Environment Canada
Environmental Protection Service

Environnement Canada
Service de la protection de l'environnement

Deep-Water Blowout Trajectory Models for the Lancaster Sound Region

Technology Development
Report EPS 4-EC-82-2

Environmental Impact Control Directorate
March 1982

ENVIRONMENTAL PROTECTION SERVICE REPORT SERIES

Technology Development Reports describe technical apparatus and procedures, and results of laboratory, pilot plant, demonstration or equipment evaluation studies. They provide a central source of information on the development and demonstration activities of the Environmental Protection Service.

Other categories in the EPS series include such groups as Regulations, Codes, and Protocols; Policy and Planning; Economic and Technical Review; Surveillance; Training Manuals; Briefs and Submission to Public Inquiries; and, Environmental Impact and Assessment.

Inquiries pertaining to Environmental Protection Service Reports should be directed to the Environmental Protection Service, Department of the Environment, Ottawa, Ontario, Canada, K1A 1C8.

Catalogue No.: En 46-4/82-2E
ISBN 0-662-11990-8

DEEP-WATER BLOWOUT TRAJECTORY MODELS FOR THE LANCASTER SOUND REGION

by

John R. Marko
Arctic Sciences Ltd.
Sidney, British Columbia

for the

Environmental Emergency Branch
Environmental Impact Control Directorate
Environmental Protection Service
Environment Canada

EPS 4-EC-82-2

ABSTRACT

Procedures were developed to simulate sea surface movements of oil released from deep-water oil blowouts. Emphasis was laid upon making realistic allowances for the horizontal spreading of oil by turbulence and current-features not included in the 5 nautical mile grid of residual currents utilized. The current values in this grid were established through the use of recent data from moored current-meters and drift-buoys. Simulations were carried out for four hypothetical blowout locations in Lancaster Sound and in the immediately adjoining sector of Baffin Bay. Separate scenarios were calculated at each site for steady winds from each of the four basic directions and for actual recorded wind sequences. Considerable contamination of shorelines occurred in most cases, except under westerly winds which generally tended to sweep oil out into the more open Baffin Bay region. Uncertainties regarding the appropriate magnitude of horizontal diffusion were explored through comparisons of scenarios computed for different values of a basic diffusivity parameter.

RÉSUMÉ

Des méthodes permettant de simuler les mouvements de surface des hydrocarbures s'échappant d'éruptions en eau profonde dans la mer ont été mise au point. Au cours des recherches, l'accent a été mis sur la prise en considération réaliste de l'étalement horizontal des hydrocarbures attribuables à la turbulence et aux courants non inclus dans la grille de 5 milles marins utilisée pour les courants résiduels. Les valeurs attribuées au courant dans cette grille ont été établies à partir de données récentes obtenues à l'aide de courantomètres fixes et de bouées dérivantes. Des simultations ont été effectuées pour quatre éruptions hypothétiques, dans quatre endroits différents du détroit de Lancaster et du secteur adjacent de la baie Baffin. Des scénarios distincts ont été élaborés pour chaque site en tenant compte de vents constants provenant des quatre points cardinaux, ainsi que des vents enregistrés en conditions réelles. Dans la plupart des cas, les rivages ont été considérablement contaminés, sauf en présence de vents d'ouest, qui, en général, tendent à pousser les hydrocarbures vers les zones plus libres de la région de la baie Baffin. Certaines incertitudes portant sur l'ampleur exacte de la diffusion horizontale ont été étudiées grâce à la comparaison de scénarios élaborés pour différentes valeurs d'un paramètre de diffusivité de base.

FOREWORD

This work was executed by J. Marko of Arctic Sciences Ltd., under the supervision of A. Milne, (formerly of Ocean Aquatic Sciences, OAS, Victoria) who acted as scientific authority. The report was supported by the Arctic Marine Oilspill Program (AMOP), with Peter Blackall as project co-ordinator, and sponsored by the Research and Development Division, Environmental Emergency Branch, Environmental Protection Service, Environment Canada.

ACKNOWLEDGEMENTS

The author acknowledges the programming and model-running contributions of Mr. C.F. Foster of Arctic Sciences Ltd. to this project. He also expresses gratitude for the contributions to his understanding of current blowout research which were gleaned from several discussions with Dr. D. Topham (Frozen Sea Research Group) and Drs. B.B. Maini and P.R. Bishnoi (Chemical Engineering Dept., University of Calgary).

TABLE OF CONTENTS

LIST OF FIGURES

LIST OF TABLES

CONCLUSIONS AND RECOMMENDATIONS

The available data on oil and gas mixtures and their behaviour in deep seawater suggest that oil released in the blowout of a sea bottom well is dispersed over a wide area, probably in excess of 10 km^2, even before reaching the sea surface. Entrainment and wave ring effects which may tend to confine oil in shallow water wells are negligible in the depths considered and even slick formation in the immediate area of the well may not be assumed as a certainty.

Simulations of the surface or near-surface movement of oil have been carried out. These include state-of-the-art knowledge of the eastern Parry Channel currents and a representation of oil spreading which makes allowance for the present understanding of real and horizontal surface turbulence. The estimated magnitudes of the latter effect, expressed in terms of an apparent diffusivity parameter, govern the width of the calculated trajectories except in regions of strong current gradients.

The scenarios of oil movement from the four selected blowout sites indicated light to heavy pollution of coastlines, particularly in the vicinity of headlands such as Cape Hay and Cape Sherard. Of the basic four wind configurations only westerlies have the general tendency to move oil out of Lancaster Sound and into the more open waters of Baffin Bay. Although large gaps in the surface current data preclude simulation accuracy, it would appear that southerly winds can move oil from the south to the north side of Parry Channel against the flow pattern which prevails east of the Cape Warrender-Borden Peninsula line.

Northerly and easterly winds generally effect the most intense coastal pollution of sites inside Lancaster Sound. This circumstance results from their tendency to remove oil from the intense easterly flowing current which parallels the southern border of Parry Channel.

The major requirements for further development in oil trajectory models are:

1) Near-surface current measurements by drogued drift buoys in the still largely unstudied central and western section of Lancaster Sound.
2) The continued accumulation of near-surface current meter time series data in order to allow the possibility of building time dependencies into the residual current grids of future models. A variability with roughly a two week period noted in eastern Lancaster Sound (Fissel and Wilton, 1978) would be expected to have a significant effect on the one week or longer simulation periods required for impact assessment.

3) Further studies on the large-scale spreading of surface slicks, possibly utilizing closer monitoring of actual accidental spills or perhaps through recording the movement patterns of groups of oil spill follower buoys. Estimates must be made of apparent diffusivity enhancements due to winds, rapid current flow and the proximity of coastline or shallow water areas.

4) Further work on the relationship between the wind scaling factor (assumed to be fixed at 3.5% in our model) and wind history. Examination of evidence that this factor can range from 1 to 7% depending upon wind duration (Aubin and Murty, personal communication). It is suggested that the wind component of motion can be studied using oil spill follower buoys in conjunction with local wind and current profiling measurements.

5) Establishment of procedures whereby wind statistics and coastline configurations may be properly combined to form a compact, easily interpretable representation of the geographical distribution of the pollution threat.

1 INTRODUCTION

The possibility of oil and gas exploration in the offshore region of eastern Parry Channel (see Figure 1) has stimulated the recent accumulation of a large mass of oceanographic and laboratory data relevent to the fate of oil spilled in this area. The work to be described below represents an attempt to incorporate this information into a model describing the movements of oil arising from deep-water well-blowouts. Blowouts are assumed to have occurred at four specific locations in Parry Channel. These sites are indicated in Figure 2 relative to the 5 nautical mile grid used in the developed model. Water depth and leaseholder information are listed for each site in Table 1.

TABLE 1 ASSUMED BLOWOUT SITE DETAILS

Site No.	Position	Water Depth	Leaseholder
1	74°7.5'W 89°33'W	280 m	Magnorth Ltd.
2	73°57.5'N 84°42'W	458 m	Ray Petroleum Ltd.
3	74°12.5'N 81°22'W	770 m	Norlands Petroleum Ltd.
4	74°37.5'N 78°32'W	549 m	Petro-Canada Ltd.

Treatment of the problem begins in Sections 2 and 3 where the available data are reviewed, while being related to the sub-surface (plume) and surface transport properties of released oil. A model compatible with these data is outlined in Section 4 and applied to the specific hypothetical blowout sites under a wide range of observed and artificial wind conditions. The results of these simulations are presented and discussed in Section 5 keeping in mind the ice-free surface conditions usually obtained in the summer season. The complications introduced by the typical ice covers of the fall and winter are considered and comparisons are made with the summer oil distribution. Conclusions and recommendations are included for further model developments.

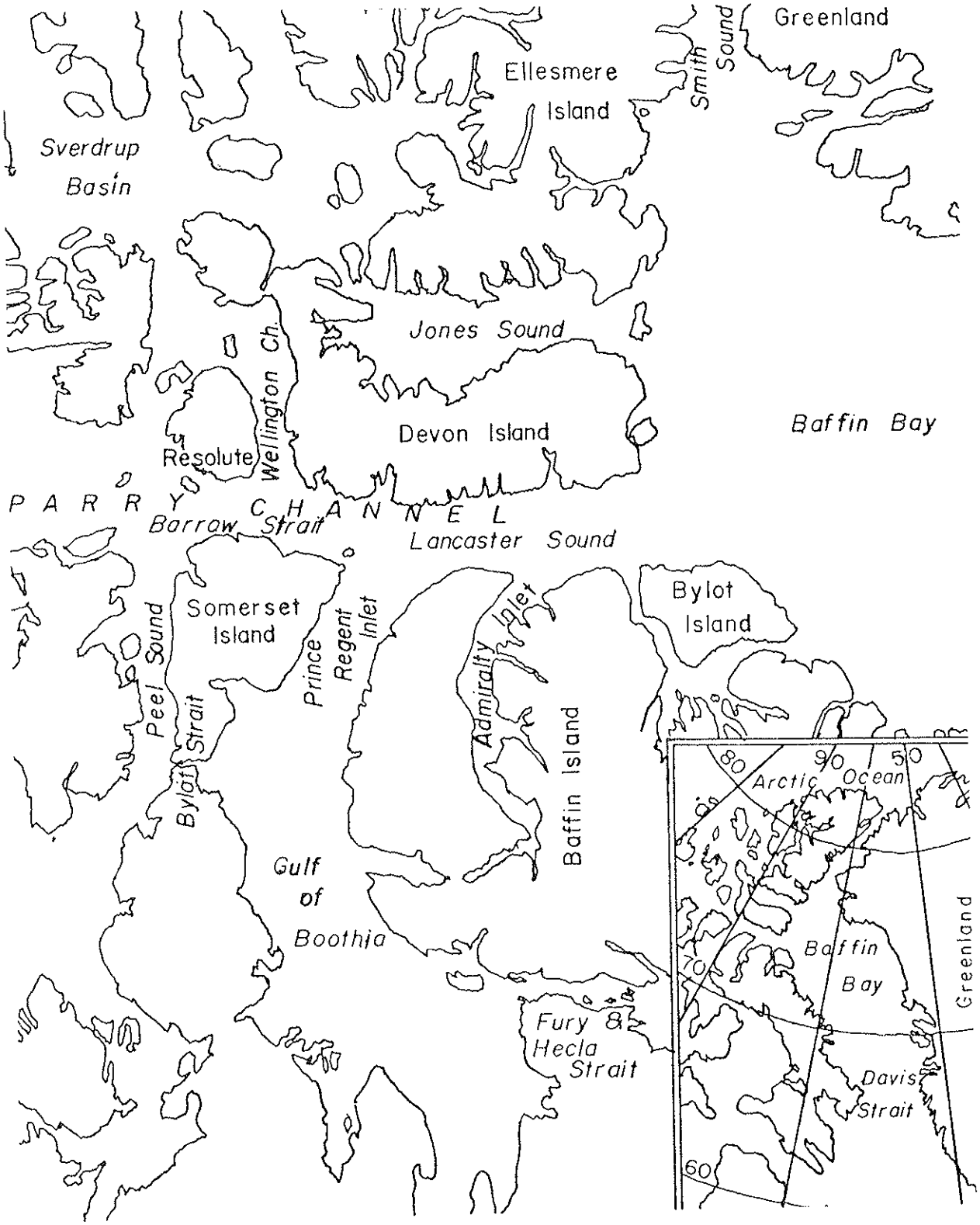

FIGURE 1 A MAP OF EASTERN PARRY CHANNEL AND ADJACENT WATER BODIES. The inset map illustrates the locations of Parry Channel in relation to Baffin Bay and the Arctic Ocean.

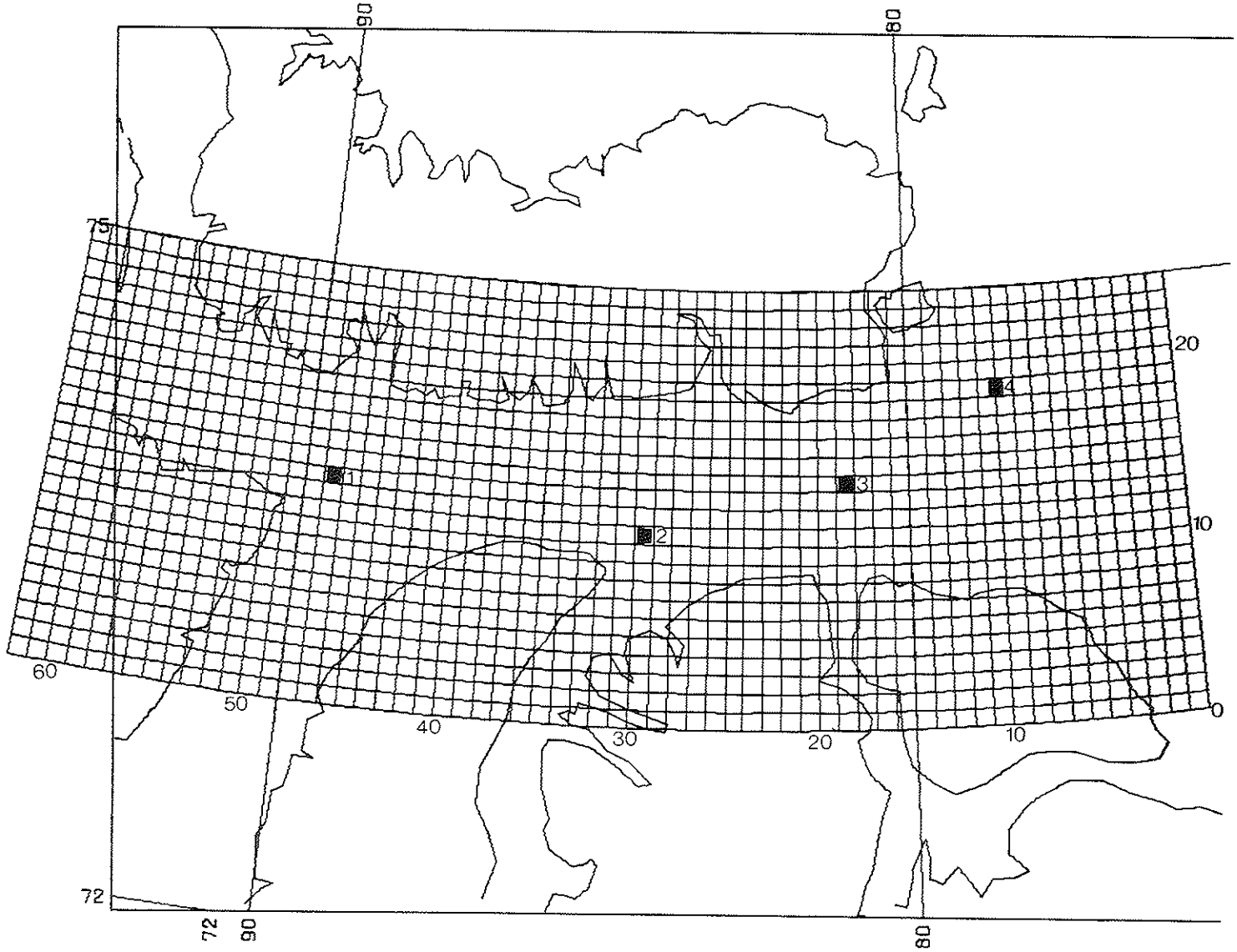

FIGURE 2 THE LOCATIONS OF THE FOUR POTENTIAL BLOWOUT SITES CONSIDERED IN THIS REPORT. The 5 nautical mile grid used in the simulations is superimposed with its origin at the lower right hand corner. In the text a grid square in the n_1th column and n_2th row is indexed as (n_1, n_2).

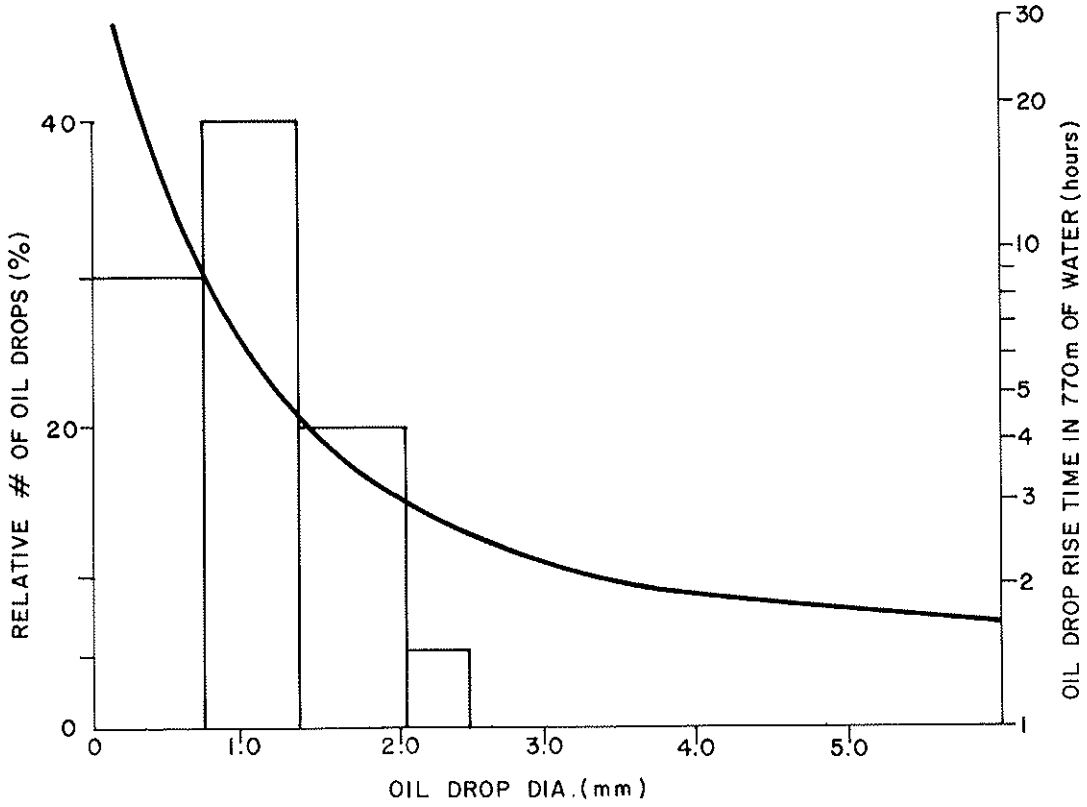

FIGURE 3 a) PERCENTAGE DISTRIBUTION OF OIL DROPLET DIAMETERS (2.2 cm DIAMETER PIPE) (ACCOMPANYING GAS VELOCITY = 1.9 m/s) (Topham 1975)

b) RISE TIME OF OIL DROPLETS AS A FUNCTION OF DROPLET DIAMETER (Milne and Smiley 1978)

2 BLOWOUT PARAMETERS AND THE SUB-SURFACE (PLUME) BEHAVIOUR OF OIL

The major parameters of an eastern Parry Channel blowout specified earlier by Milne and Smiley (1977) in their evaluation of the likely pollution threats to Lancaster Sound have been assumed. Estimates of 950 m^3 (6000 barrels) of oil and 2850 m^3 of gas flow per day were obtained assuming saturation of the gas in the oil at a 3000 m formation depth. This oil and gas mixture was assumed to emerge from a 15 cm diameter outlet pipe on the sea floor in a slug type flow of alternating masses of gas and oil. In this case the corresponding gas and oil exit velocities are 1.9 m/s and 0.6 m/s respectively (Milne and Smiley used a combined value of 0.62 m/s).

The laboratory measurements of Topham (1975) at similar rates of gas and oil flow indicated that this process produces a fine dispersion of oil droplets. The detailed distribution of droplet diameters appears to be a strong function of the exit velocities, pipe diameter and oil type. The percentage distribution of 100 randomly selected drop diameters is indicated in Figure 3 for a Norman Wells oil-gas mixture exiting a 2.2 cm pipe into sea water. The gas velocity at the outlet pipe in this case was 1.9 m/s corresponding well with the hypothetical Milne and Smiley case.

However, direct application of the distribution in Figure 3 to the case at hand is not completely justified in view of Topham's additional results which indicate that even slower flow rates in larger (7.7 cm) diameter pipes produced finer dispersions of the oil, i.e. all observed droplet diameters were less than 0.5 mm.

The precise nature of the oil droplet size distribution in the vicinity of the wellhead exit pipe is critical to the subsequent characteristics of the plume of rising oil. The size is dependent on the rate at which a droplet rises through the water column under the force of its own buoyancy. Calculated rise times in 770 m of water (corresponding to our deepest site No. 3) are indicated in Figure 3 for the relevant range of droplet sizes.

The spread of droplet rise times allows a similar spread in the drifts of each droplet under the action of the horizontal currents in the water column. The resulting linear dimensions of the "patch" of rising oil is approximately given by the product of some mean current speed and the difference in the rise times corresponding to the smallest and largest significant droplet size categories. In the case of the distribution of Figure 3, this rise time difference is on the order of eight hours. A further reduction of droplet size to less than 0.5 mm; as suggested by Topham's large pipe results,

could increase this spread to 20 or 30 hours with a corresponding tripling or quadrupling of the linear patch dimensions.

Nevertheless, in the absence of further data on droplet sizes, the validity of the Topham distribution (Figure 3) in all further considerations of the plume of rising oil is assumed. The outline of this plume has been calculated assuming typical values for the current speeds in the upper, middle and lower portions of the water column. These speeds are indicated in Figure 4 along with the calculated outline of the plume. The latter actually corresponds to the trajectories of the smallest and largest droplet size categories. The indicated local oil concentrations highlight the rapid dilution of the oil mass as it rises in the column. The length of the patch of surfacing oil itself is approximately 5 km, with 85% of the oil being concentrated within 1 km of the trailing patch edge. If all oil rises to and stays on the surface, the thickness of the resulting slick is approximately 0.16 mm.

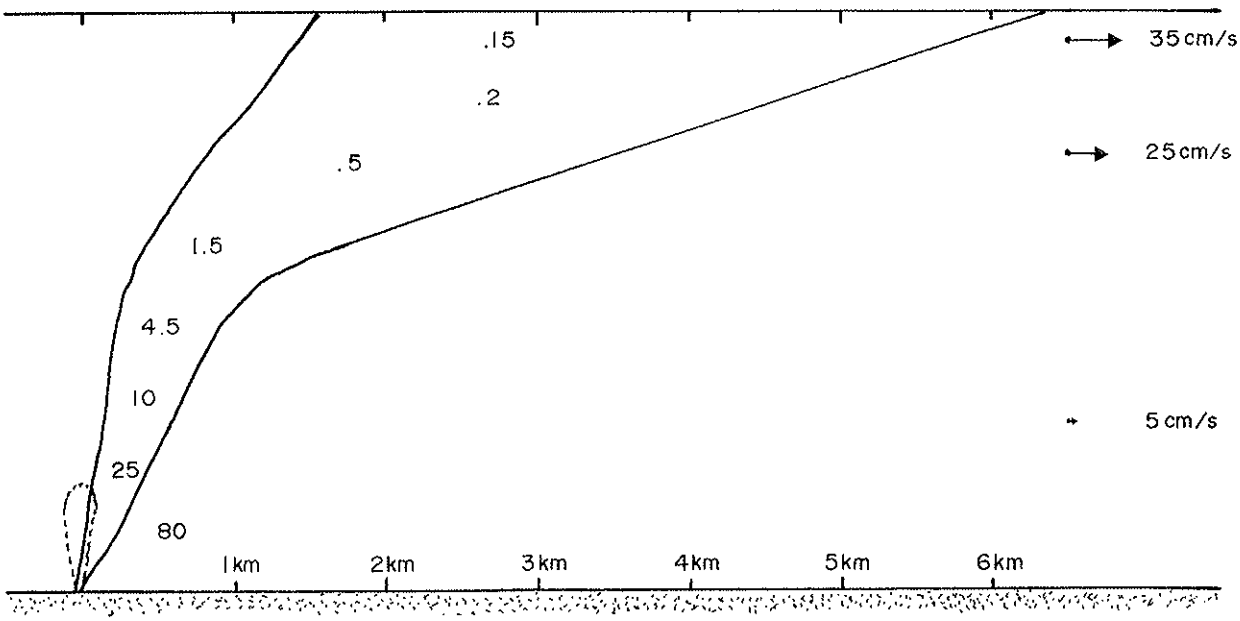

FIGURE 4 A SIDE VIEW OF THE STEADY STATE OIL PLUME ARISING FROM A 6000 bbl/day BLOWOUT WELL IN 770 m OF WATER. The droplet size distribution and rise time data of Figure 2 have been utilized and the indicated current speeds assumed applicable in the 0 to 121 m, 121 to 378 m and 378 to 770 m layers. The accompanying release of natural gas is assumed to be totally converted to solid gas hydrate particles at some point in the water column as indicated by the broken line envelope sketched in above the wellhead.

Assuming an aspect ratio (the ratio of transverse to longitudinal dimensions) of 0.2, these results indicate that the mass of rising oil at any given time covers approximately 5 km^2 of sea surface even before it begins to be dispersed by the actions of surface winds and currents. This large initial patch size was not accounted for in an earlier model (Imperial, 1978) which assumed a size-independent entrainment of oil droplets in the vertical current set up by a rapidly rising mass of gas bubbles. This picture neglected the gradual separation of the oil and gas columns by diffusion, and, even more importantly, did not account for rapid gas-hydrate formation rates in water deeper than 400 meters. The latter effect, according to the data of Maini and Bishnoi (1979), will extinguish the gas flow at some point in the lower water column, replacing it with a widely distributed cloud of slowly rising, hydrate fragments (specific gravity of hydrate = 0.94). Furthermore, the gas which comes out of solution in the oil droplets undergoes immediate conversion to the hydrate; coating, in the process, each droplet with a dense outer skin. This effect further increases the oil droplet rise time and, hence, the linear patch dimensions.

The complications produced by either the finer initial dispersal of oil droplets or solid hydrate formation will not be detailed further. More experimental data are needed in each case before these effects can be properly included in a quantitative picture of the oil plume. Nevertheless it should be emphasized that the starting point for the on or near-surface spread of oil represents, in all likelihood, is an underestimate of the actual initial spatial extent. In any case, however, the conservatively estimated 5 km^2 patch size is still well in excess of the regime where the surface tension and viscosity dominated spreading mechanisms of Fay (1971) and Blokker (1964) have any applicability.

3 OIL AT THE AIR-WATER INTERFACE

Perhaps the most complete study to date of the distribution of oil arising from a well blowout was carried out by Murray et al (1970) in connection with an actual blowout site in the Gulf of Mexico. Although the approximate 50 foot water depth and warmer temperatures at this site preclude direct application to the cases at hand, the detailed observations and accompanying analysis made by Murray and co-workers offer valuable insights into the likely characteristics of the surface movements of oil arising from deepwater wells.

For example, it was found that the slick above the wellhead aligned itself from 10° to 40° to the right of the surface wind apparently under the influence of the dominant tidal component of the local surface current. The general form of the slick is as indicated in part A of Figure 5. The edges of the slick tended to be a fraction of a micron thick and large areas of more thickly concentrated oil were seen within its perimeter. Murray (1972) showed in detail that the shape of the portion of the slick still attached to the wellhead area undergoes a change from linear ($y \propto x$) to parabolic, ($y \propto x1/2$), behaviour before deteriorating into more complicated "pinch out" regime at greater distances from the well site. It was also shown that these shapes were consistent with a Fickian diffusion mechanism of spreading (Murray 1972). In this approach, little difference was seen between the motion of surface oil and that of the uppermost water layer. Murray's analysis of the shape and size data were consistent with an apparent diffusivity coefficient D ranging from 1.5×10^5 to 2.0×10^5 cm^2/s. Evidence for temporary increases in this quantity associated with the higher turbulence levels produced under high wind conditions was also cited.

Consideration of diffusion from a linear source indicated the area of the visible portion of the oil slick "A" has the following dependences.

$$A \propto \frac{Q^3}{DU^2} \qquad (1)$$

where: Q - is the volume rate of oil flow;
D - is the diffusivity; and
U - is the surface current speed.

Slick areas in the 10 to 20 km^2 range were recorded but the data were insufficient to verify Equation (1).

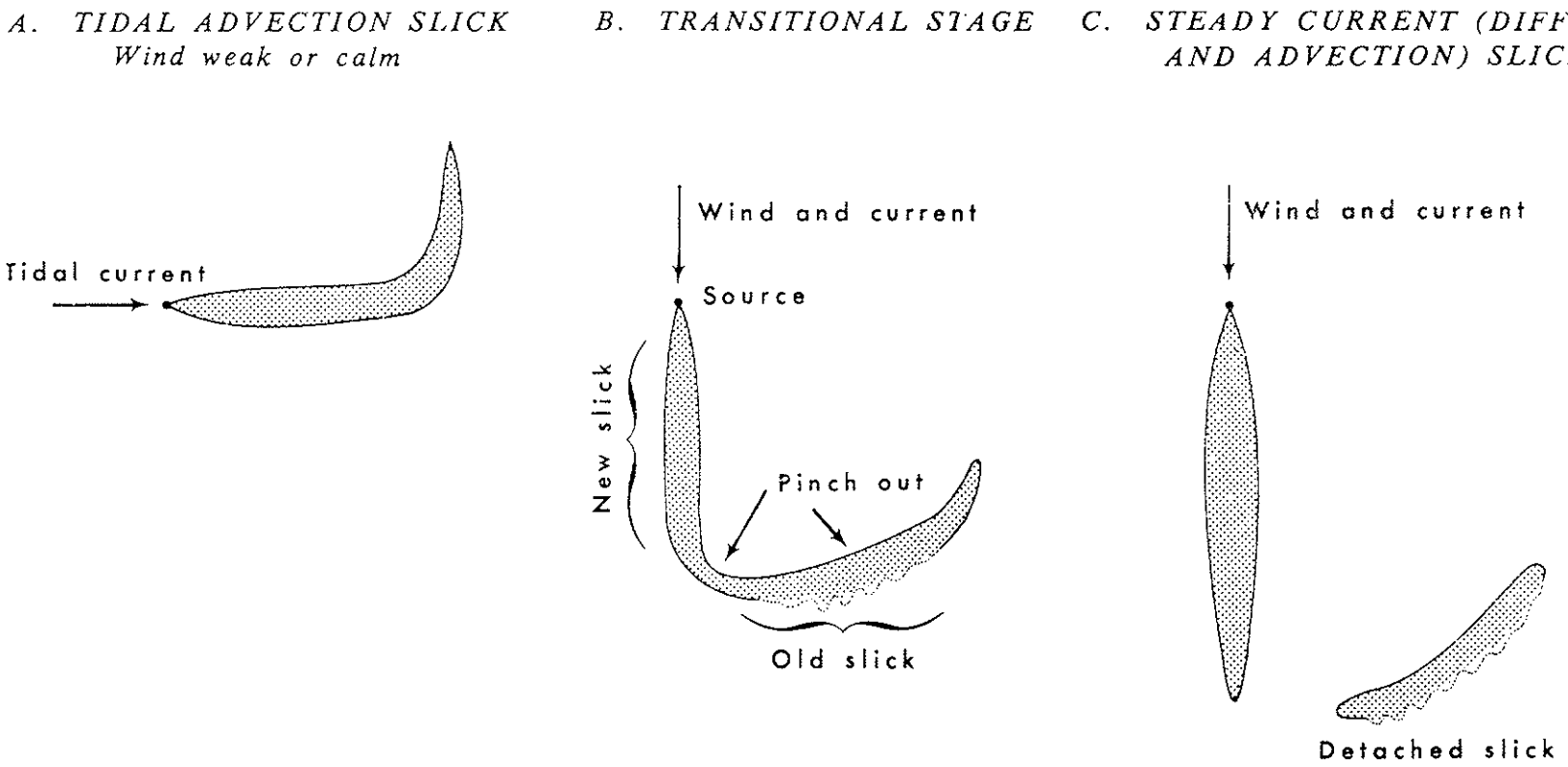

FIGURE 5 AN ILLUSTRATION OF A MECHANISM WHEREBY TIDAL AND WIND CHANGES SEPARATE OIL FROM THE IMMEDIATE AREA OF A SHALLOW WATER BLOWOUT (from Murray (1972)).

A major contribution of the Murray study was the identification of a mechanism whereby oil is visibly spread to areas well separated from the blowout site. This process, illustrated in Figure 5, requires the production of a weak link between the older and more recently released portions of the oil slick. It depends upon changes in the direction of the predominant wind or current forcing and the subsequent breaking of the linkages releasing individual, self-contained slicks which then move freely with the surface water layer until they are either dissipated by evaporation and dispersion or are driven onto shorelines.

A good portion of the available oil slick size versus time data is represented in Figure 6. Areas are included in this figure for: small controlled spills of oil and oil-water mixtures; large accidental releases from the Torrey Canyon sinking and Santa Barbara seepage; and a pseudo oil spill in which the area enclosed by three independently drifting oil spill follower buoys was monitored (Fissel, Lemon and Wilton, 1979). If one neglects the poorly characterized and internally contradictory oil-water mixture data, a fair representation of the area vs time relationship can be achieved with a simple power law:

$$A = 1.6t^{1.52} \qquad (2)$$

where A = the area in square meters
and t = the elapsed time in seconds

This relationship is stronger than the linear time dependence expected in the case of simple Fickian diffusion. The deviations from the Fickian law seem to be general and not solely connected with slick properties; as similar results were obtained in the dye tracer diffusion experiments studied by Okubo (1971).

Nevertheless Equation (2) is unsatisfactory in itself because of its neglect of any dependence of the slick size-time relationship upon oil volume. There appears to be ample evidence, Smith (1970), Jeffreys (1973), that after an initial period of rapid expansion, the slick size stabilizes, at least temporarily, at a value which bears some relationship to the available pool of spilled oil. Unlike the area encompassed by an initially specified patch of surface water, which expands indefinitely through diffusion, the area of an oil slick is governed by a complicated mixture of processes in which oil is not only diffused away in non-visible quantities but also moves back and forth between the thicker and thinner portions of the slick.

To our knowledge the best documentation of long term slick behaviour was provided by Smith in his study of the Torrey Canyon spill (1970). Although the volume of oil in the chosen slick was uncertain (corresponding data points in Figure 6 are labelled as 2×10^4 tons but uncertainties in both the released volume of oil and its relative

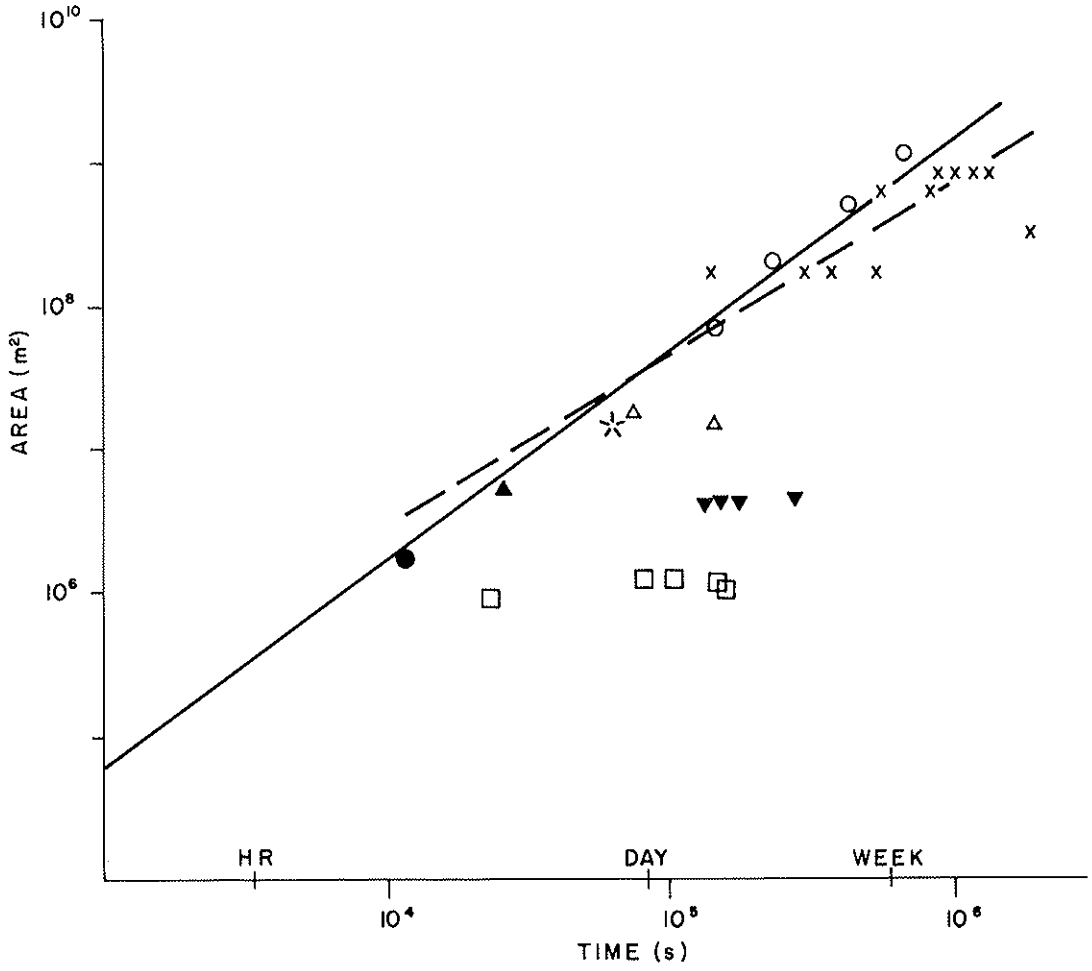

FIGURE 6 EXPERIMENTAL DATA ON THE SURFACE SPREAD OF OIL, OIL AND WATER MIXTURES AND OIL SPILL FOLLOWER BUOYS AS A FUNCTION OF ELAPSED TIME. (x) 2×10^4 tons; (▲) 80 bbl oil; (●) 30 bbl oil; (o) Santa Barbara seep (▼) 110 bbl oil-water; (△) 90 bbl oil-water; (□) 25 bbl oil-water; (✳) oil spill followers. The solid line depicts the assumption made to derive equation (2). The broken line represents a linear fit, $A \propto t$, to the data in accord with simple Fickian diffusion theory.

division among several slicks make this value more appropriate as an order of magnitude estimate), the almost daily recording taken of slick sizes and shapes (Figure 7) illustrate many of the characteristics of freely drifting oil masses. It was observed that the daily positions of the slick could be quite accurately predicted assuming oil movement parallel to the direction of the daily mean surface wind and at 3.4% of wind speed. The slick tended to elongate in the direction of this motion and after the initial period of growth (the slick was first studied some 48 hours after the initial release of oil) its size remained relatively unchanged at ~150 km^2 until March 25 (Figure 7) when a sudden expansion to ~450 km^2 was observed. This event was followed by a further period of relative stability in slick size.

It should be noted that the included period of expansion coincided with the closest approach of the slick to a major land mass. Net winds were low during this period and it remains a strong possibility that the source of expansion lay in an effective increase in the level of horizontal diffusion associated with the more complicated surface current regimes of coastal areas. Tidal current anomalies, rips and other local current structures; although not truly random or turbulent in nature, contribute to the expansion of a drifting oil slick in a way which is difficult to distinguish from the effect of a local enhancement of diffusivity. This effect was anticipated in Ahlstrom's (1975) development of a general spill simulation where it was suggested that the complications introduced by shoreline structures are equivalent to an order of magnitude increase in diffusivity.

Finally, any consideration of the distribution of released oil must account for its losses of water soluble and volatile components and its dispersal in low concentrations away from the observed areas of contamination.

In view of the fine initial dispersion of the oil into droplets and their subsequent slow rise to the surface, it seems reasonable to expect that the roughly 5% water soluble component of a Norman Wells-type crude (Milne and Smiley, 1977) would enter completely into solution prior to reaching the surface.

Evaporation rates are less well known and strongly dependent upon the nature of the surface oil mass (i.e. the percentages in thick or thin films, mousse or tarballs) and related external parameters such as the wind speed. According to Kreider (1971) most of the volatile carbon components, up to C_{12}, evaporate in the first 24 hours of surface exposure. The loss of heavier components up to C_{25}, continues for an additional short period. An estimated total loss of 45% of oil volume seems appropriate for the initial two day period following slick formation.

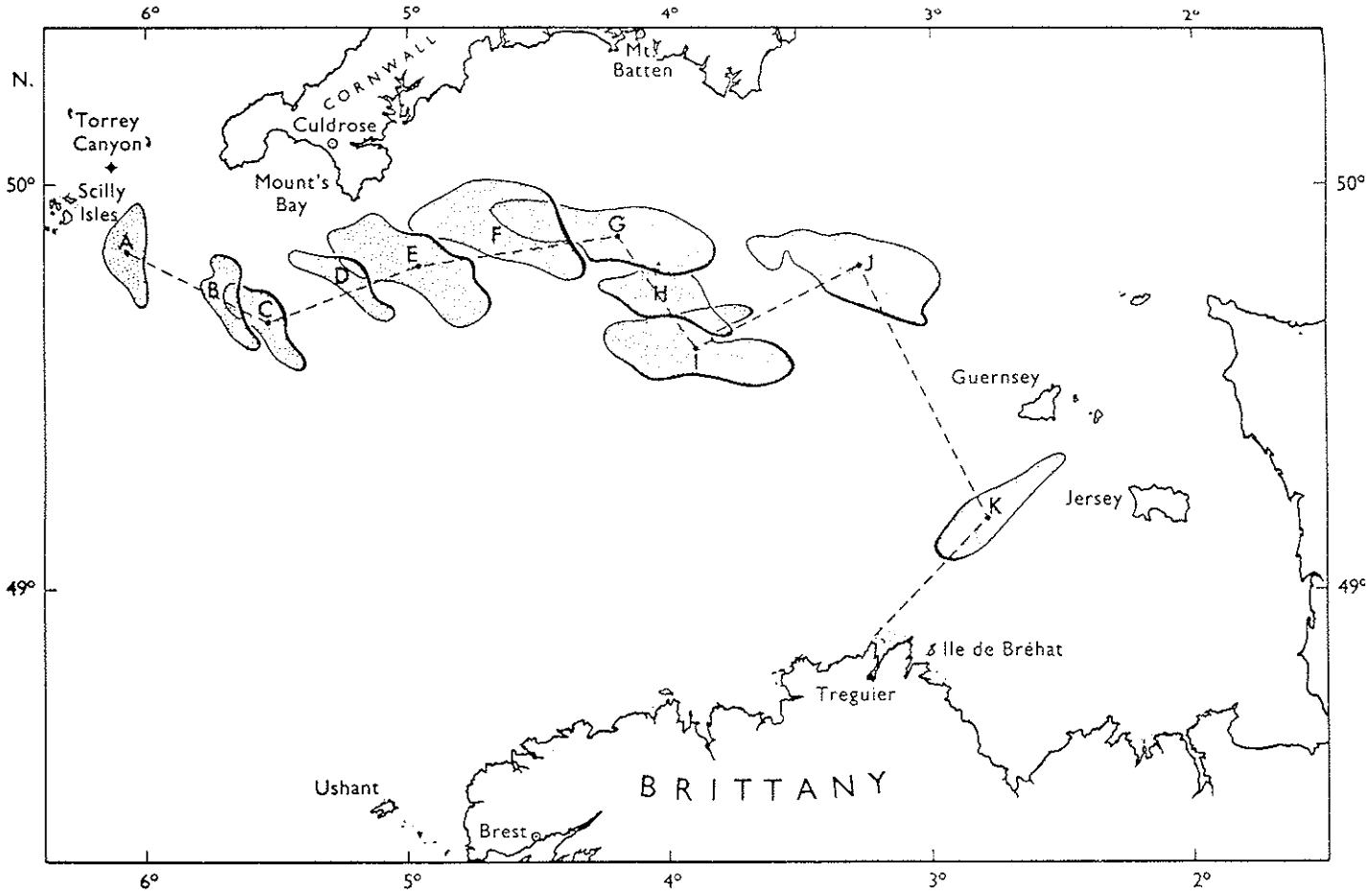

FIGURE 7 THE CONFIGURATIONS OF A SINGLE OIL SLICK RELEASED FROM THE TORREY CANYON. A, 20 March, 07.00 h; B, 22 March between 06.00 and 08.00 h; C, 23 March, between 06.00 and 07.00 h; D, 25 March between 06.00 and 07.00 h; E, 26 March, 13.00 h; F, 27 March between 06.00 and 09.00 h; G, 28 March between 05.45 and 11.00 h; H, 30 March between 06.00 and 11.30 h; I, 1 April, 09.00 h; J, 4 April between 08.45 and 11.50 h; K, 8 April about midday. (from Smith (1970)).

Major uncertainties remain in the estimating procedures for assessing loss rates due to dispersion processes. Problems arise since the mere horizontal or vertical separation of a mass of oil droplets from the body of a slick may not be equivalent to dissipation. Instead, under a later reduction in wave state, this oil may rise again to the surface to either rejoin its parent slick or to form an independent oil mass. True dissipation requires some combination of the natural processes of biodegradation, sedimentation and oxidation with the gradual diffusion away of oil particles in low concentrations. Our estimates of the likely dispersion loss rates tend toward the lower or more conservative end of the ranges given by Blaikely et al (1977) based on rather short form field tests and observations in the North Sea.

4 AN OIL SLICK TRAJECTORY MODEL

Our approach to modelling the movements of on or near-surface oil in Lancaster Sound and Barrow Strait follows the general simulation scheme outlined by Ahlstrom (1975). Because of the detail available on surface currents in selected areas, calculations were performed utilizing the 5 nautical mile grid indicated in Figure 2.

The continuous 950 m^3 or 6000 barrel daily flow of the hypothetical blowout was represented as a series of smaller, discrete releases of oil "batches" at uniform intervals in time. Our batch sizes and release intervals, 750 barrels and 3 hours respectively, were chosen: 1) to simulate the rate at which freely drifting oil slicks would become detached from the immediate area of the blowout by changes in tidal and wind flow; and 2) to insure that the oil volume contained within each batch is sufficient to support the "internal" component of slick expansion assumed in the model described below.

In this model each batch forms a distinct slick independent of its overlap or interaction with adjoining slicks. Two components of motion are considered for each batch: 1) a net advection or displacement of its centroid; and 2) an expansion of its area of coverage. The magnitude of the latter, internal component was approximated assuming the applicability of equation (2) with an initial advance in time equal to roughly 6 hours in order to account for the assumed 5 km^2 initial size of a just-released oil batch. A 200 km^2 upper limit was also placed upon the size of each slick in accord with the evidence for the apparent stabilizing of much larger oil masses near such a limiting value. In our case this resulted in the cessation of internal slick spreading some 45 hours after internal batch release.

To simplify matters, the individual batches are represented as rectangles with constant aspect ratios = 0.2 and aligned with the long axes parallel to the net displacement over the previous 24 hour period. The instantaneous configurations of five released batches are sketched in Figure (8).

The displacement of the centroid of each batch over the time interval between t_n and $t_n + 1 = t_n + \Delta t$ is assumed to be given by:

$$\vec{d}_{n,\, n+1} = (\vec{v}_r + \vec{v}_w)\ \Delta t + \vec{d}_d$$

where $\vec{v}_r$ and $\vec{v}_w$ respectively represent the residual near-surface and wind driven-current components. The displacement of the batch by diffusive or pseudo-random motions of the sea surface is given by $\vec{d}_d$. As defined here, the residual current is the time-averaged

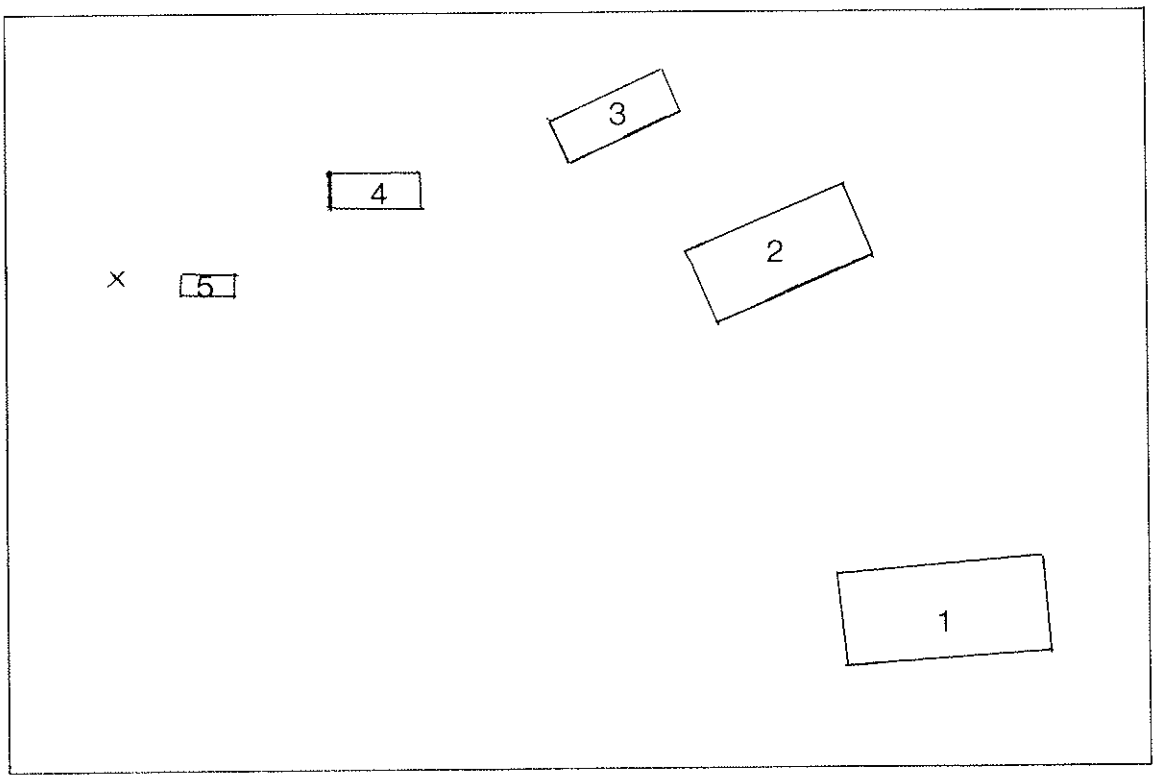

FIGURE 8 A SIMULATED CONFIGURATION OF RELEASED OIL. The continuous flow of oil from the sea-bottom source (x) is broken into batches which are released at fixed intervals of time. Each batch is assumed, for simplicity, to take on a rectangular shape with its area increasing with time and its long dimension oriented to parallel its net displacement over the previous 1 day period.

current less the component directly associated with surface wind forcing. It includes contributions to motion arising from the water mass distribution, sea slope, river discharges, etc. which are, in themselves, prohibitively difficult to quantitatively characterize. Tidal effects are neglected in this formulation, since to first order, they give no contribution to the time-averaged net displacement of a surface slick.

The residual currents used in our simulation of a summer season, ice-free blowout were primarily derived from the observed trajectories of 25 Nimbus satellite RAMS-monitored drifting buoys which moved through the areas of interest as part of the 1977 and 1978 field programs of the Institute of Ocean Sciences, Patricia Bay, Norlands Petroleum Ltd. and Petro-Canada Ltd. (Fissel and Marko, 1978 and Fissel, Lemon and Wilton, 1978). These buoys were fitted with drogues centered at approximately 7 m depths in order to maximize coupling to the sub-surface, non-wind driven current component (residual current). The resulting position data were smoothed, filtered and utilized to calculate trajectories and vector averaged drift velocities in each square of our grid. The resulting set of local drift velocities is indicated in Figure 9. Data are heavily concentrated in eastern Lancaster Sound and Prince Regent Inlet.

Data from moored current meters (Figure 10) and from consideration of individual buoy tracks (with allowance for wind-driven components of motion) were used to supplement Figure 9 in the production of the residual current grid of Figure 11.

This grid differs from an earlier version (FENCO, 1978) in many respects, most prominently, perhaps, in the large current velocities indicated for the Cape Sherard -Cape Warrender area of northeastern Lancaster Sound.

Very strong southerly flow was found north of Navy Board Inlet and a large zone of relatively slow, complicated motion was identified at the eastern end of Lancaster Sound bounded on the north and south respectively by the coastal flows of southeastern Devon and northern Bylot Islands. Evidence of a small, (~10 km scale), eddy-like structure northeast of Cape Hay and north and east of Cape Fanshawe was acknowledged by the inclusion of similarly located circulating structures in our coarse grid representation.

It should be noted that the low density of buoy drift data in areas west of roughly 81.5° W longitude (excluding of course the area of Prince Regent Inlet) undermines the applicability of the representation of Figure 11 to the central portion of Lancaster Sound. There is evidence (Fissel and Marko, 1978, Marko , 1978) of large

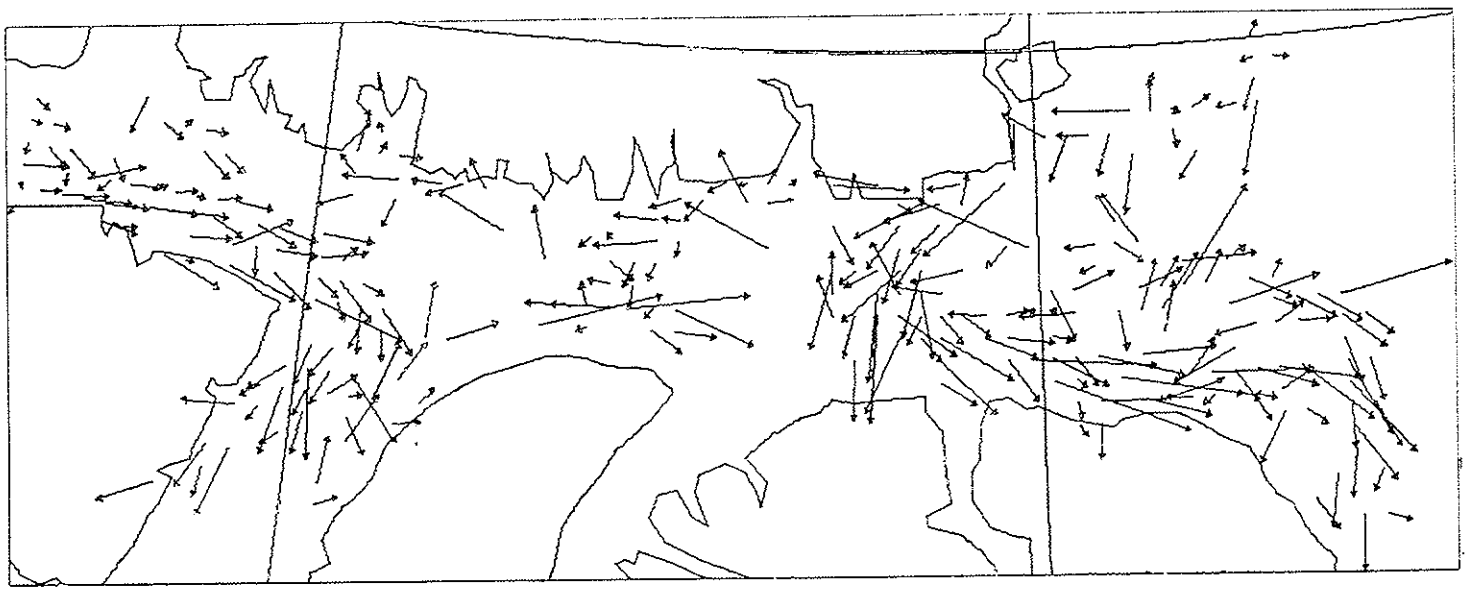

FIGURE 9 AVERAGE BUOY DRIFT VELOCITIES AS DEDUCED FOR TWENTY-FIVE NIMBUS SATELLITE RAMS- MONITORED DROGUED BUOYS RELEASED DURING THE SUMMERS OF 1977 AND 1978, SUPERIMPOSED ON A 5 NAUTICAL MILE GRID.

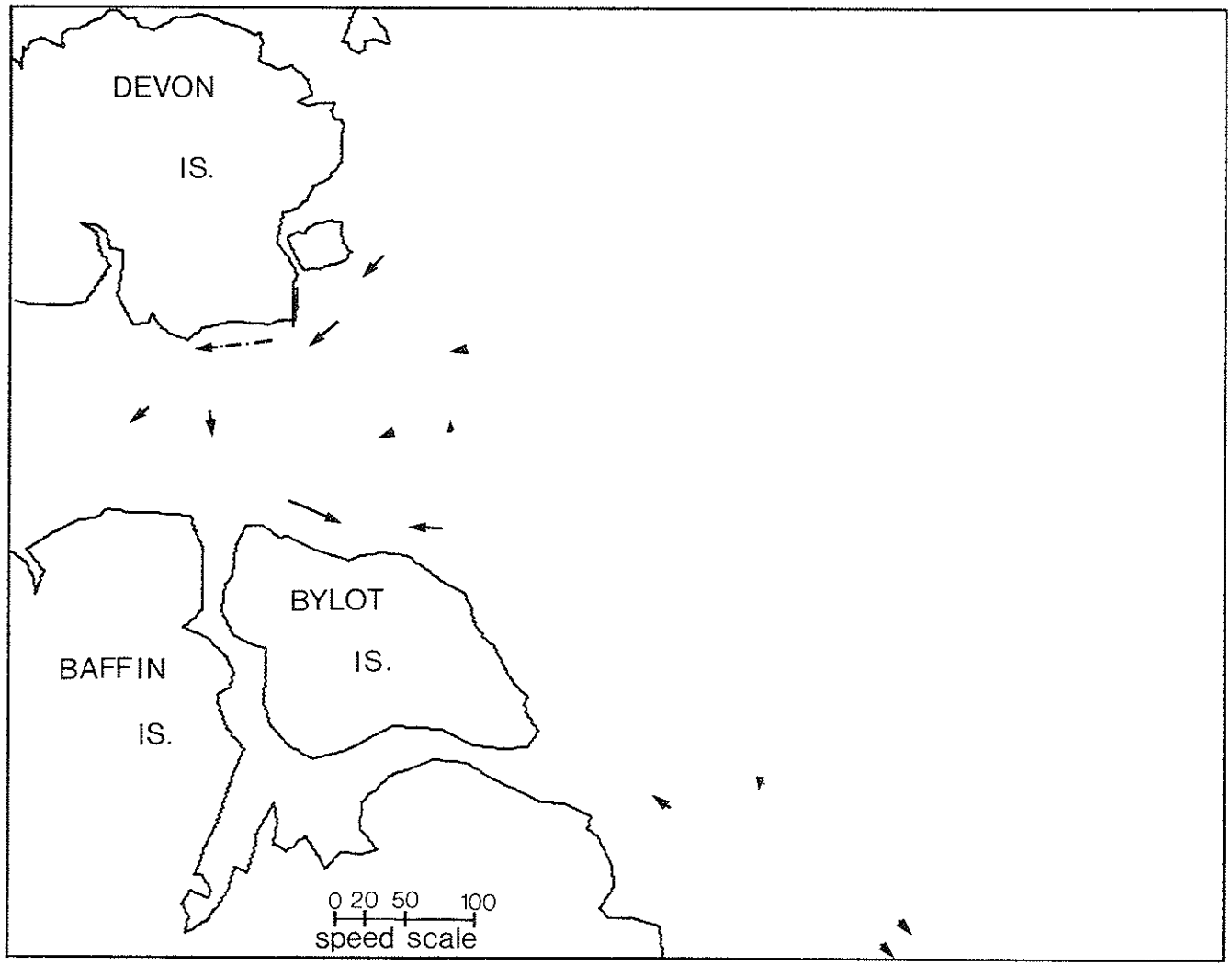

FIGURE 10 MEAN CURRENTS AT 35 TO 50 m DEPTH AS OBTAINED FROM MOORED CURRENT METERS IN LANCASTER SOUND FOR THE SUMMER SEASONS OF 1977 AND 1978 (Fissel and Wilton, 1978 and Fissel, Lemon and Wilton, 1979)

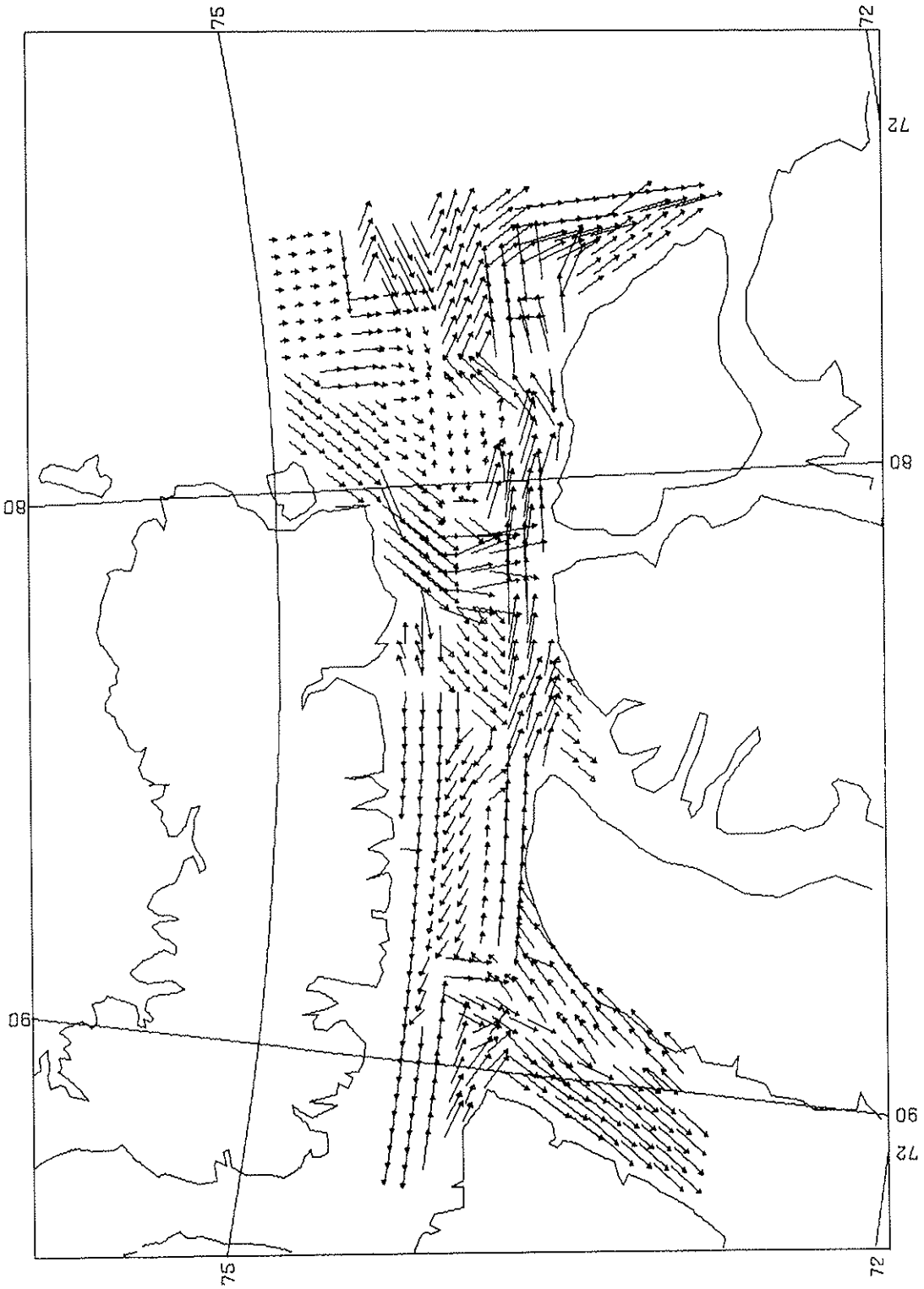

FIGURE 11 THE RESIDUAL CURRENT GRID USED IN ALL SIMULATION RUNS

(50 km scale) eddy-like structures in this area. However, in the absence of further data on the permanence and localization of such features, the current vectors of Figure 11 were intended to represent a general, not particularly strong westerly flow believed to be characteristic of northern Lancaster Sound west of Dundas Harbour. The indicated mid-Channel currents of this area represent one particular observed flow configuration whereby a north-south interchange of water masses may occur.

In view of the apparent dominant influence of residual currents in most areas, the active controversies over the optimum representation of the wind-driven slick component have not been given further consideration. Variations in coupling coefficient as a function of wind speed have been neglected and the approach of Smith (1970) has been slightly modified, in assuming that the oil moves directly downwind at 3.5% of its speed.

Treatment of the diffusive contribution to the centroid motion of each batch follows the standard procedure of earlier simulations (Ahlstrom, 1975, Sahota et al, 1978) in that displacement magnitude and direction are determined from a subroutine-generated source of random numbers "R" such that $0<R<1$, according to:

$$|\vec{d}_d| = 2\sqrt{3}\ R\sqrt{D\Delta t} \qquad (3) \text{ and}$$

$$\Theta = 2\pi R \qquad (4)$$

where D is the horizontal eddy diffusivity, and Δt is the time interval separating successive positions of each batch.

Diffusive displacements were computed for values of D ranging from 2×10^5 to 2×10^6 cm^2/s. The lowest of these values is approximately the value deduced by Murray (1972) in his study of slick size and shape in the vicinity of the blowout site.

Our tendency toward consideration of values of D in excess of Murray's value can be justified on several grounds including the need for methodological consistency between Murray's measurement and the general results of Okubo (1971). The latter indicated the apparent diffusivity, with single point source releases, increased according to strong power law relationships with both the time of diffusion and the spatial scale (proportional to the size of the eddies responsible for the observed diffusive movements). The difference between the scales of the internal spreading and centroidal diffusion motions would be expected to produce a diffusivity in the latter case in excess of 2×10^5 cm^2/s. Direct application of Okubo's results to deduce an appropriate value for the extent of the increase is not possible at this time due to the sensitivity of Okubo's

results to initial conditions (Buckley and Humphrey, 1979) and as a result of fundamental differences between diffusion from a single instantaneous release and a quasi-continuously emitting source.

Additionally, as suggested above, high values of surface winds, currents and the presence of shoreline associated current structures might be expected to produce real or apparent increases in the horizontal turbulence manifesting itself in the order of magnitude range allowance for the diffusivity parameter.

The assumptions made during three hour of intervals calculation of loss rates of oil in each batch, are listed in Table 2.

TABLE 2 OIL LOSS RATES ASSUMED IN SIMULATIONS

Dissolution	37.5 bbl (5%) lost prior to t = 0 and the beginning of surface movement.				
Evaporation	day 1	37.5 bbl/interval			
	day 2	4.25 bbl/interval			
	day 3 etc.	nil			
Dispersion	day 1	wind speed	<	7 m/s	7.5 bbl/interval
	day 1	wind speed	>	7 m/s	10.5 bbl/interval
	day 2	wind speed	<	7 m/s	7 bbl/interval
	day 2	wind speed	>	7 m/s	10 bbl/interval
	day 3	wind speed	<	7 m/s	6 bbl/interval
	day 3	wind speed	>	7 m/s	9 bbl/interval
	day 4	wind speed	<	7 m/s	5 bbl/interval
	day 4	wind speed	>	7 m/s	7 bbl/interval
	day 5	wind speed	<	7 m/s	4 bbl/interval
	day 5	wind speed	>	7 m/s	6 bbl/interval

The simulation procedure also accounts for the losses from each batch through shoreline contamination. This is done by assuming fractional losses of the batch contents in any interval equal to the fraction of batch slick area which overlaps land areas. Shoreline accumulations of oil on this basis are stored for each coastal square of our grid.

The general simulation scheme outlined above was programmed for operation on the Sperry Rand 1106 computer of the Institute of Ocean Sciences, Patricia Bay. Program codes are included in Appendix A.

5 RESULTS

5.1 General

A major difficulty in the use of an oil spill trajectory simulation model is associated with the necessary choice of "representative" environmental (in this case, wind) conditions. This problem becomes particularly complicated and acute when critical coastline areas are positioned within several hours drift of the spill source or from any portion of the mean oil trajectory. In this case evaluation of the environmental hazard would ideally have to make allowance even for very low probability, but appropriately directed wind configurations which could, in a very brief period, cause severe shoreline contamination.

At present no general procedures exist for the compact representation of the relative distribution of threat, short of the rather tedious, site-specific accumulation of hypothetical shoreline contamination statistics under applied actual or simulated synoptic wind fields.

For the purposes of the present report, simulations have been confined to wind configurations of moderate to high probability and little or no time dependence. It has been intended that these data will allow the reader to make his own estimates of oil movements under other specific, more complicated wind configurations. The procedure involved separate simulation of the oil flow at each site under:

a) time-independent, gentle (10 knot) and fresh (20 knot) winds from each of the four basic wind directions. The probability of each wind configuration may be evaluated from Table 3 which gives the breakdown of wind statistics over the years 1903 -1973 in a 2° latitude by 10° longitude area centered on the centerpoint of Lancaster Sound. These data were taken directly from the "Synoptic Meteorological Tables for the Canadian Arctic". The indicated distribution of wind direction and magnitude seems roughly consistent with land-based, near sea-level measurements obtained in 1977 near Cape Charles Yorke (FENCO, 1978). In this instance a single mid-range, $D = 10^6$ cm^2/s diffusivity value was used.

b) time dependent wind fields which were derived from the 1977 Cape Charles Yorke anemometer data and from geostrophic calculations utilizing the four times daily surface pressure charts produced by the Atmospheric Environment Service for two September, 1978 periods. The chosen windfields, plotted in Appendix B, correspond primarily to the predominant north, east and west wind configurations. The

TABLE 3 THE PERCENTAGE DISTRIBUTION OF WINDSPEEDS AND DIRECTIONS IN MARINE SQUARE II, ARCTIC CANADA

	Wind Speed (knots)				
Direction	<1	1-10	11-21	22-33	>34
Calm	6.9				
N		5.0	4.7	0.8	0.2
NE		4.5	5.6	2.1	0.6
E		6.1	6.7	4.8	0.7
SE		4.5	1.9	1.1	0.1
S		3.7	0.9	0.3	-
SW		3.9	3.4	0.7	-
W		8.9	8.4	1.9	0.1
NW		3.7	5.2	1.1	0.1

resulting slick movement simulations differ from those developed under (a) above, in their allowance for realistic variability in wind speed and direction and the possible uncertainty in diffusivity by including calculations for both the lower ($D = 2 \times 10^5$ cm^2/s) and upper ($D = 2 \times 10^6$ cm^2/s) limits of the estimated range of the diffusivity parameter.

5.2 Simulation Results and Discussion

Space limitations necessitated confinement of considerations of the simulation results primarily to those obtained under the steady-winds and mid-range diffusivity of case (a). Data were selected from the oil distributions computed for one day intervals in the seven day period following each blowout occurrence. For a given site, daily configurations were selected to illustrate significant steps in the movement of oil such as the initial drift, the first contamination of a given shoreline and changes in direction of the leading edge of the flow. An annotated map of the area with "squared off" coastal outlines is included in Figure 12 to assist the reader in the interpretation of the individual site simulations presented in Figures 13 - 16. The configurations in the latter figures are labelled according to, blowout site, wind direction, wind speed (kts), and time (days).

Thus the first diagram in Figure 13, labelled **1 N10-1,** corresponds to a site No. 1 blowout under a 10 knot northerly wind as viewed 1 day after the initial release of oil. A tabulation of the daily amounts and locations of shoreline oil accumulations follows each set of site simulations (Tables 4 - 7).

The main features of these results with respect to oil impact are summarized in the following paragraphs. General conclusions regarding the relative importance of wind and horizontal diffusion are addressed in Section 5.3 with a brief consideration of the simulation performed for the time-varying wind conditions of case (b).

5.2.1 Site No. 1. Over the seven day periods of the northerly wind simulations moderate accumulations of oil occurred along the western coastline of the Borden Peninsula. An increase in wind speed from 10 to 20 knots advanced the first arrival of oil from the fourth to the third day. Account must be taken of the fact that while the plotted configurations do not indicate impact on the eastern coast of Somerset Island such contamination undoubtedly occurred after oil crossed the southern boundary of our modelling area. Evidence for this assertion may be found in the drift buoy groundings which have occured in this area (Fissel and Marko, 1978). The stronger 20 knot winds increased the flow both across the boundary of the modelling grid and into the eastern half of the Inlet. This had the effect of producing a narrower, less concentrated, offshore flow of oil in western areas.

Easterly winds led to drastic pollution of northeastern Somerset Island. An increase in the strength of this wind moved the impact area northward along the coastline and, by decreasing the time between oil release and shoreline impact, allowed an increase in movement of less-weathered oil into shoreline areas.

West winds shifted pollution to the northern and northwestern ends of the Brodeur Peninsula. In this case heightened, 20 knot, winds appeared to actually lessen the oil impact by increasing the fraction which entered into the strong stream of easterly flow along the southern side of Lancaster Sound. It was seen that in this case, oil required four days to drift to a position north of the Borden Peninsula.

In the relatively low probability southerly wind case, the resulting pattern of oil spreading was seen to be strongly dependent upon wind speed. Thus for 10 knot winds a near- cancellation of the wind driven and residual current driven-flows occurred, leading to a large accumulation of oil immediately to the south of the blowout site. A slow leakage to the southwest touched the northeastern corner of Somerset Island with moderate amounts of oil roughly one week after blowout. On the other hand, under 20

TABLE 4 SHORELINE OIL ACCUMULATIONS IN BARRELS FOR SPILLS AT SITE NO. 1. Time is recorded in days since the surface-spreading of oil and locations of contaminated shore points are given according to the grid of Figure 2.

Site No. 1	Daily Accumulation (Barrels)					
	Day 2	Day 3	Day 4	Day 5	Day 6	Day 7
West Brodeur Peninsula (44,6 - 7) Wind-North, 10 kts			70	520	860	1264
West Brodeur Peninsula (43,7-8)(44,6-7)(45,5) (46,1) Wind-North, 20 kts		339	614	755	958	962
East Somerset Island (50,9-10)(51,8)(52,6-7) Wind-East, 10 kts		850	2685	4653	6283	8771
East Somerset Island (50,9-10)(51,8)(52,6-7)	253	2008	4353	5739	8133	9899
North Somerset Island (50,12) Wind-East, 20 kts					23	118
West Brodeur Peninsula (38,10-11)(39-40,10)			630	1455	2308	3587
East Brodeur Peninsula (35-36,11) Wind-West, 10 kts					109	109
West Brodeur Peninsula (38,10-11)(39-40,10)		269	530	1221	1842	2222
East Brodeur Peninsula (35-36,11) Wind-west, 20 kts		27	67	74	81	136
East Somerset Island (50,9-11)(51,8) Wind-South, 10 kts				136	460	1088
West Devon Island (45-46,26)(47,19-21) Wind-South, 20 kts	372	2452	4016	6138	9024	10368

TABLE 5 SHORELINE OIL ACCUMULATIONS IN BARRELS FOR SPILLS AT SITE NO. 2. Time is recorded in days since the surface-spreading of oil and locations of contaminated shore points are given according to the grid of Figure 2.

Site No. 2	Daily Accumulations (Barrels)						
	Day 1	Day 2	Day 3	Day 4	Day 5	Day 6	Day 7
West Borden Peninsula (26,8-9)(27,8) Wind-North, 10 kts		1345	4068	6366	9004	11522	13764
West Borden Peninsula (26,8-9)(27,8) Wind-North, 20 kts	68	2467	4913	7591	10227	12822	15566
East Borden Peninsula (25-26,9) Wind-East, 10 kts		153	1534	2945	4975	6732	8422
East Borden Peninsula (25-26,9)(28,8)			8	24	130	141	168
East Brodeur Peninsula (32,9)(33,8) Wind-East, 20 kts			568	1029	2009	3101	4153
Mid-Devon (32-34,19) Wind-South, 20 kts			1730	3408	4966	6493	8297

TABLE 6 SHORELINE OIL ACCUMULATIONS IN BARRELS FOR SPILLS AT SITE NO. 3. Time is recorded in days since the surface-spreading of oil and locations of contaminated shore points are given according to the grid of figure 2.

Site No. 3	Daily Accumulations (Barrels)						
	Day 1	Day 2	Day 3	Day 4	Day 5	Day 6	Day 7
Cape Hay (15-16,9) Wind-North, 10 kts		1438	3972	6614	9462	11756	14513
Cape Hay (15-16,9)	22.6	1751	4014	6602	9002	11455	14000
Bylot Island, except Cape Hay (17,9) Wind-North, 20 kts		665	1318	1705	2038	2670	3018
Cape Hay (13-14,8)(15-16,9) Wind-East, 10 kts			578	1125	2462	3741	5063
Cape Hay (13-14,8)(15-16,9)				136	531	754	1162
Bylot Island except Cape Hay (17,9) Wind-East, 20 kts			3.9	3.9	4.6	44	82
East Devon Island (17-18,19) Wind-South, 20 kts					1.8	7	14.7

TABLE 7 SHORELINE OIL ACCUMULATIONS IN BARRELS FOR SPILLS AT SITE NO. 4. Time is recorded in days since the surface-spreading of oil and locations of contaminated shore points are given according to the grid of Figure 2.

	Daily Accumulations (Barrels)					
Site No. 4	Day 2	Day 3	Day 4	Day 5	Day 6	Day 7
East Devon Island (17,19)		206	356	689	689	703
Bylot Island (15-16,9)(13-14,8) Wind-East, 10 kts					13.6	212
East Devon Island (17,19) Wind-East, 20 kts	709	2240	3538	5574	7281	8419
East Devon Island (17,19-22) Wind-South, 10 kts				899	1938	2940
Philpots Island (14,23-24) Wind-South, 20 kts	61	1751	3296	5010	6514	8541

knot southerly winds, the Devon Island coastline is inundated near Maxwell Bay roughly two days after blowout. It should be noted, however, that this particular simulation is suspect because of the very weak data base underlying the residual current grid assumed for northwestern Lancaster Sound.

A reassuring aspect of the simulations is the apparent absence of impact on the Prince Leopold Island shore because of the strong easterly flows in this area (this land feature is not included in the map outlines of Figures 2 and 13, but its position is indicated in Figure 1).

5.2.2 Site No. 2. In evaluating the flow of oil from Site No. 2 it should be noted that the water depth in this case is significantly less than the 400 m value associated with strong gas hydrate formation in laboratory experiments. Therefore, the possibility remains that a smaller initial spread of the rising oil column will occur. However, in view of the conservative nature of the initial 5 km^2 patch size of the modelling scheme, no special shallow water corrections were made at any of the blowout sites.

The north wind configuration at Site No. 2 gave the second highest level of shoreline pollution obtained in any of the simulations. Both the 10 and 20 knot winds moved the oil to the southeast and directly onto the northwestern corner of the Borden Peninsula. Major volumes of oil arrived in this area roughly one and a half days after the blowout.

Ten knot east winds led to contamination in almost the same area of the Borden Peninsula affected by north winds, with roughly a one day further delay in oil arrival. The 20 knot east winds on the other hand produced a major change in the oil distribution leading to contamination of the Brodeur Peninsula and almost certain introduction of oil into the Admiralty Inlet ecosystem.

Mild west winds led to moderate accumulations of oil along the northern shore of the Borden Peninsula and after 4 days, in the Cape Hay area at the northeastern corner of Bylot Island. The main portion of the oilstream in this case eventually broke away from the Bylot Island coastline and entered Baffin Bay. An increase of the west wind to 20 knots, as in the case of Site No. 1, tended to sweep oil out of Lancaster Sound by passing most land areas (a small amount of oil came ashore at Cape Hay).

Southerly winds at this site again brought oil to the Devon Island coastline. In the case of the lower wind value, nearly 7 days was required for contact compared to a 2 day delay in the 20 knot case. However, the paucity of current data on the north side of Lancaster Sound again strongly undermines confidence in the predicted contamination patterns.

5.2.3 **Site No. 3.** North winds at this site moved the released oil directly, with a one or at most 2 day delay, onto the shoreline of northeastern Bylot Island and particularly in the Cape Hay region. According to the simulation, no significant amounts of oil managed to escape into the eastward moving current and hence into Baffin Bay.

Mild, 10 knot easterly winds tended to give more moderate pollution levels in the same Cape Hay region with only a small amount of oil (see day 6 configuration) moving to the east and northeast and into the Baffin Bay flow stream. Twenty knot easterly winds built up large concentrations of oil offshore, north of Navy Board Inlet before contaminating the Cape Hay area with relatively moderate amounts some five days after blowout.

West winds at this site were, as usual, protective of coastline areas and oil remained well offshore on a rather direct trajectory into Baffin Bay.

Under southerly winds our simulated oil flows took the form of counter-clockwise gyres reaching almost to the southeastern Devon Island coastline. Measurable contamination levels were recorded only for the twenty knot wind case.

5.2.4 Site No. 4. Under 10 knot northerly winds the major portion of oil from this site moved south and then east-southeast into Baffin Bay, following the east coast of Bylot Island some 10 to 15 nautical miles offshore. However, some oil parcels did continue directly south to approach the Bylot Island coast to the east of Cape Hay in day 7. Under 20 knot northerly winds, the oil trajectory followed the east Bylot Island coastline very closely, although, no contacts were recorded.

East winds moved oil into eastern Lancaster Sound where it followed the basic pattern of movement observed in Site No. 3 results. En route, however, oil did come ashore near Cape Sherard at the southeastern corner of Devon Island. Contamination was particularly prompt (day 2) and intense (8400 barrels by day 7) under the 20 knot winds configurations.

West winds both mild and fresh moved oil directly to the east and away from land areas.

Ten knot southerly winds brought oil slowly (day 5) but heavily to the Devon Island shoreline south of Philpots Island. An increase in windspeed to 20 knots led to a quicker and equally heavy contamination of the latter island.

5.3 Additional Simulations

As previously indicated, simulations were also performed for the temporally and spatially varying windfields plotted in Appendix B. These fields were extracted from real meteorological data to approximate typical surface conditions of the summer-fall period. The changes in directionality, with time, in any of the three basic (north, east, west) wind fields were relatively small, leaving wind speed as the major time-varying parameter.

Simulations were performed for each of the two extreme diffusivity values, $D = 2 \times 10^5$ cm^2/s and $D = 2 \times 10^6$ cm^2/s, to allow later assessments of the magnitude relating to the horizontal diffusion term of Equation 2.

By and large, these simulations reproduced the trajectories of the corresponding time-independent wind cases of 5.2. Additionally, however, the varying winds produced wider surface dispersals of oil particularly in areas having large spatial gradients in the residual current field.

The wholesale inclusion of data from these simulations would be impractical and redundant. Instead treatment of these results was confined to a few comparisons of simulated oil configurations which illustrate the significance of time-dependence and the diffusivity parameter.

To these points, the configurations in Figure 17a, b which correspond respectively to the low and high diffusivity day 5 distributions of oil flowing from Site No. 4 under a variable westerly wind are considered. The spatial extent of the slick even in the low diffusivity ($D = 2 \times 10^5$ cm^2/s) case exceeded that previously calculated (see Figure 16) for the steady 10 knot wind case with $D = 10^6$ cm^2 /s. This is the result of the complicated residual current field in the vicinity of the blowout site which, under changing wind conditions, acts to scatter the individual slicks. Nevertheless, a tenfold enhancement in diffusivity (Figure 17b) had visible effect in terms of a broader, more uniform distribution of oil.

The role of diffusivity in determining the predicted spatial extent of shoreline pollution is illustrated in the pair of configurations represented in Figure 18a, b. These are respectively associated with the low and high diffusivity patterns four days after a blowout at site No. 2. The strong relationship which is evident between the assumed diffusivity and the predicted length of affected coastline suggests a possible test for the appropriate value(s) of the former parameter utilizing, in lieu of oil, the beaching locations of released oil spill follower buoys.

5.4 Oil Trajectories in Ice

The restriction of the simulation techniques to ice-free surface conditions may, in fact, be relaxed to allow the inclusion of situations where drifting ice is present in low overall (less than 3/10) concentrations and in accumulations comparable to or smaller than the size of our 25 square nautical mile modelling grid.

On the other hand, landfast ice growth along shorelines and/or over major portions of the surfaces of major water bodies such as Prince Regent Inlet, Barrow Strait and Lancaster Sound significantly alters the details of oil pollutant transport in these areas. In this case there is ample evidence (Milne and Smiley, 1977; Sahota et al, 1978) that oil tends to accumulate beneath and gradually become incorporated into the ice cover. There is, as a result, an effective identity between the large scale movements of oil and the host ice pack.

Modelling oil movements in the heavy ice concentrations of Lancaster Sound and Prince Regent Inlet is complicated by the questionable utility of "mean" ice

movements in these areas. As detailed elsewhere (Marko, 1978), the major event of the winter surface of eastern Parry Channel is the formation of a stable boundary extending roughly north-south across the Channel separating landfast ice on its west from spasmodically drifting ice to its east. The position of this boundary ranges from western Barrow Strait (near Griffith Island) to the eastern end of Lancaster Sound (near Cape Warrender). This year to year variability produces drastic changes in the mean winter and spring ice velocities in the areas of most potential blowout sites.

Average fall to spring ice velocities obtained from 4 years of satellite data (Marko, 1978) are sketched in Figure 19 for the major zones of eastern Parry Channel. These velocities are not true indicators of the average motion in that they were compiled specifically during periods of visible motion and hence do not properly reflect the considerable fraction of time during which ice conditions are largely static. As indicated above, ice movements are spasmodic in nature being triggered, at least in part, by the prior or present occurrence motion differs dramatically from the residual current grid deduced under low or negligible ice coverages. Movement is confined to the east-west long axis of Parry Channel and there is no evidence of net westerly motion anywhere in Lancaster Sound. The current structures and large scale turbulence evident in summer surface water data are not visible in a concentrated ice cover. In the absence of accompanying under-ice current measurements, it is impossible to assess whether this represents an alteration of the wintertime residual current flows or is merely a damping effect induced by the ice cover.

In any case a much simpler model of oil movements under heavy ice conditions is possible corresponding to an almost spatially uniform (allowance can be made for the observed south to north fall off in mean drift velocity) eastward drift in areas both east of the cross-channel landfast ice boundary and outside the shoreline-hugging landfast ice zones. Nevertheless, traditional models of sea ice motion (e.g. Neralla et al (1977)) relating ice and wind velocities through a simple scaling factor and rotation are not likely to be directly applicable under the required conditions of strong confinement and with the likelihood of thresholds associated with motion in a continuously refreezing ice cover.

The necessary linkage of ice and wind motions can be established only on the basis of actual comparisons of ice movements with local surface wind values. Ice drift data are now readily available from satellite imagery and/or satellite-monitored drift stations. Unfortunately, corresponding sources of local surface wind data are not

currently available. As a result no quantitative modelling of oil drift in heavy ice was attempted in the present study.

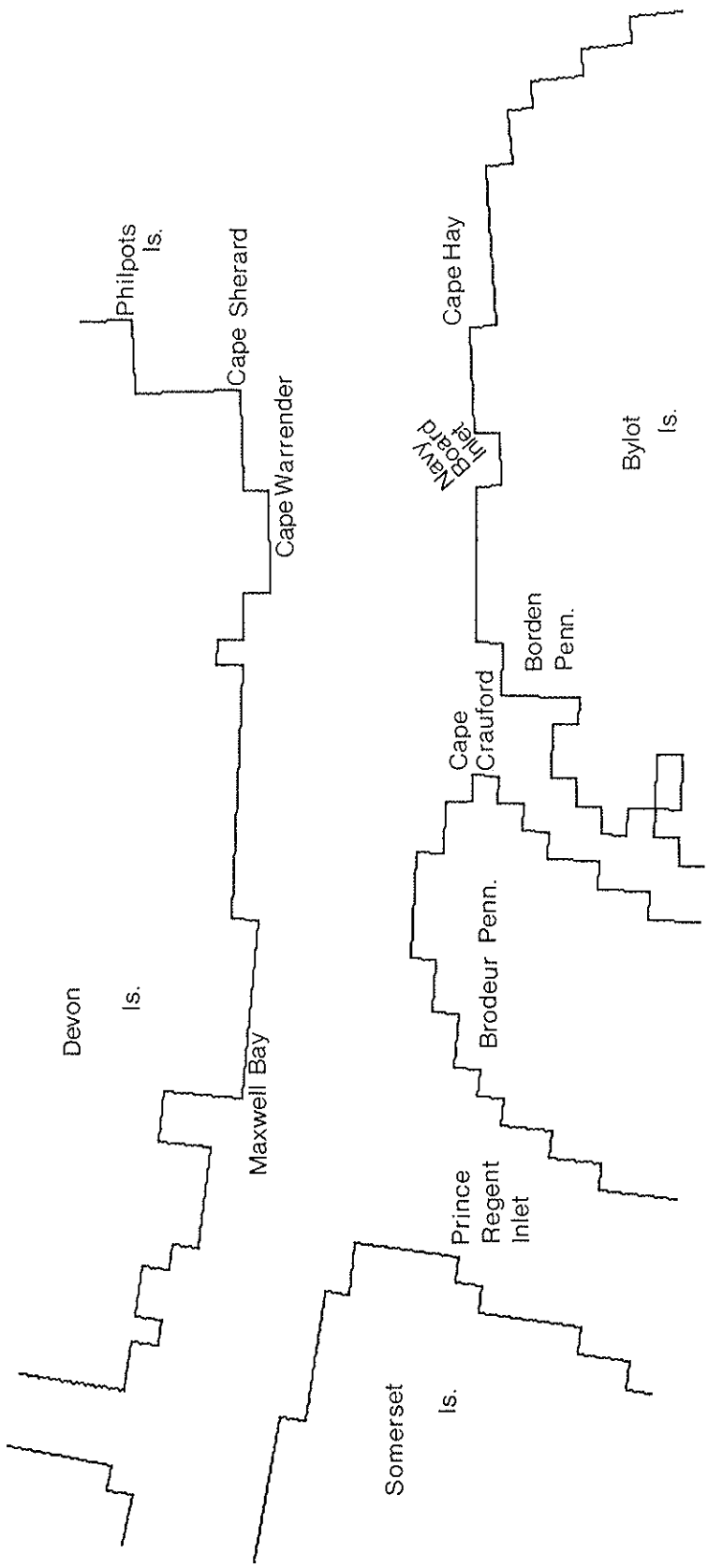

FIGURE 12 AN ANNOTATED VERSION OF THE SQUARED-OFF COASTLINE MAP USED IN ALL SIMULATIONS

13 a) 1 N 10-1 - Site one; Blowout under 10 knot northerly wind; viewed one day after release of oil

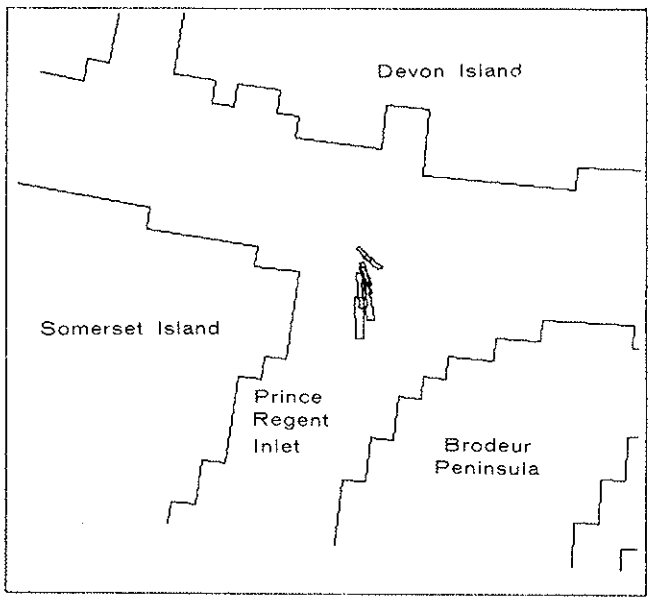

13 b) 1 N 10-3 - Site one; Blowout under 10 knot northerly wind; viewed three days after initial release of oil.

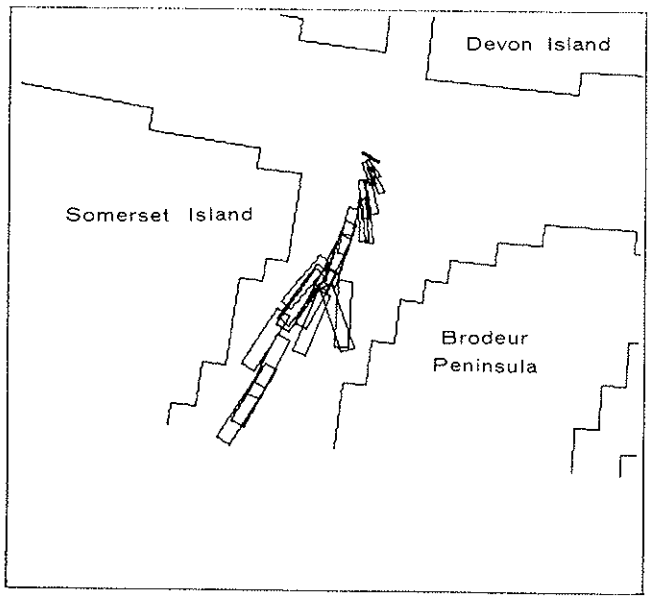

FIGURE 13 SCENARIOS OF OIL DRIFT IN THE AREA OF A SITE NO. 1 BLOWOUT UNDER TIME-INDEPENDENT NORTH, EAST, WEST AND SOUTH WINDS

13 c) 1 N 10-7 - Site one; Blowout under 10 knot northerly wind; viewed seven days after initial release of oil.

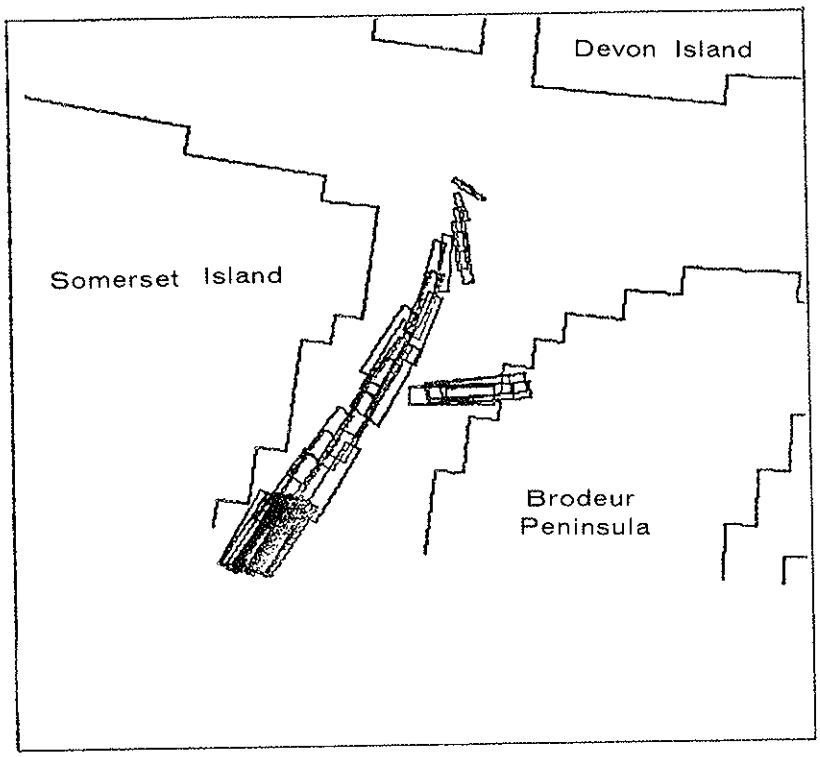

13 d) 1 N 20-1 - Site one; Blowout under 20 knot northerly wind; viewed one day after initial release of oil.

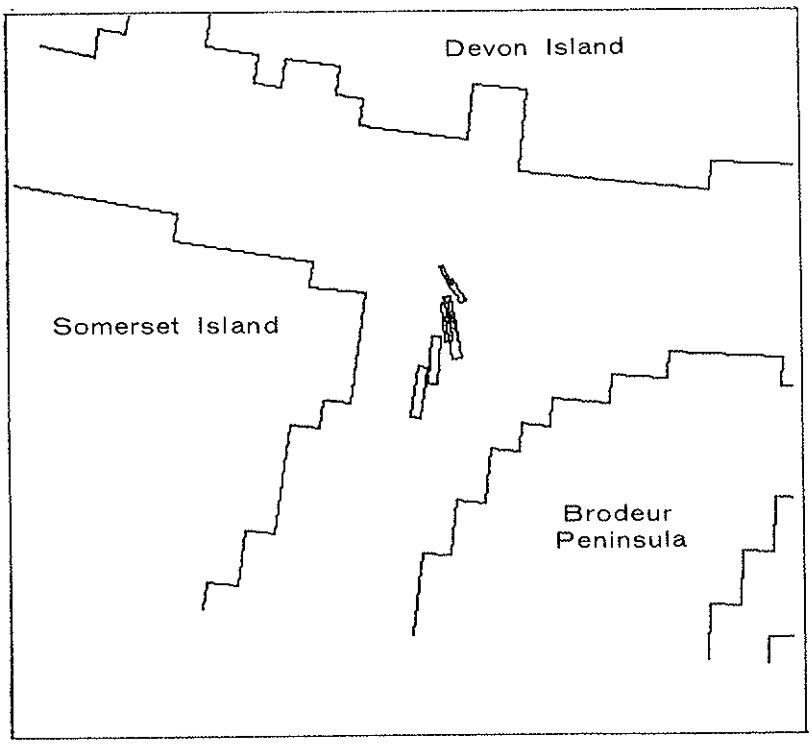

13 e) 1 N 20-3 - Site one; Blowout under 20 knot northerly wind; viewed three days after initial release of oil.

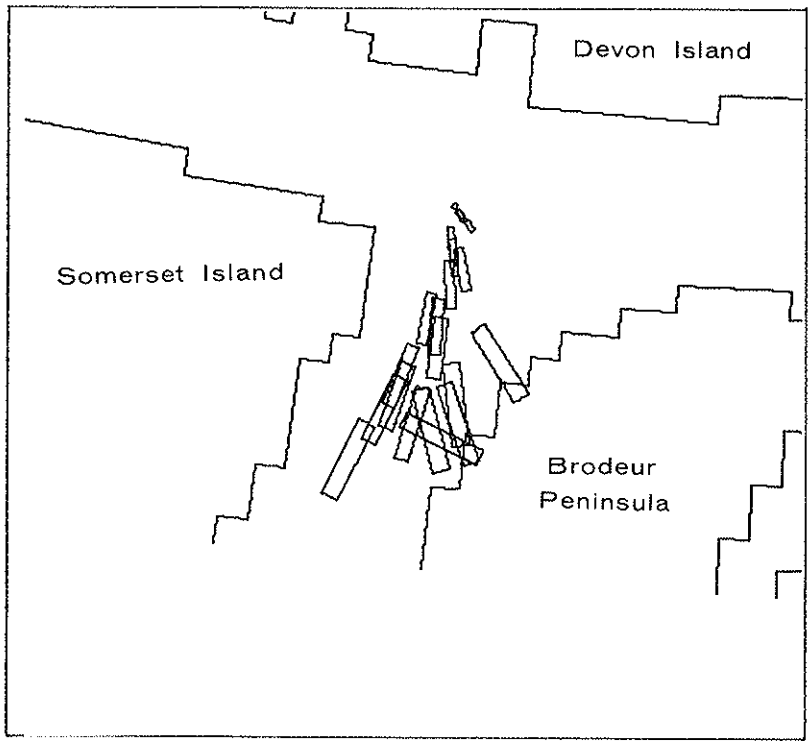

13 f) 1 N 20-5 - Site one; Blowout under 20 knot northerly wind; viewed five days after initial release of oil.

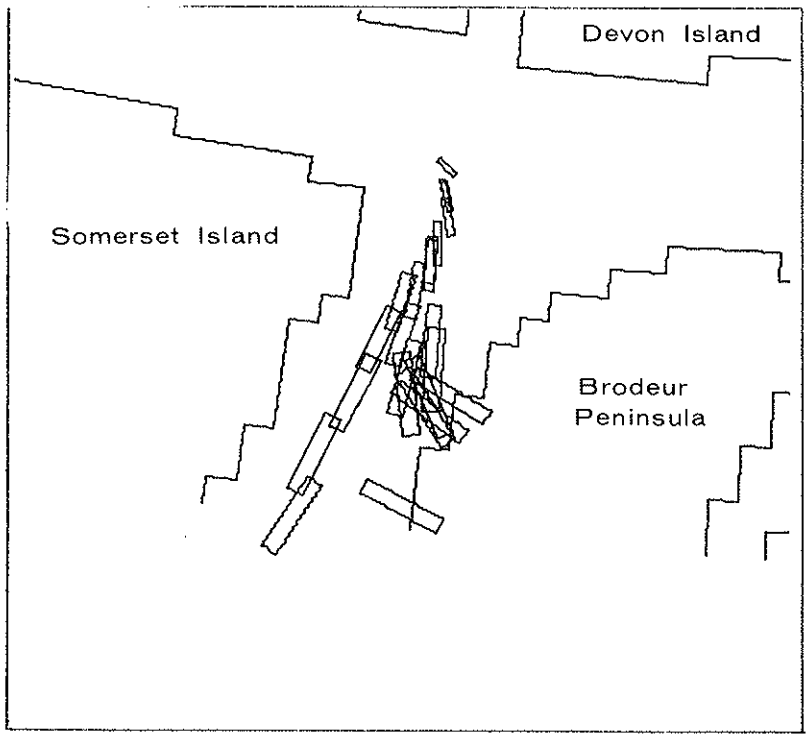

13 g) 1 E 10-2 - Site one; Blowout under 10 knot easterly wind; viewed two days after initial release of oil.

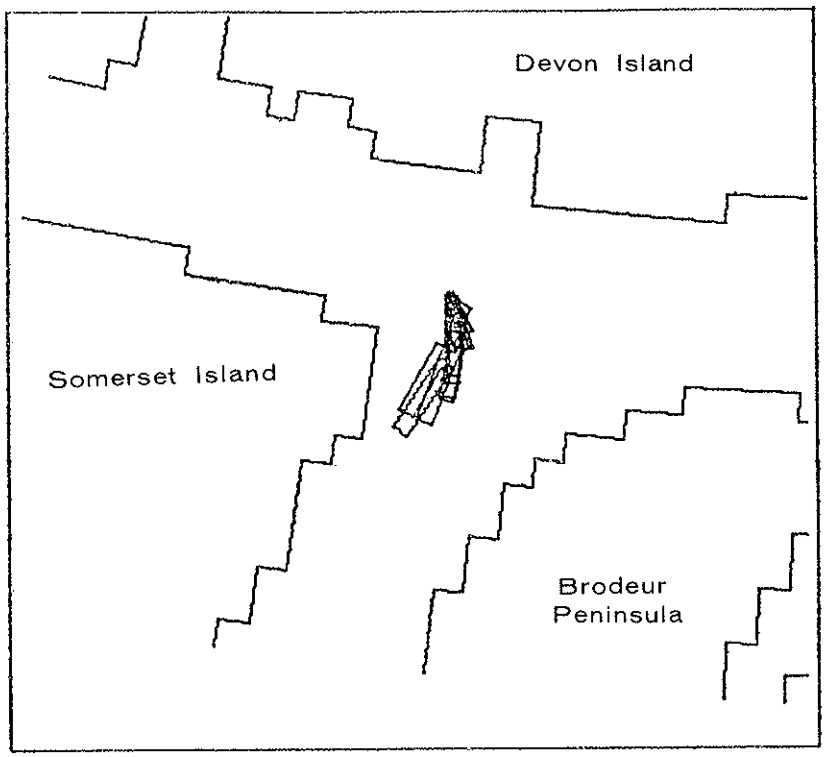

13 h) 1 E 10-3 - Site one; Blowout under 10 knot easterly wind; viewed three days after initial release of oil.

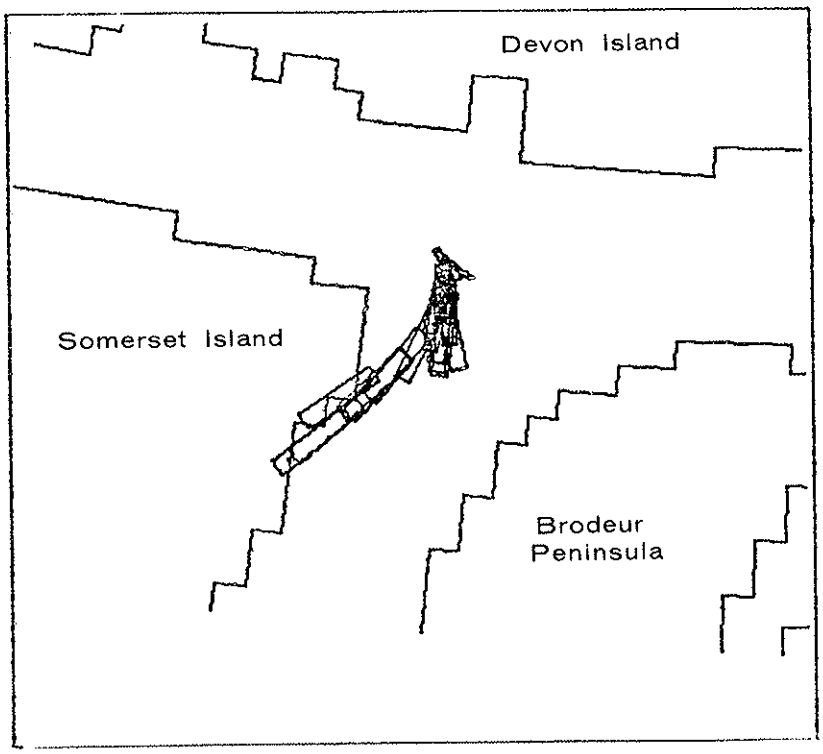

13 i) 1 E 10-7 - Site one; Blowout under 10 knot easterly wind; viewed seven days after initial release of oil.

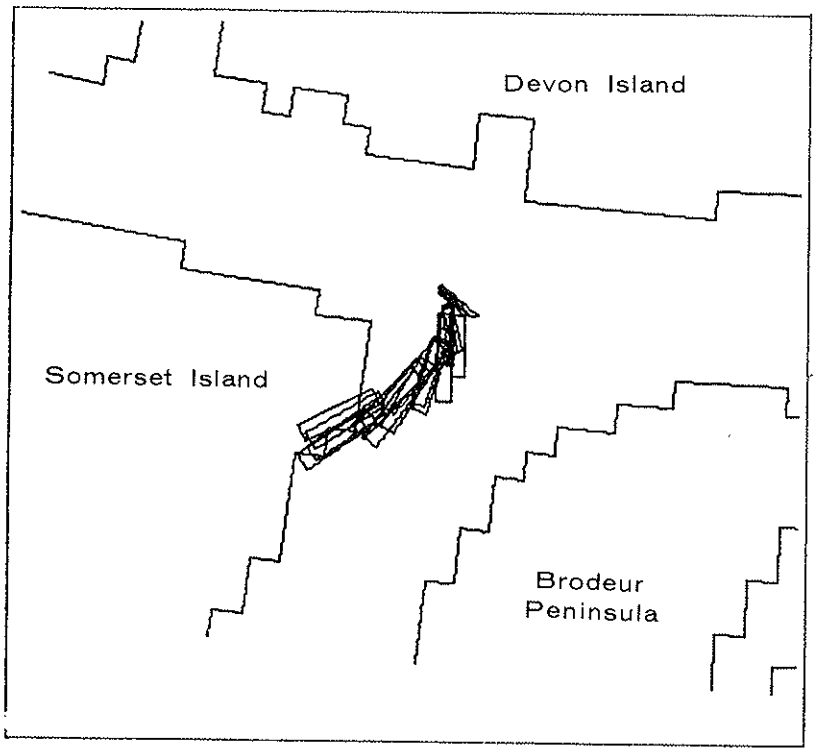

13 j) 1 E 20-2 - Site one; Blowout under 20 knot easterly wind; viewed two days after initial release of oil.

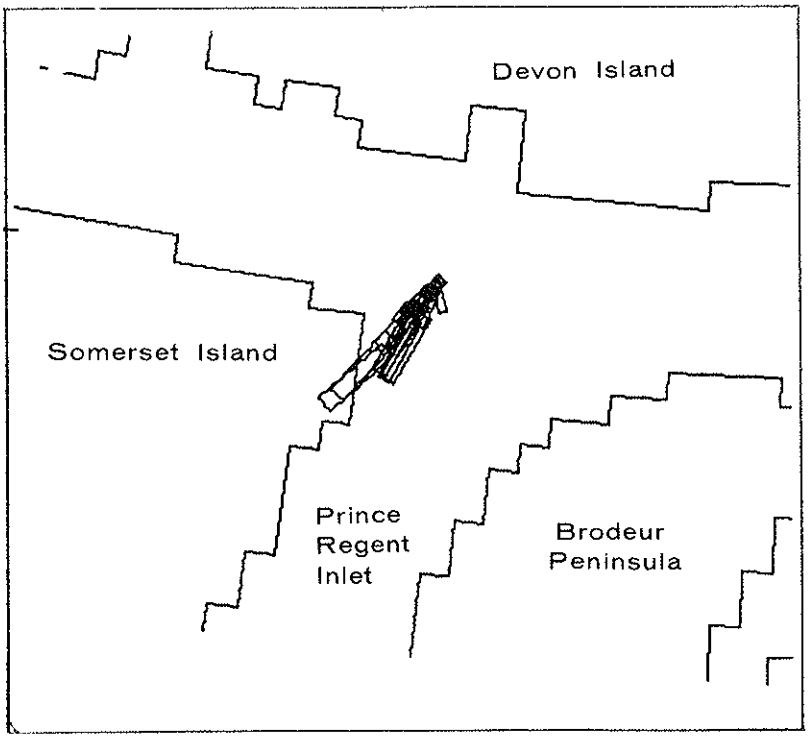

13 k) 1 E 20-4 - Site one; Blowout under 20 knot easterly wind; viewed four days after initial release of oil.

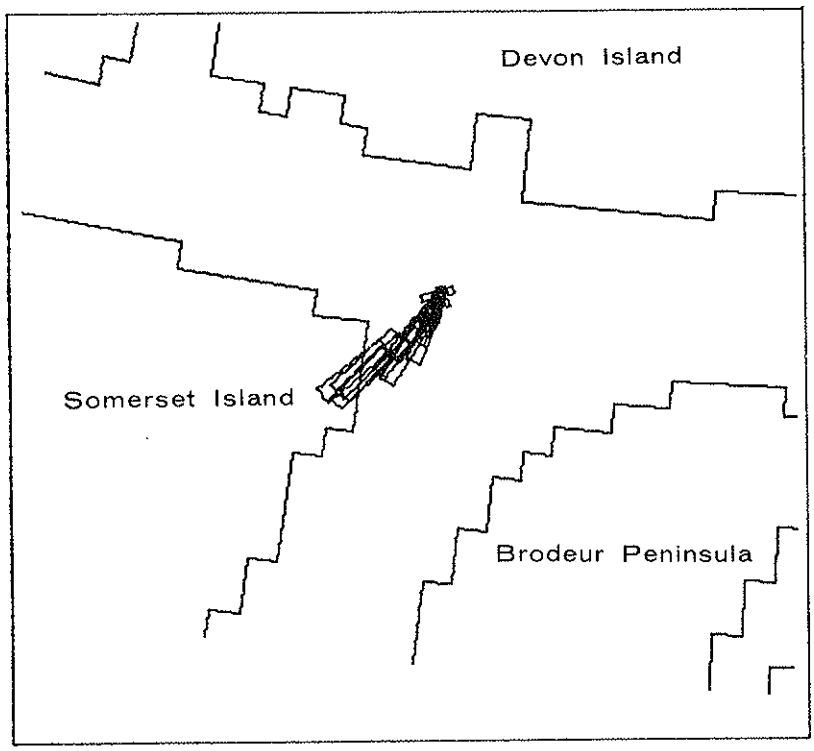

13 l) 1 W 10-1 - Site one; Blowout under 10 knot westerly wind; viewed one day after initial release of oil.

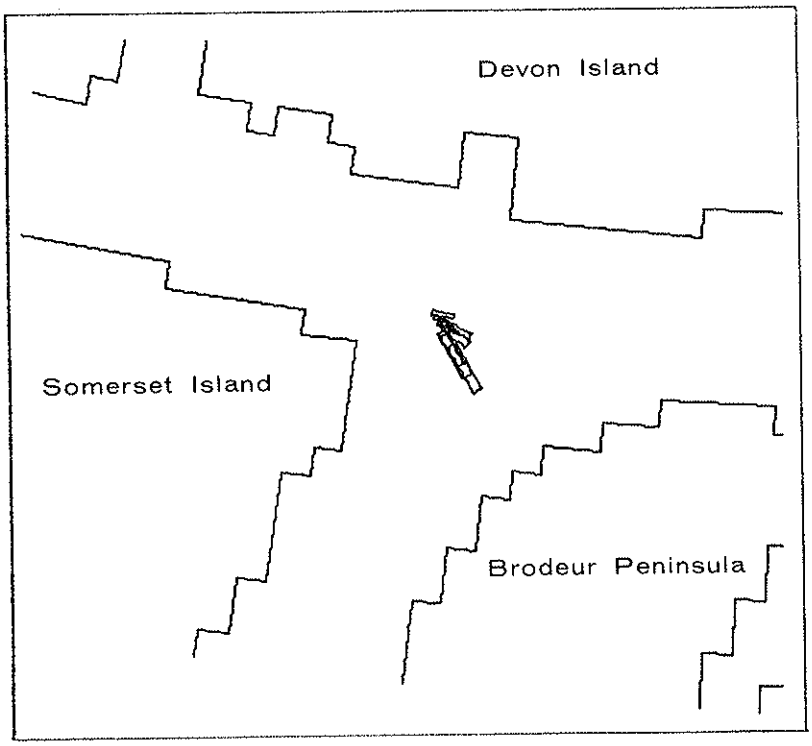

13 m) 1 W 10-3 - Site one; Blowout under 10 knot westerly wind; viewed three days after initial release of oil.

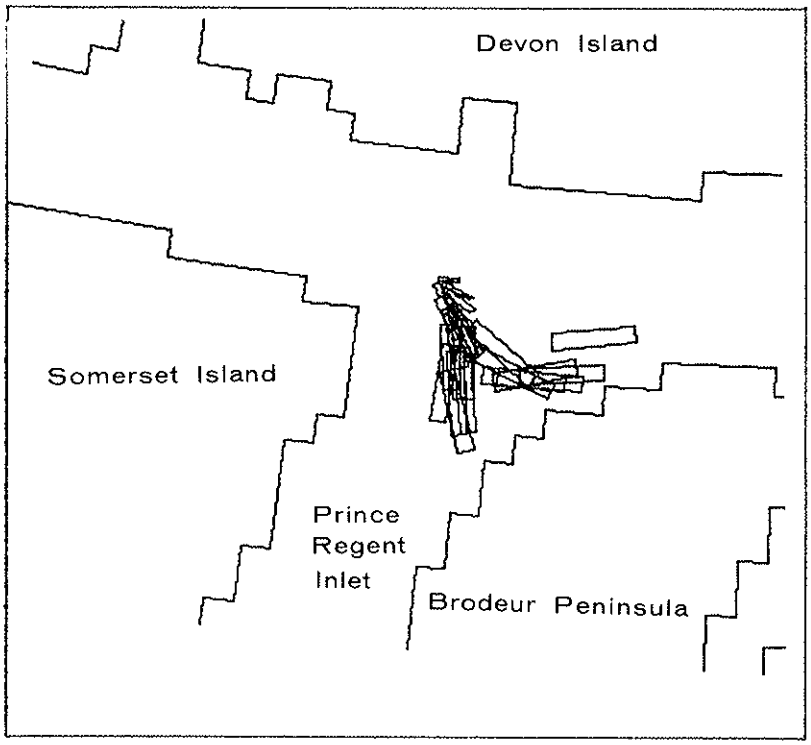

13 n) 1 W 10-6 - Site one; Blowout under 10 knot westerly wind; viewed six days after initial release of oil.

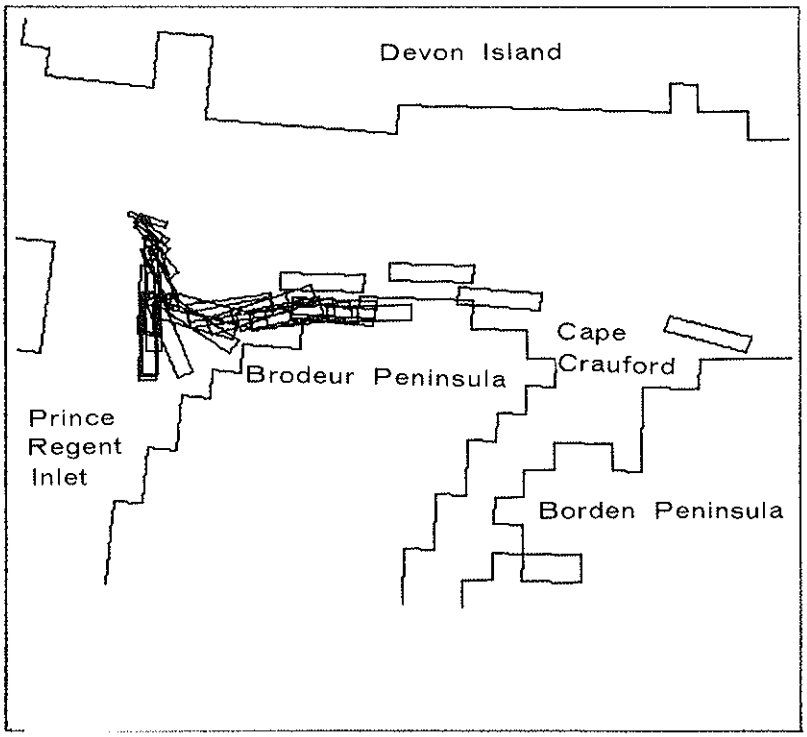

13 o) 1 W 20-2 - Site one; Blowout under 20 knot westerly wind; viewed two days after initial release of oil.

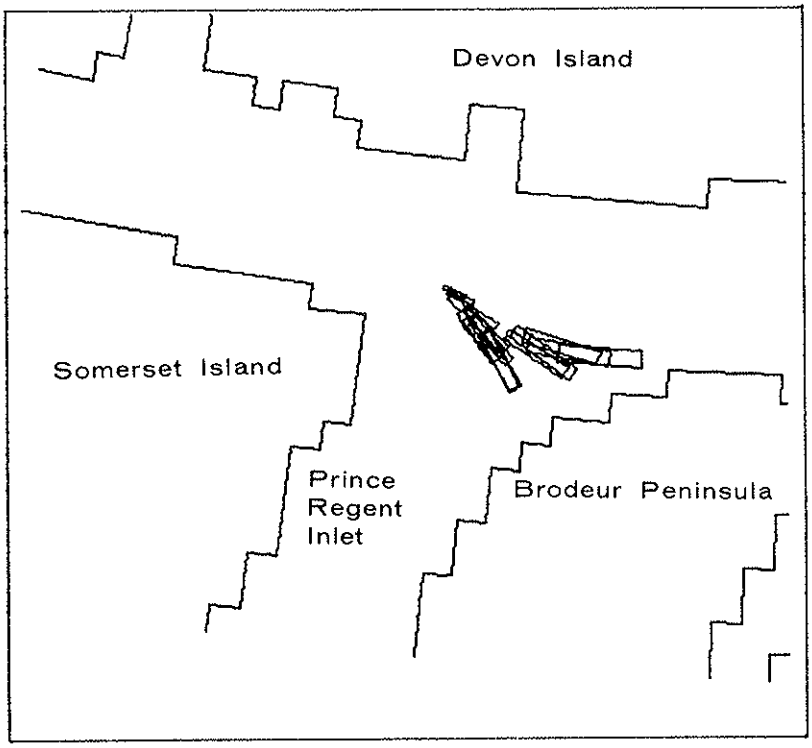

13 p) 1 W 20-4 - Site one; Blowout under 20 knot westerly wind; viewed four days after initial release of oil.

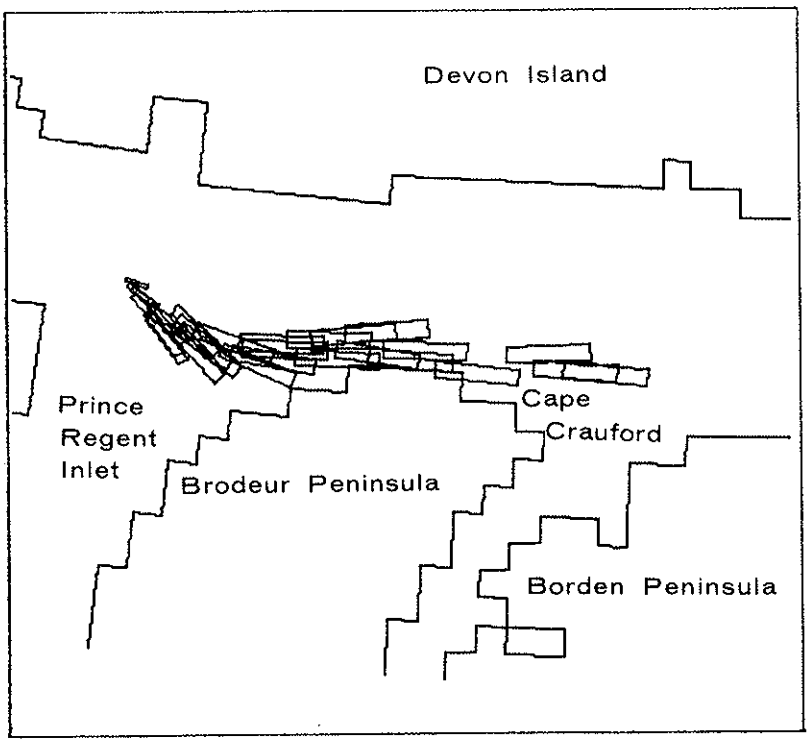

13 q) 1 W 20-5 - Site one; Blowout under 20 knot westerly wind; viewed five days after initial release of oil.

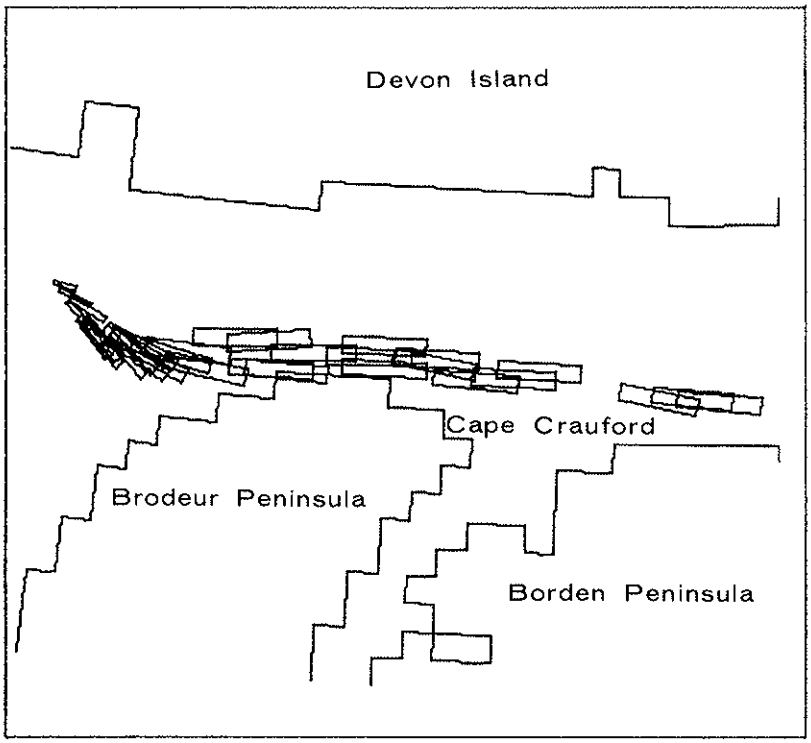

13 r) 1 S 10-1 - Site one; Blowout under 10 knot southerly wind; viewed one day after initial release of oil.

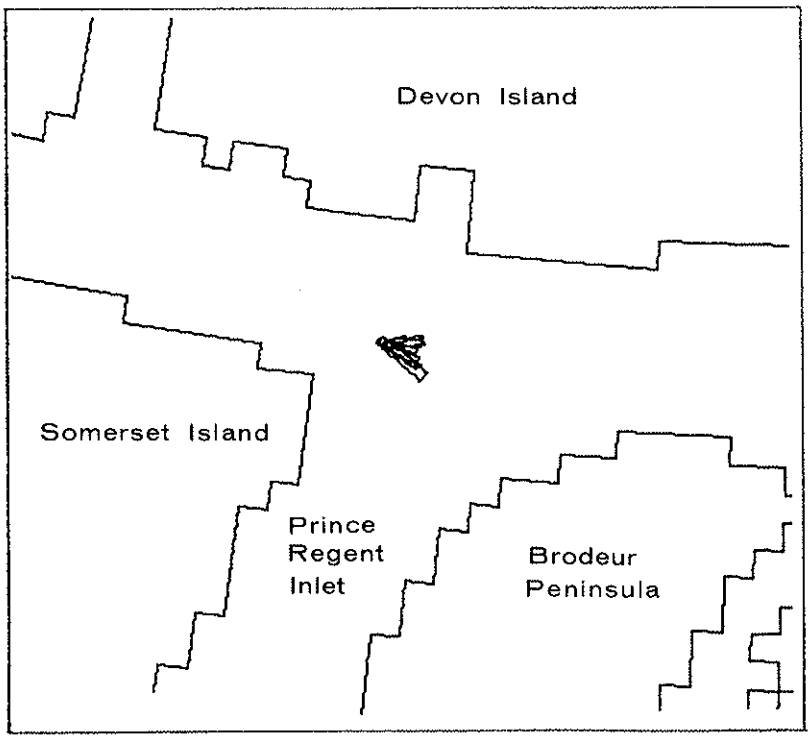

13 s) 1 S 10-4 - Site one; Blowout under 10 knot southerly wind; viewed four days after initial release of oil.

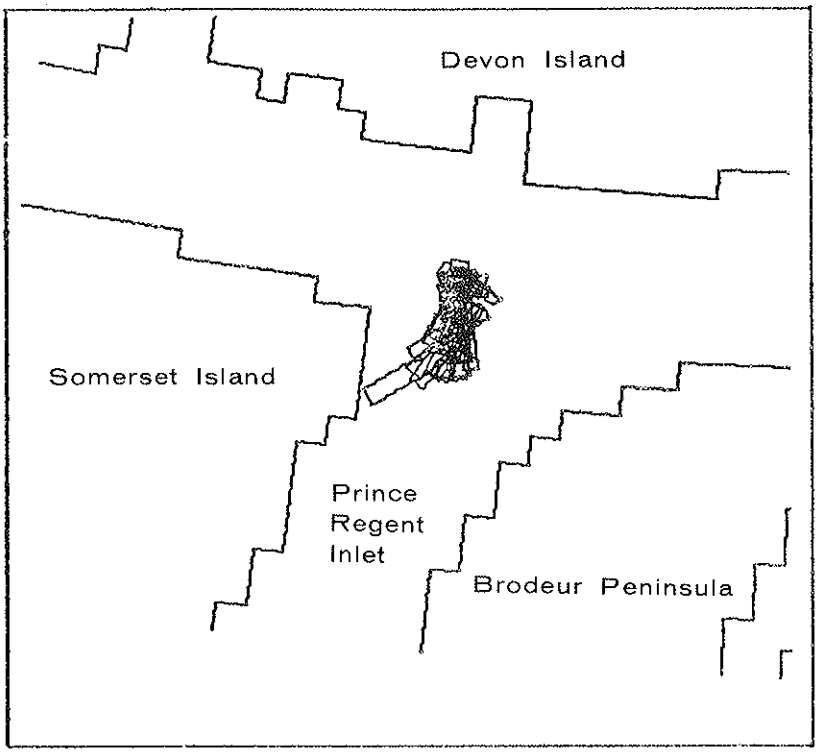

13 t) 1 S 10-6 - Site one; Blowout under 10 knot southerly wind; viewed six days after initial release of oil.

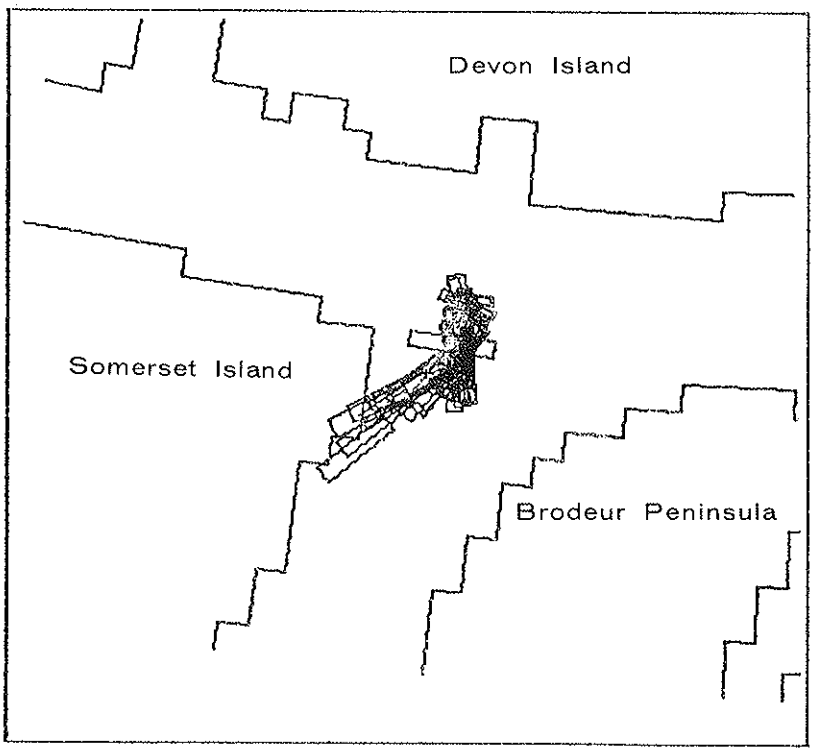

13 u) 1 S 20-1 - Site one; Blowout under 20 knot southerly wind; viewed one day after initial release of oil.

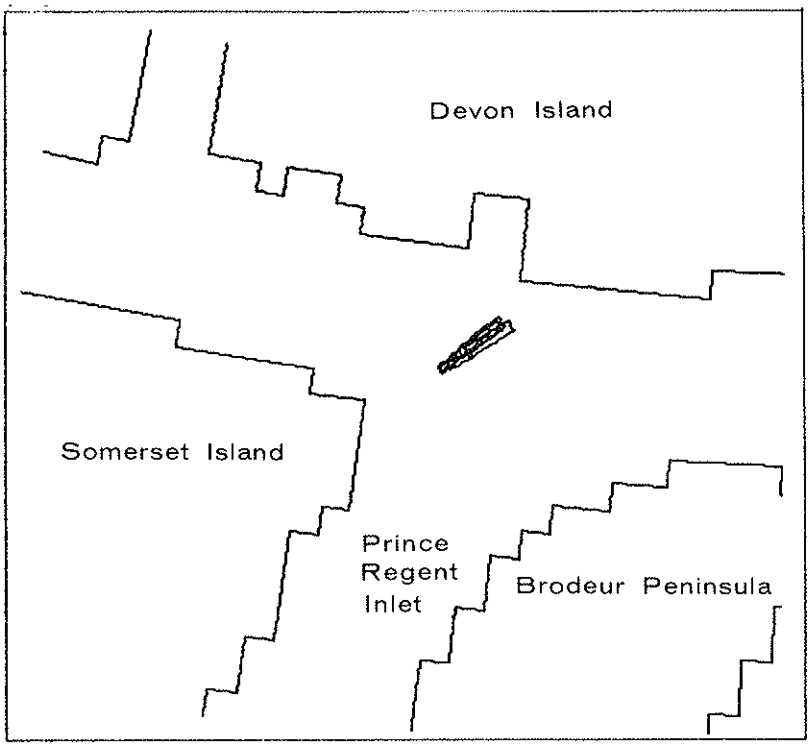

13 v) 1 S 20-2 - Site one; Blowout under 20 knot southerly wind; viewed two days after initial release of oil.

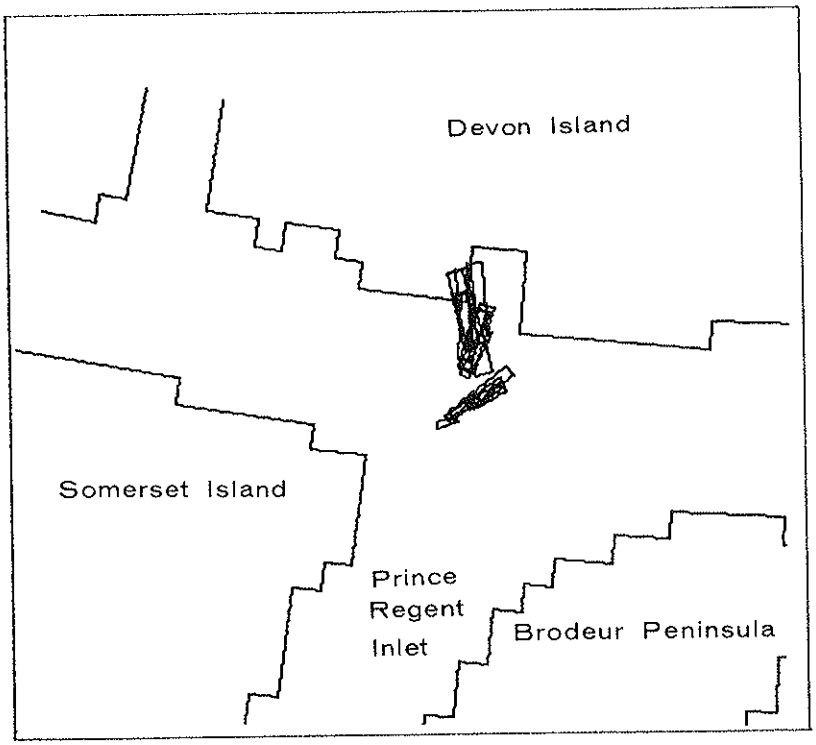

13 w) 1 S 20-7 - Site one; Blowout under 20 knot southerly wind; viewed seven days after initial release of oil.

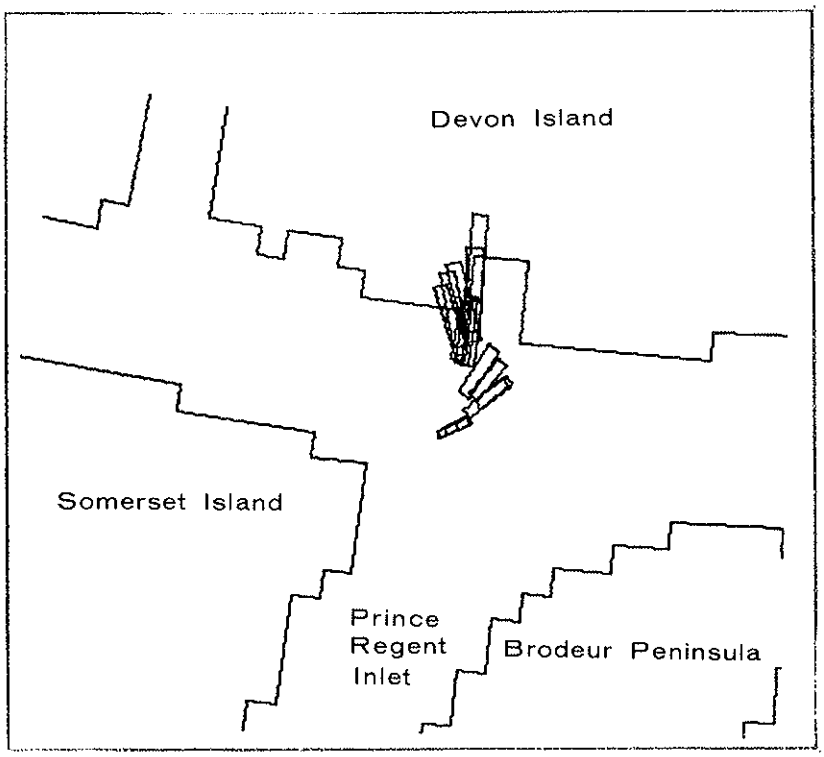

14 a) 2 N 10-1 - Site two; Blowout under 10 knot northerly wind; viewed one day after initial release of oil.

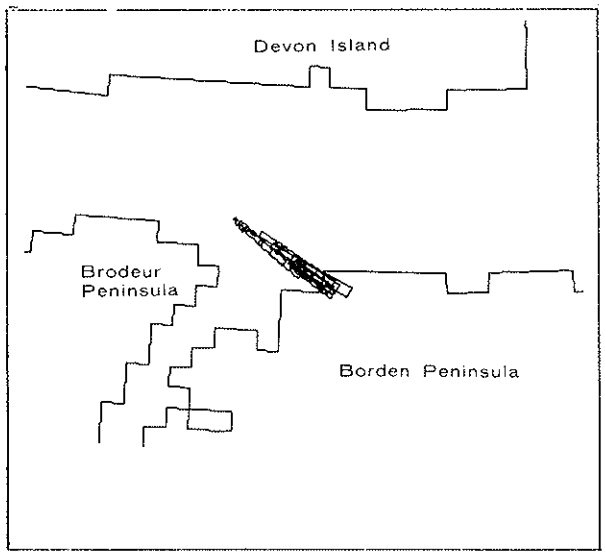

14 b) 2 N 10-2 - Site two; Blowout under 10 knot northerly wind; viewed two days after initial release of oil.

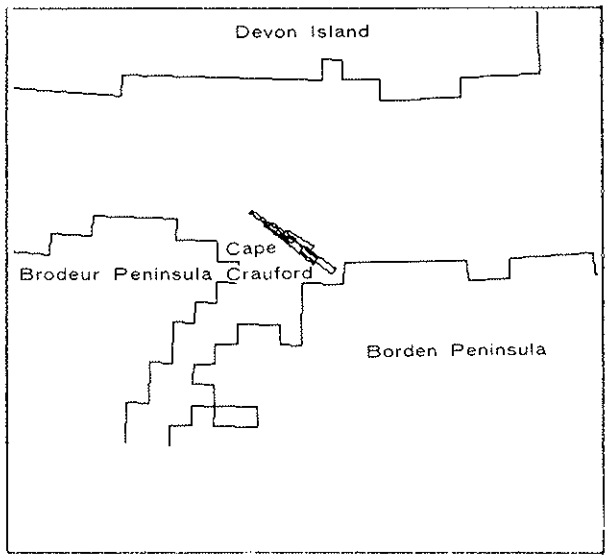

FIGURE 14 SCENARIOS OF OIL DRIFT IN THE AREA OF A SITE NO. 2 BLOWOUT UNDER TIME-INDEPENDENT NORTH, EAST, WEST AND SOUTH WINDS.

14 c) 2 N 20-1 - Site two; Blowout under 20 knot northerly wind; viewed one day after initial release of oil.

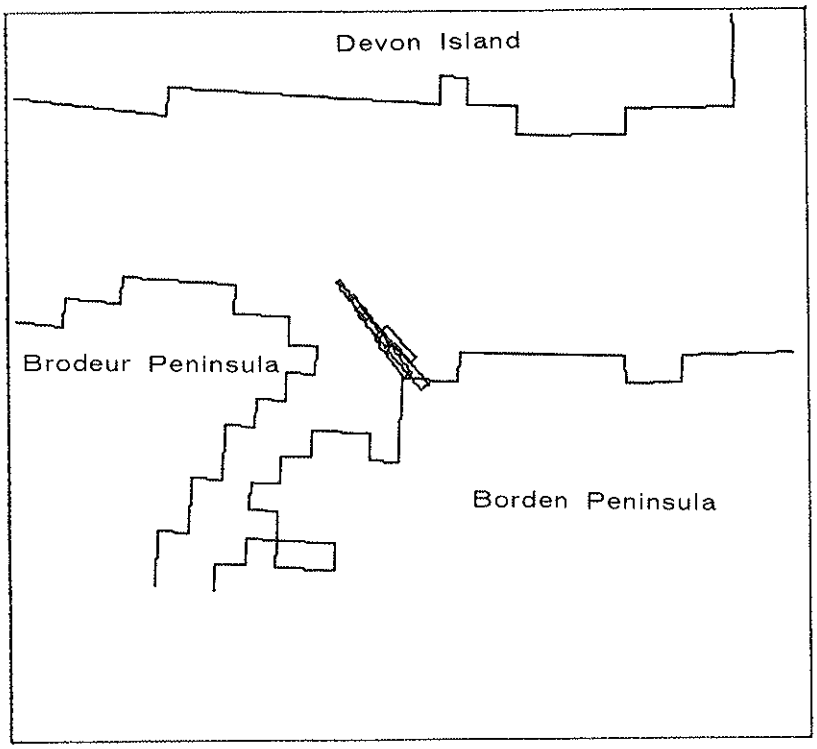

14 d) 2 E 10-2 - Site two; Blowout under 10 knot easterly wind; viewed two days after initial release of oil.

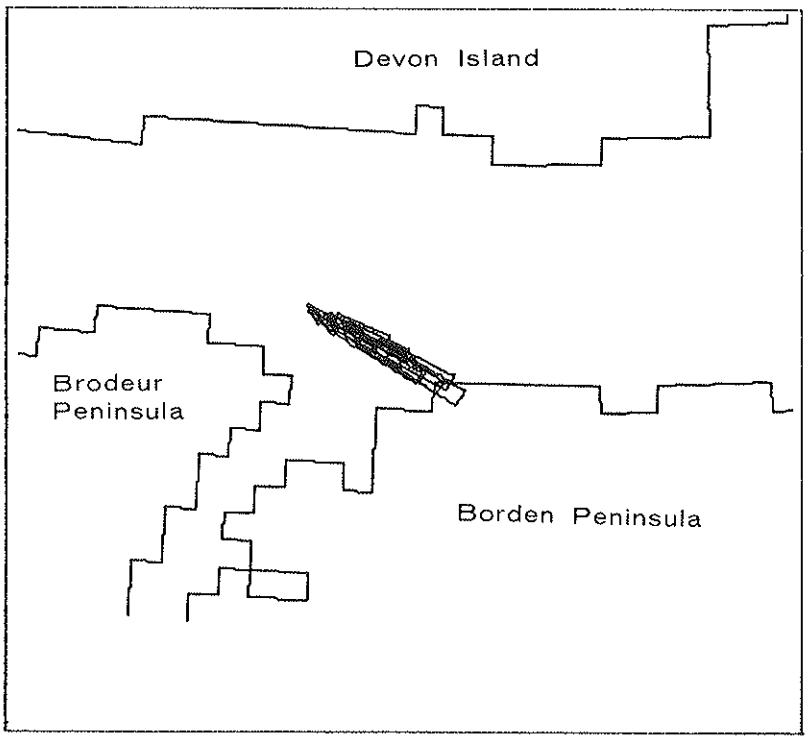

14 e) 2 E 20-2 - Site two; Blowout under 20 knot easterly wind; viewed two days after initial release of oil.

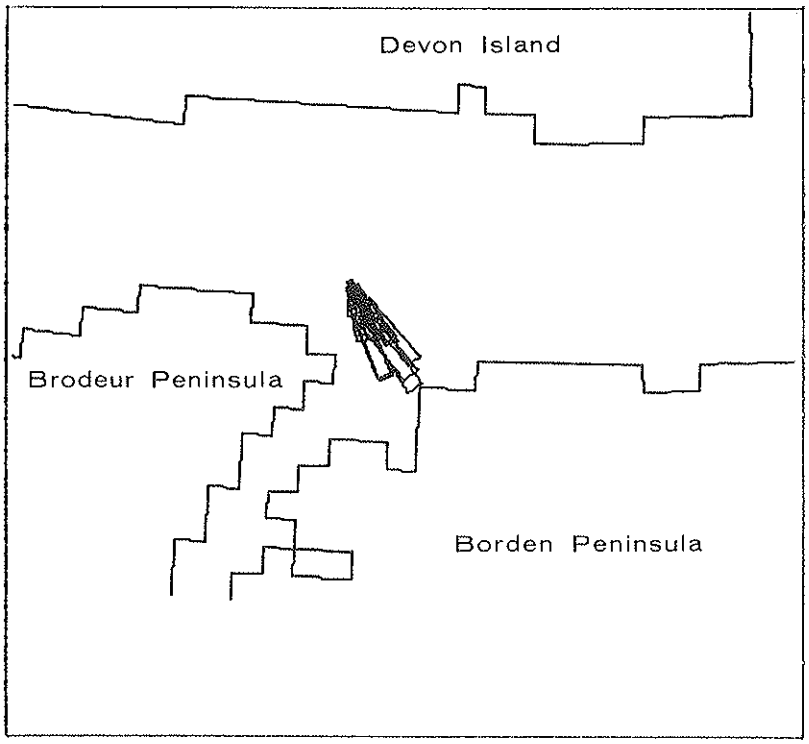

14 f) 2 E 20-3 - Site two; Blowout under 20 knot easterly wind; viewed three days after initial release of oil.

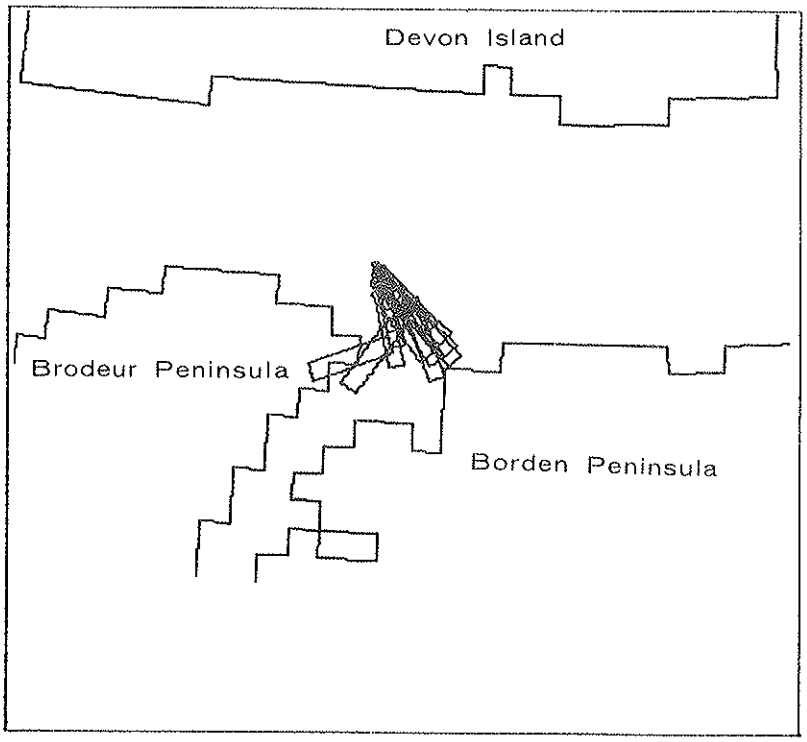

14 g) 2 E 20-7 - Site two; Blowout under 20 knot easterly wind; viewed seven days after initial release of oil.

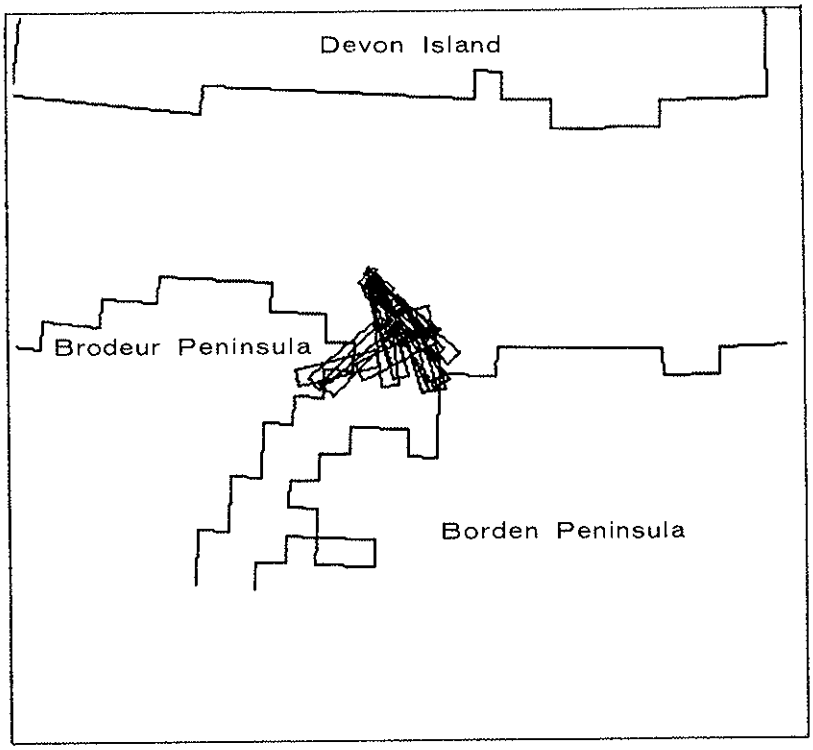

14 h) 2 W 10-1 - Site two; Blowout under 10 knot westerly wind; viewed one day after initial release of oil.

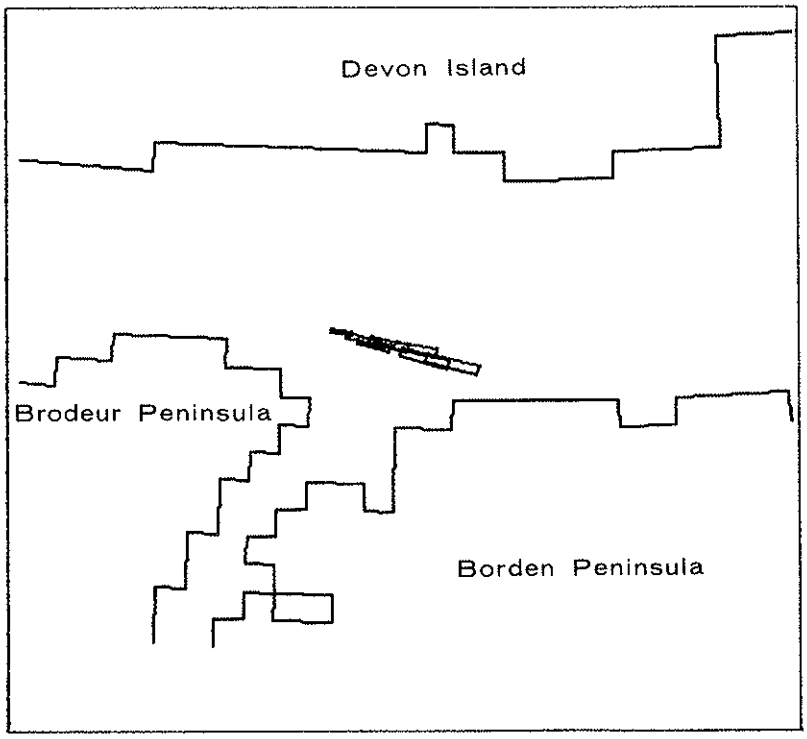

14 i) 2 W 10-5 - Site two; Blowout under 10 knot westerly wind; viewed five days after initial release of oil.

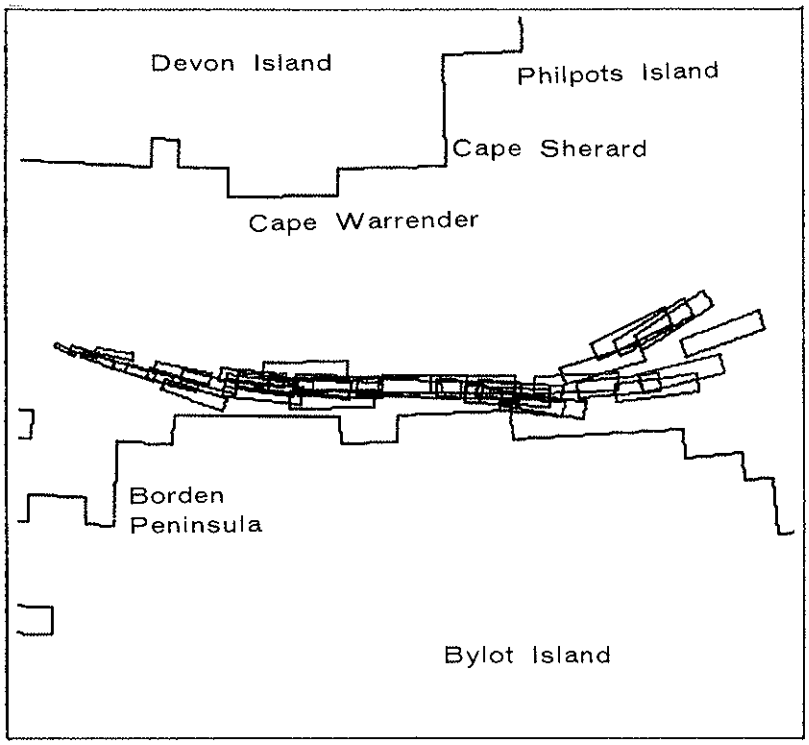

14 j) 2 W 10-7 - Site two; Blowout under 10 knot westerly wind; viewed seven days after initial release of oil.

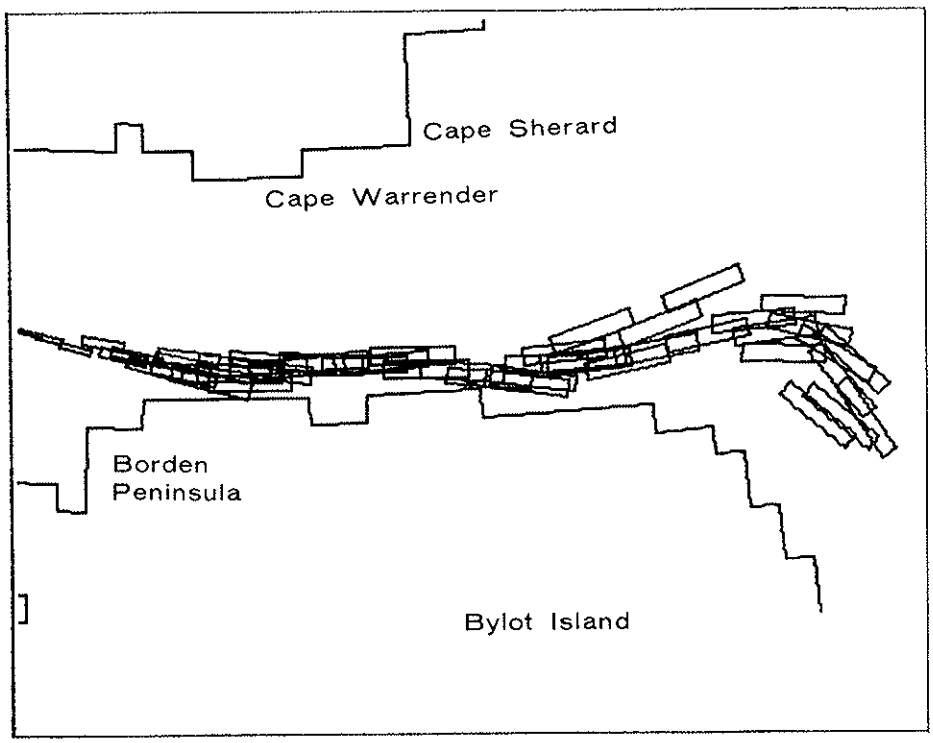

14 k) 2 W 20-1 - Site two; Blowout under 20 knot westerly wind; viewed one day after initial release of oil.

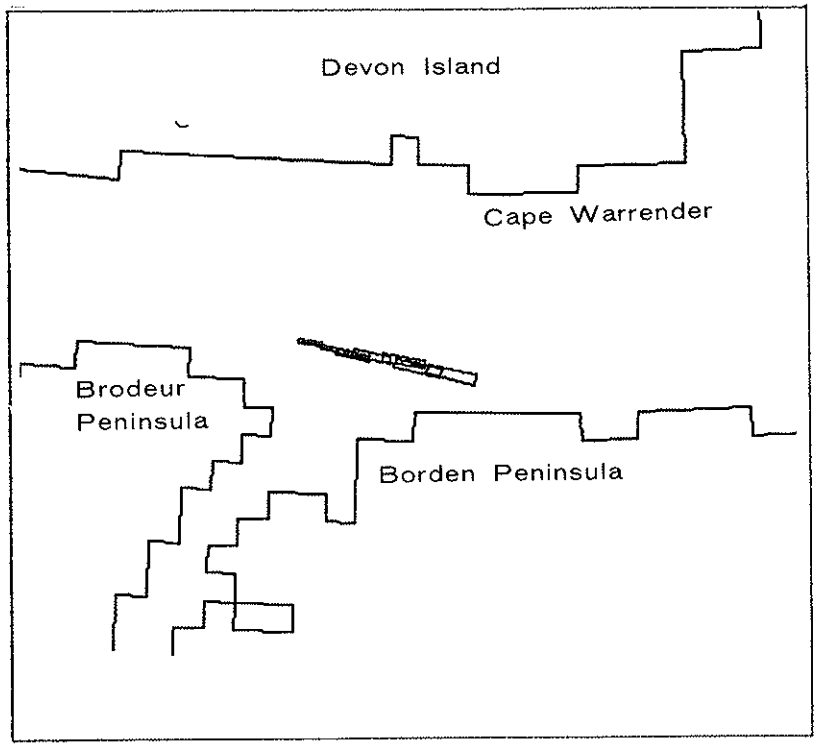

14 l) 2 W 20-3 - Site two; Blowout under 20 knot westerly wind; viewed three days after initial release of oil.

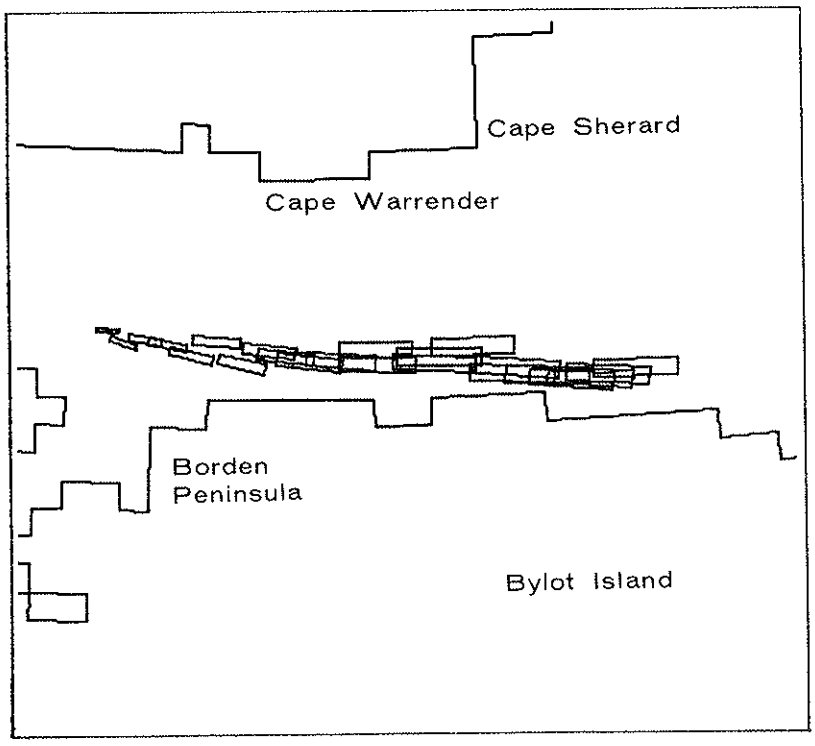

14 m) 2 W 20-5 - Site two; Blowout under 20 knot westerly wind; viewed five days after initial release of oil.

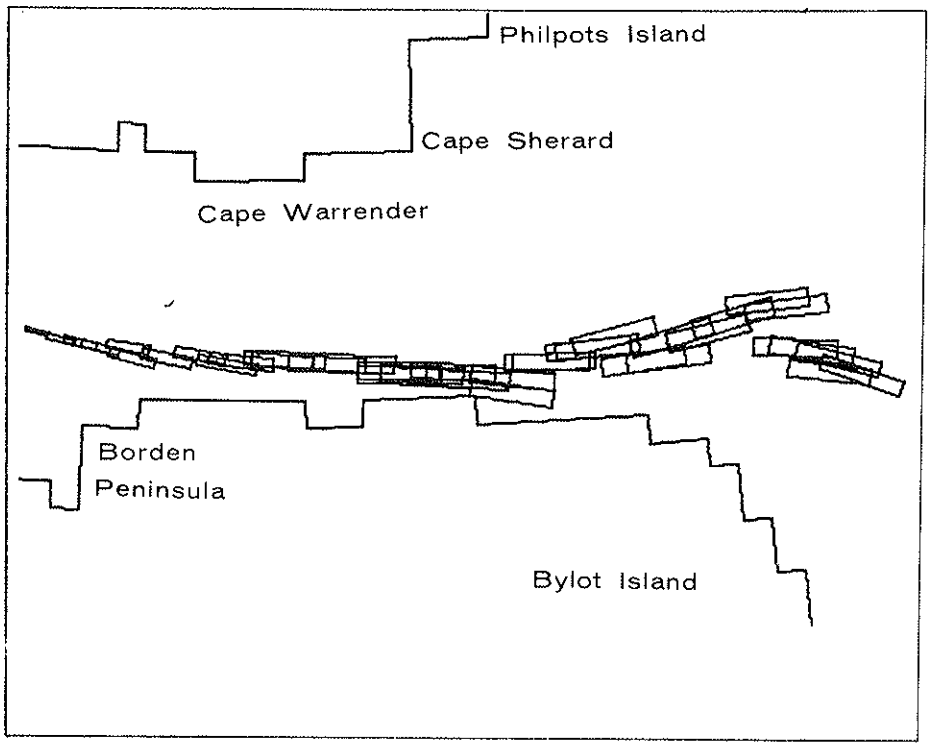

14 n) 2 S 10-1 - Site two; Blowout under 10 knot southerly wind; viewed one day after initial release of oil.

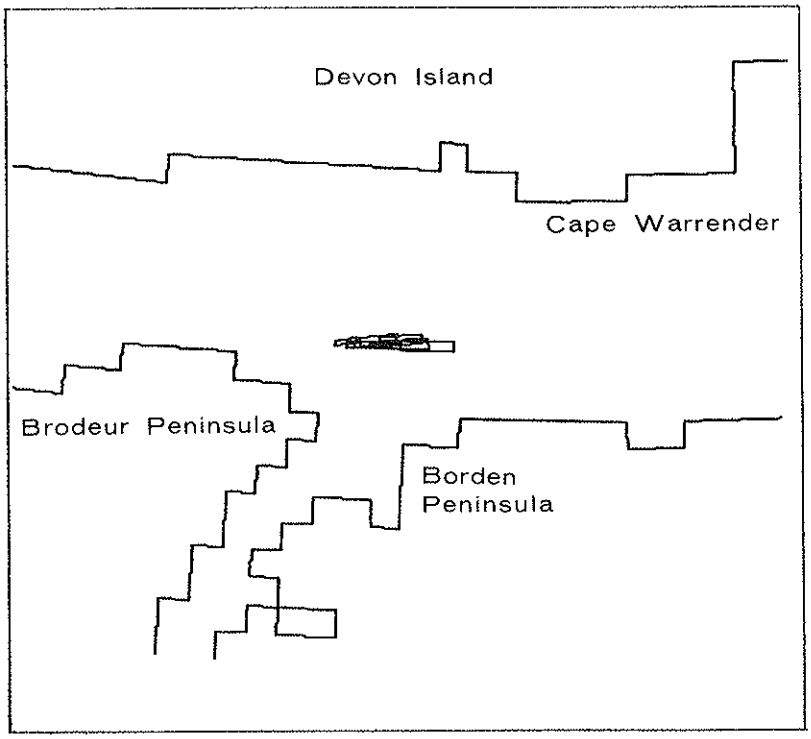

14 o) 2 S 10-4 - Site two; Blowout under 10 knot southerly wind; viewed four days after initial release of oil.

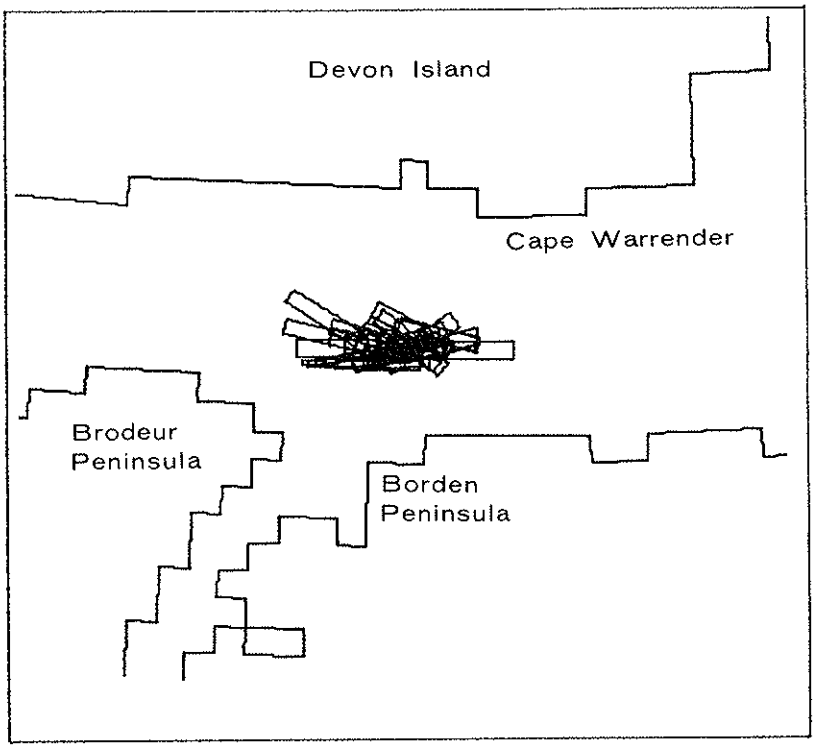

14 p) 2 S 10-6 - Site two; Blowout under 10 knot southerly wind; viewed six days after initial release of oil.

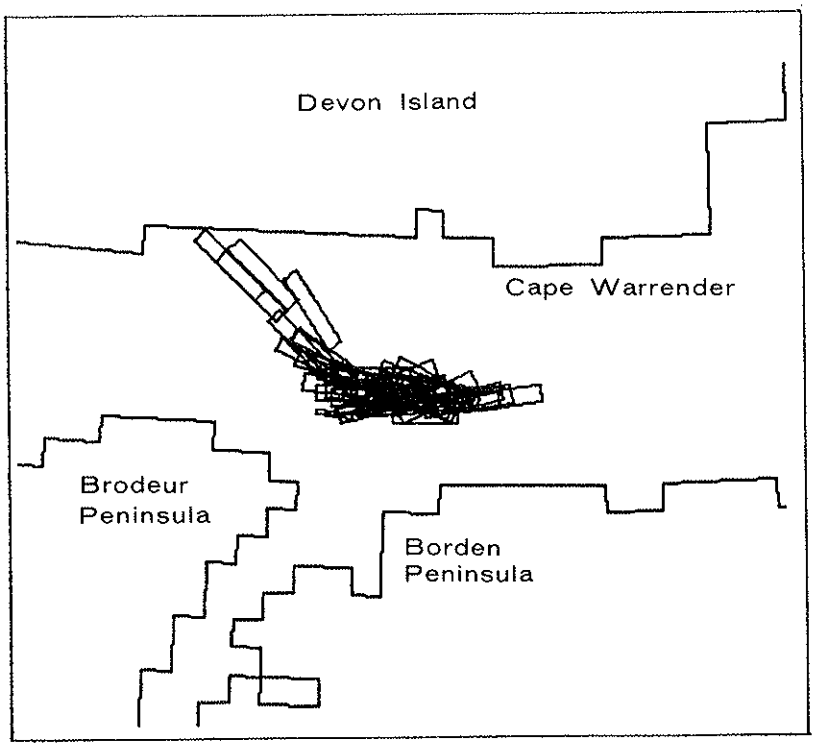

14 q) 2 S 10-7 - Site two; Blowout under 10 knot southerly wind; viewed seven days after initial release of oil.

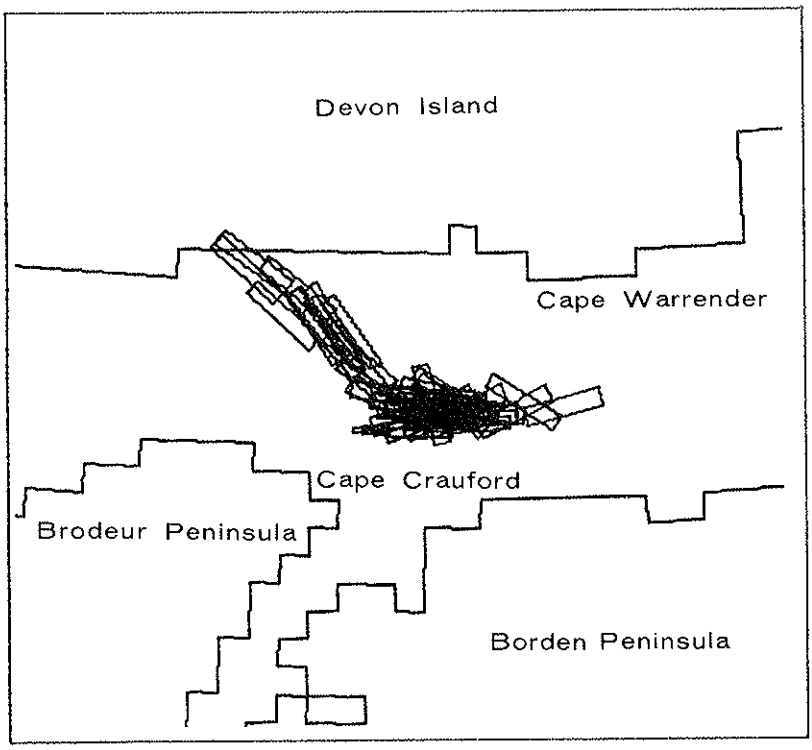

14 r) 2 S 20-1 - Site two; Blowout under 20 knot southerly wind; viewed one day after initial release of oil.

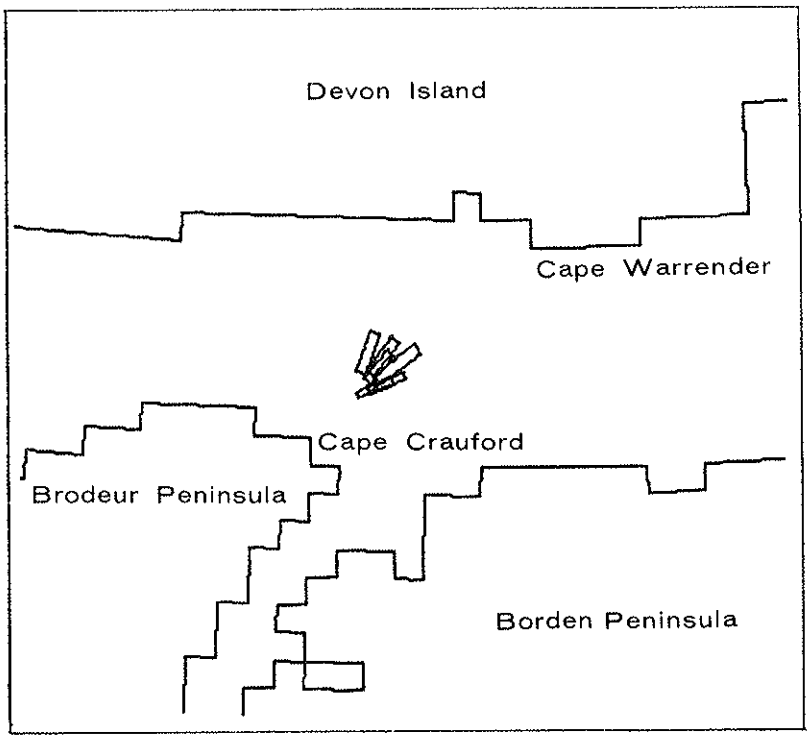

14 s) 2 S 20-2 - Site two; Blowout under 20 knot southerly wind; viewed two days after initial release of oil.

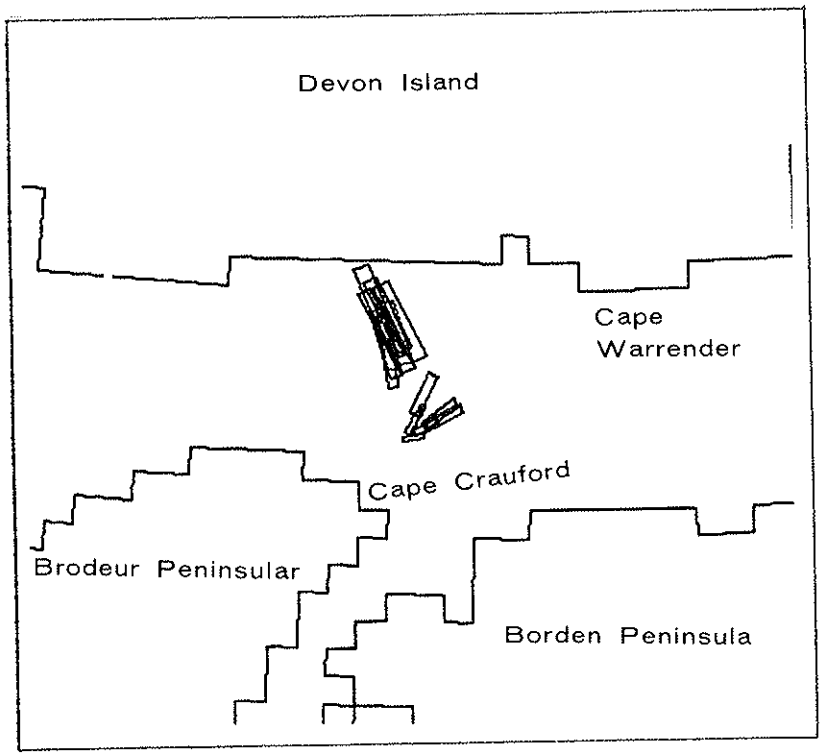

14 t) 2 S 20-3 - Site two; Blowout under 20 knot southerly wind; viewed three days after initial release of oil.

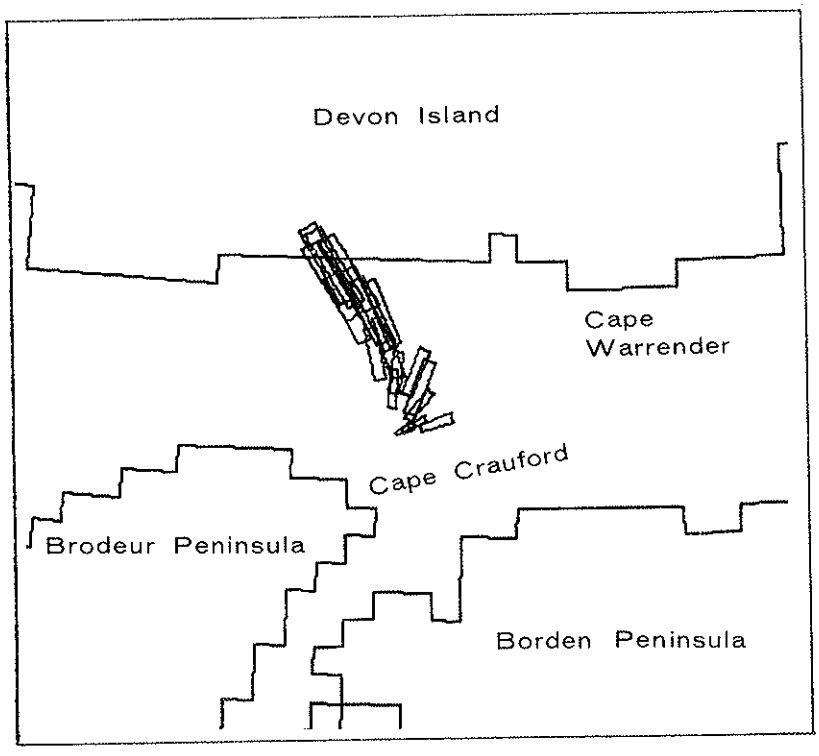

15 a) 3 N 10-1 - Site three; Blowout under 10 knot northerly wind; viewed one day after initial release of oil.

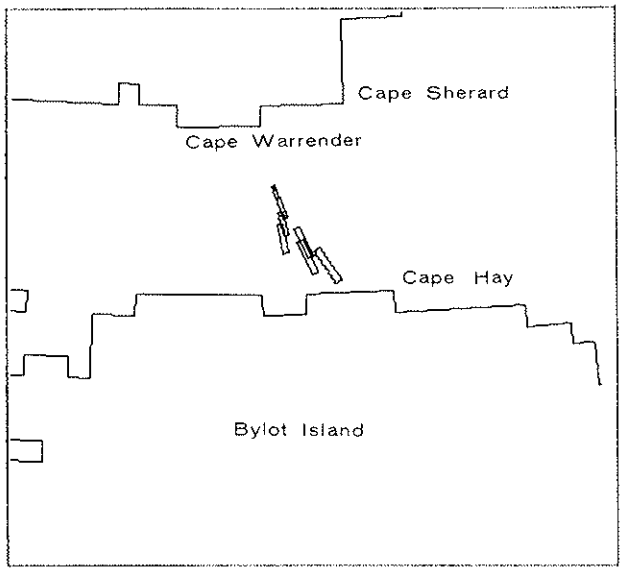

15 b) 3 N 10-2 - Site three; Blowout under 10 knot northerly wind; viewed two days after initial release of oil.

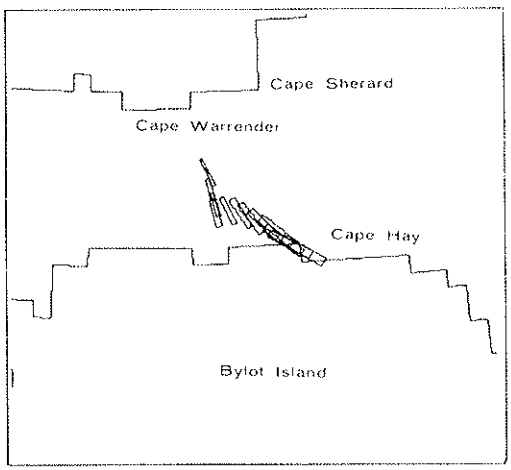

FIGURE 15 SCENARIOS OF OIL DRIFT IN THE AREA OF A SITE NO. 3 BLOWOUT UNDER TIME-INDEPENDENT NORTH, EAST, WEST AND SOUTH WINDS.

15 c) 3 N 20-1 - Site three; Blowout under 20 knot northerly wind; viewed one day after initial release of oil.

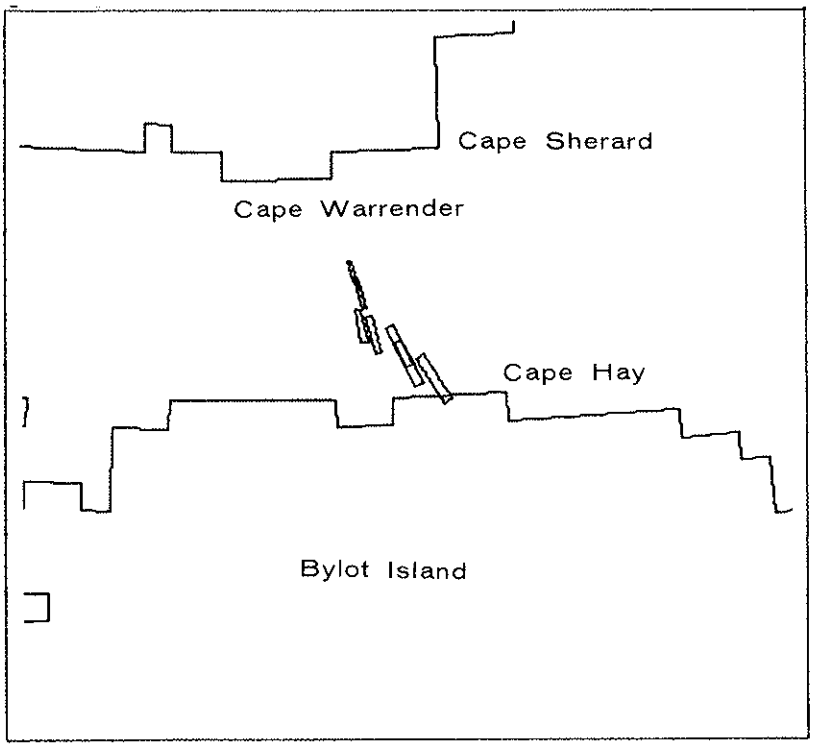

15 d) 3 N 20-3 - Site three; Blowout under 20 knot northerly wind; viewed three days after initial release of oil.

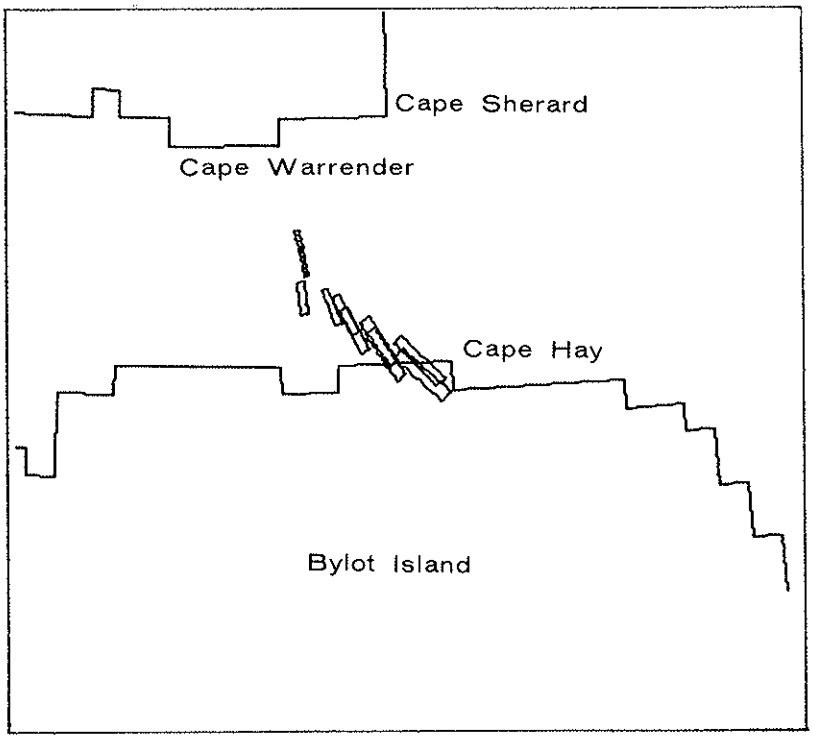

15 e) 3 E 10-1 - Site three; Blowout under 10 knot easterly wind; viewed one day after initial release of oil.

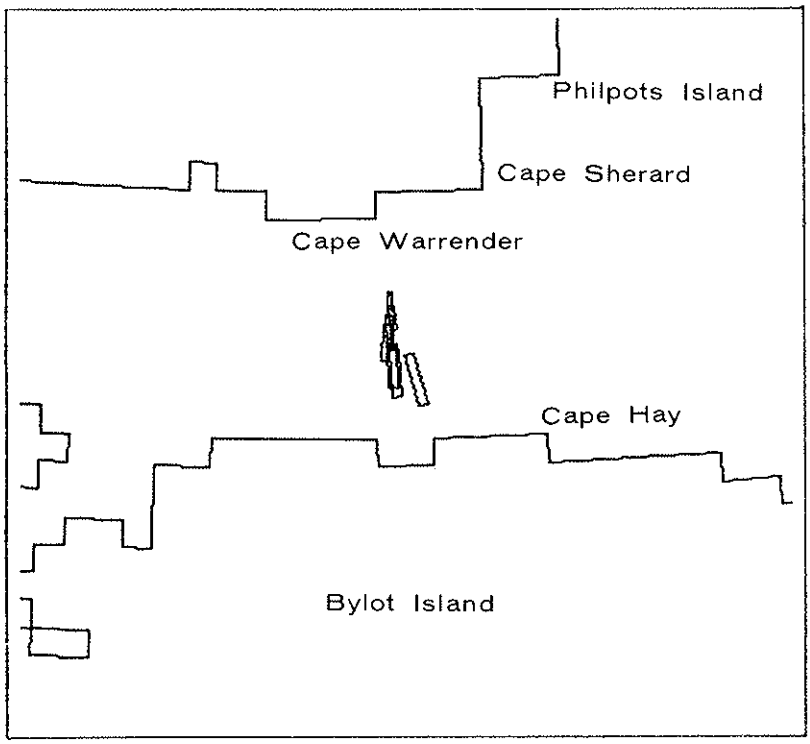

15 f) 3 E 10-2 - Site three; Blowout under 10 knot easterly wind; viewed two days after initial release of oil.

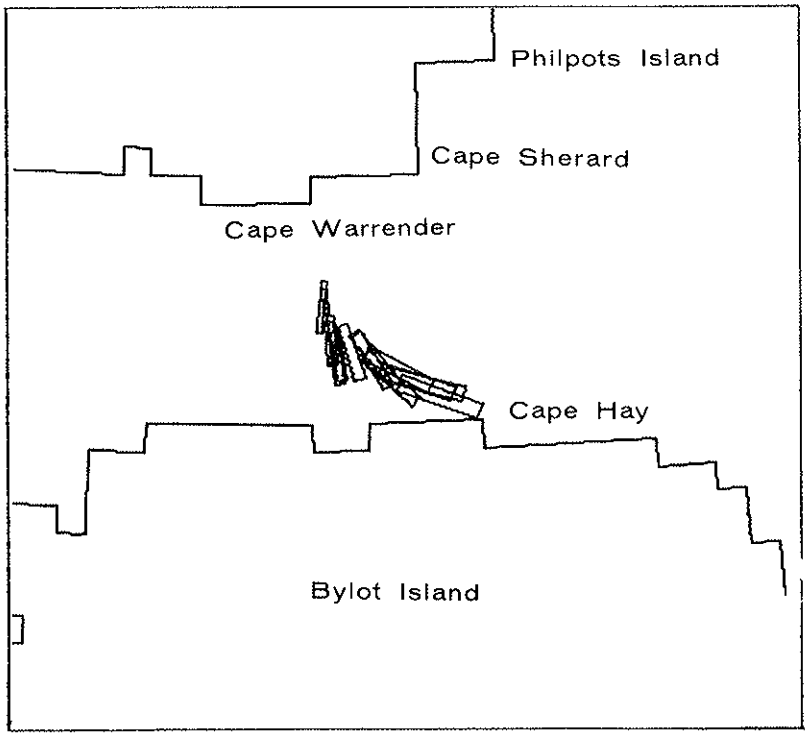

15 g) 3 E 10-6 - Site three; Blowout under 10 knot easterly wind; viewed six days after initial release of oil.

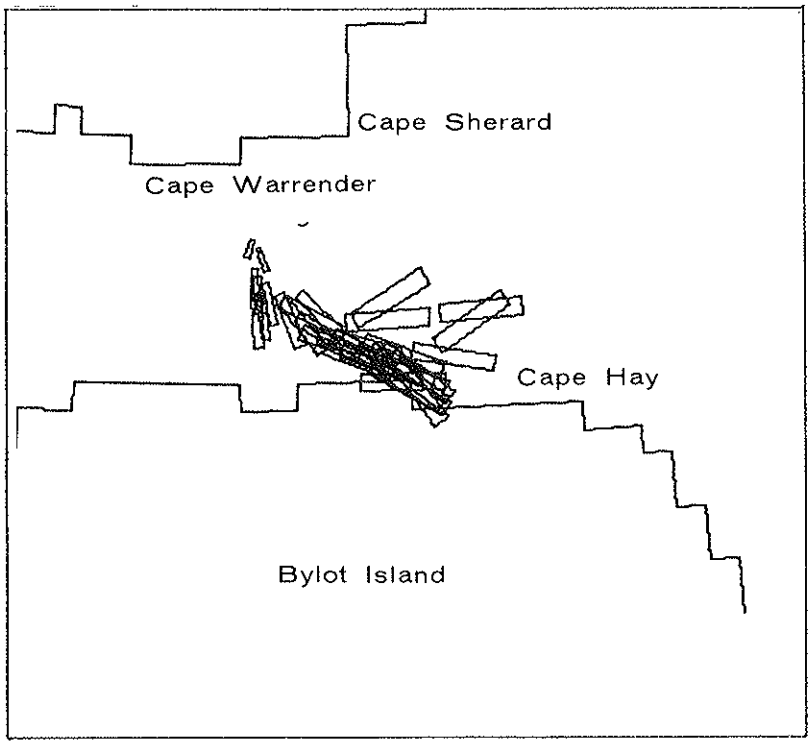

15 h) 3 E 20-1 - Site three; Blowout under 20 knot easterly wind; viewed one day after initial release of oil.

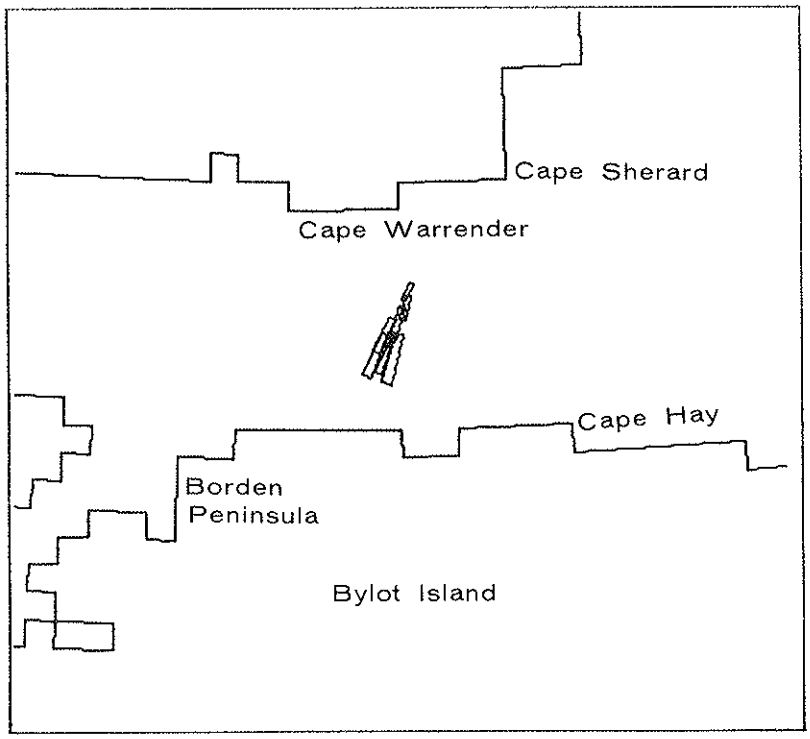

15 i) 3 E 20-3 - Site three; Blowout under 20 knot easterly wind; viewed three days after initial release of oil.

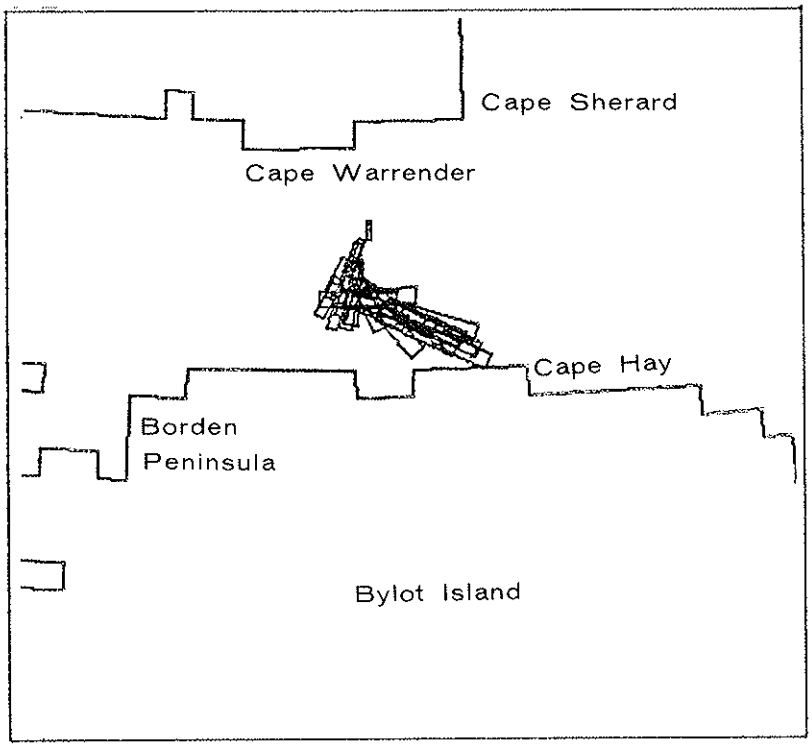

15 j) 3 E 20-4 - Site three; Blowout under 20 knot easterly wind; viewed four days after initial release of oil.

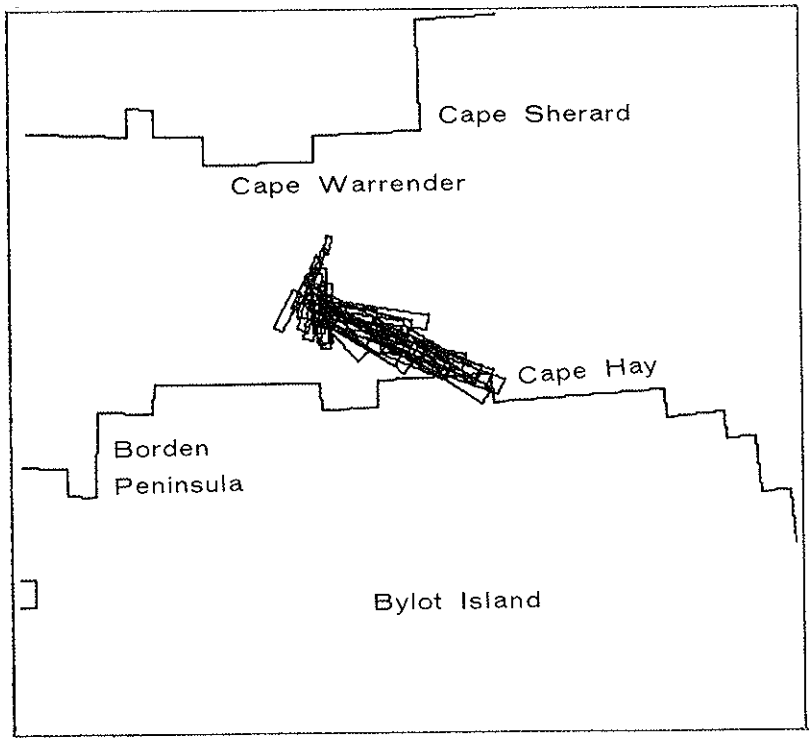

15 k) 3 W 10-1 - Site three; Blowout under 10 knot westerly wind; viewed one day after initial release of oil.

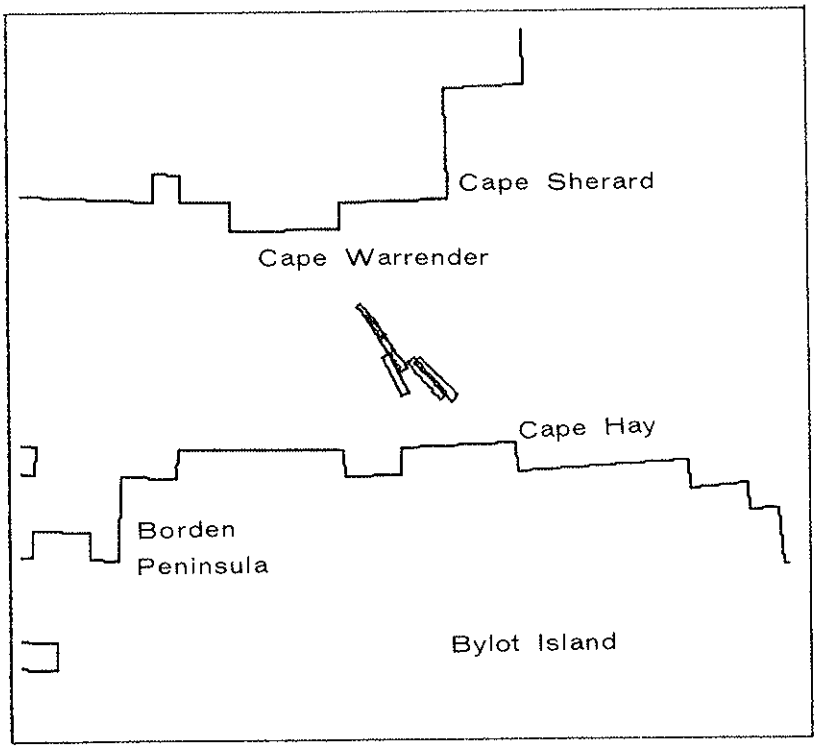

15 l) 3 W 10-4 - Site three; Blowout under 10 knot westerly wind; viewed four days after initial release of oil.

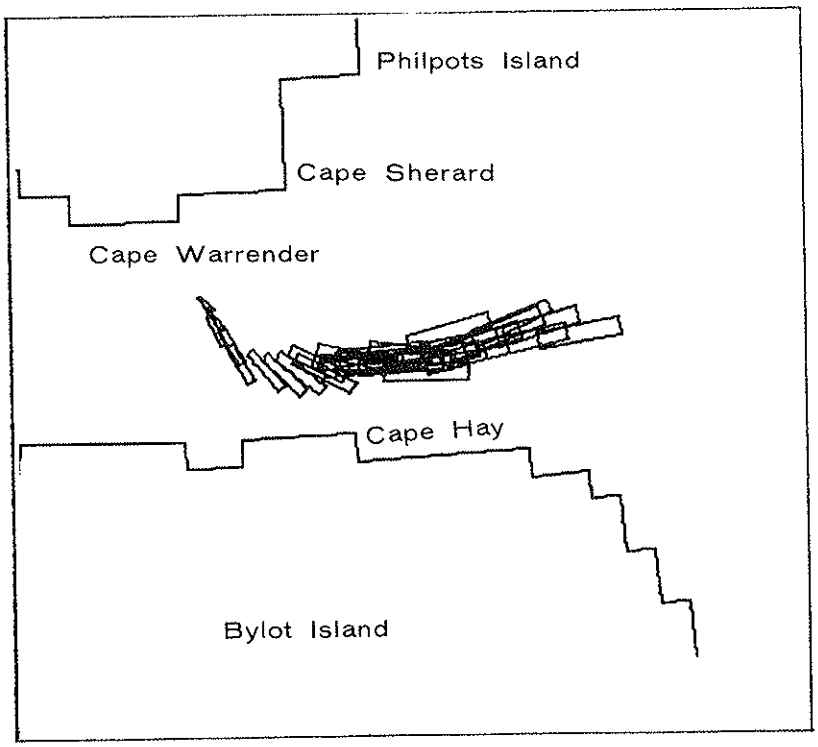

15 m) 3 W 10-6 - Site three; Blowout under 10 knot westerly wind; viewed six days after initial release of oil.

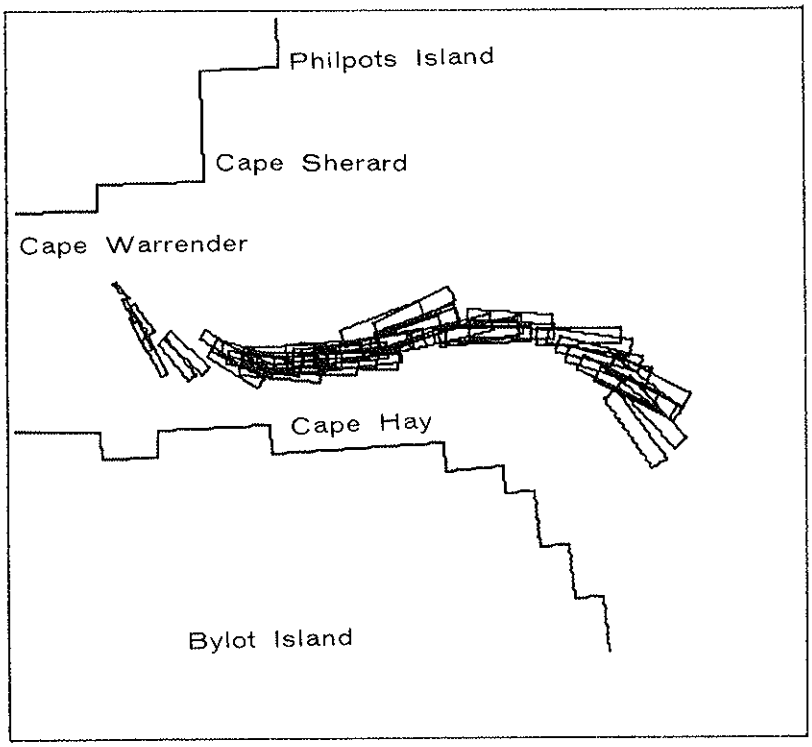

15 n) 3 W 20-1 - Site three; Blowout under 20 knot westerly wind; viewed one day after initial release of oil.

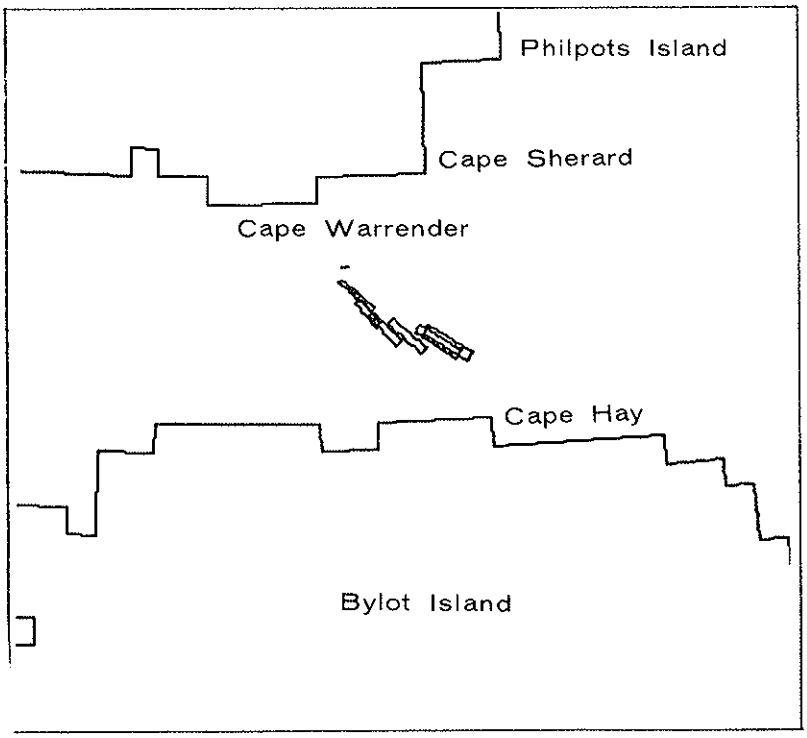

15 o) 3 W 20-3 - Site three; Blowout under 20 knot westerly wind; viewed three days after initial release of oil.

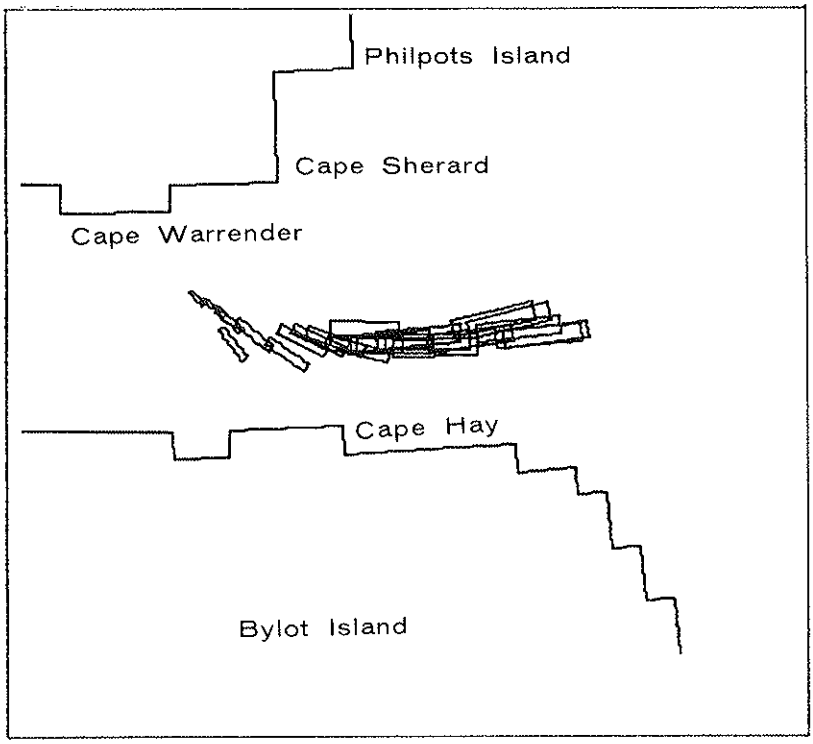

15 p) 3 W 20-4 - Site three; Blowout under 20 knot westerly wind; viewed four days after initial release of oil.

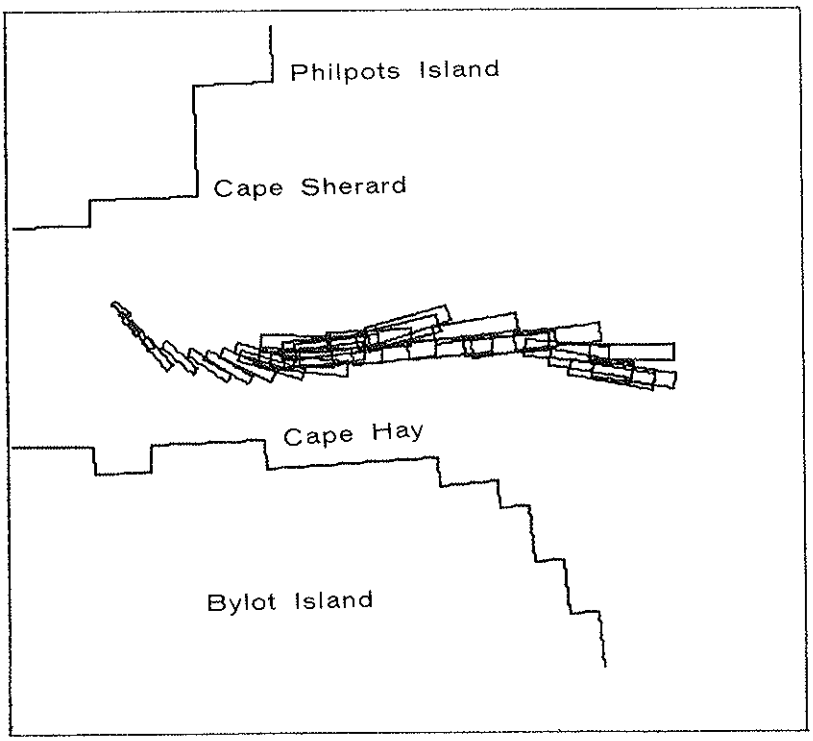

15 q) 3 S 10-1 - Site three; Blowout under 10 knot southerly wind; viewed one day after initial release of oil.

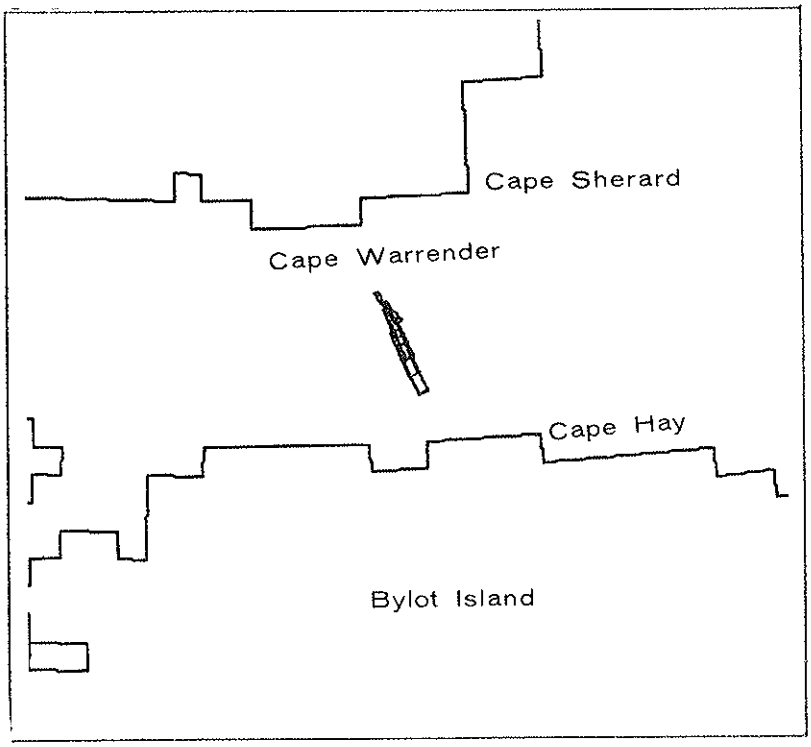

15 r) 3 S 10-3 - Site three; Blowout under 10 knot southerly wind; viewed three days after initial release of oil.

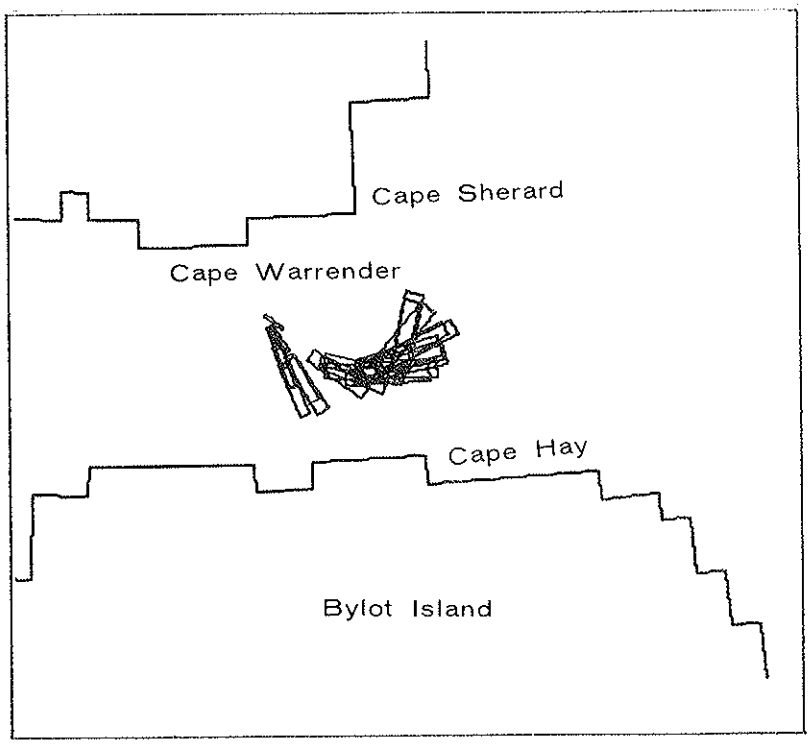

15 s) 3 S 10-6 - Site three; Blowout under 10 knot southerly wind; viewed six days after initial release of oil.

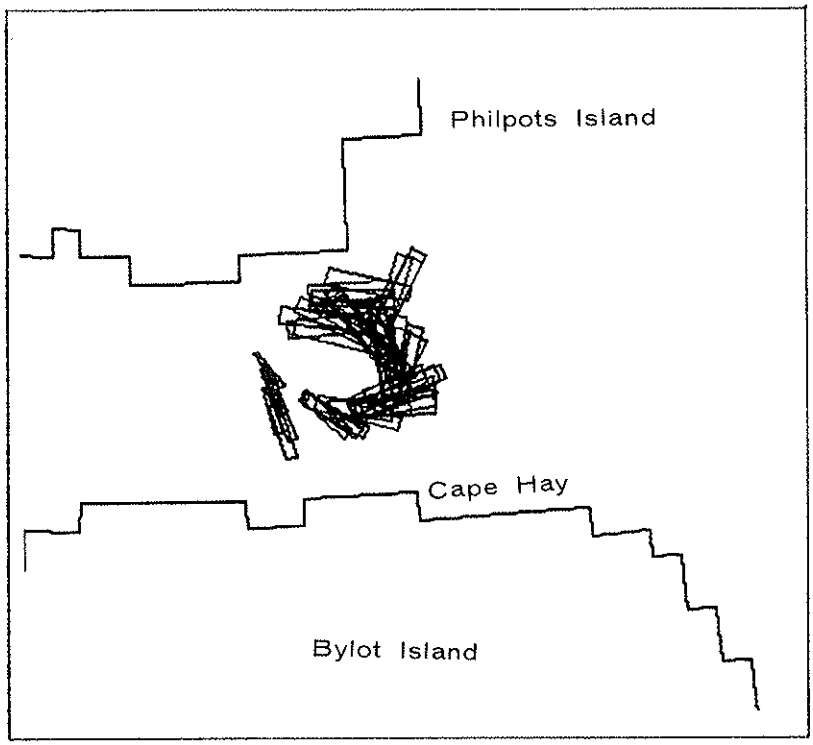

15 t) 3 S 10-7 - Site three; Blowout under 10 knot southerly wind; viewed seven days after initial release of oil.

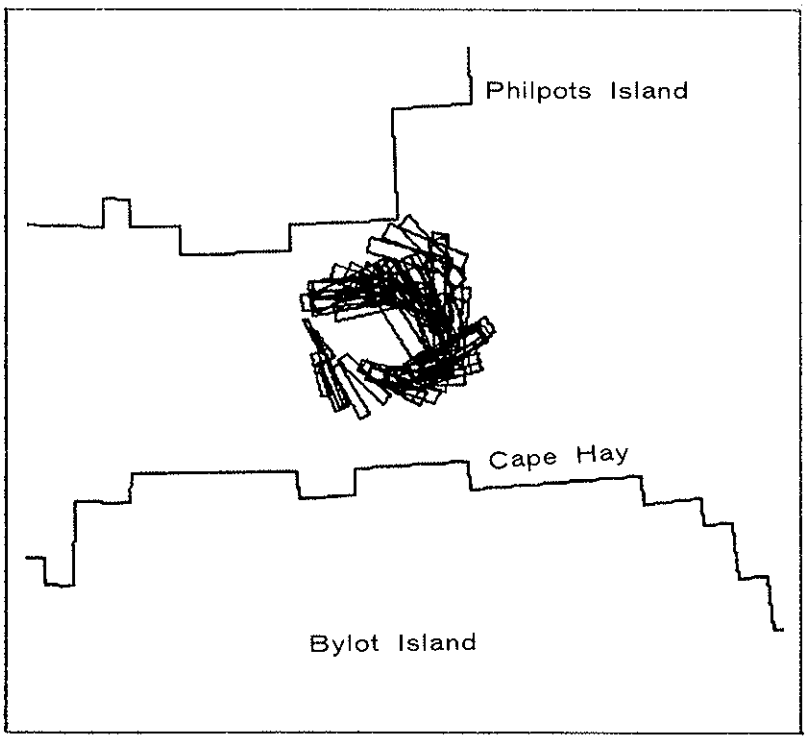

15 u) 3 S 20-2 - Site three; Blowout under 20 knot southerly wind; viewed two days after initial release of oil.

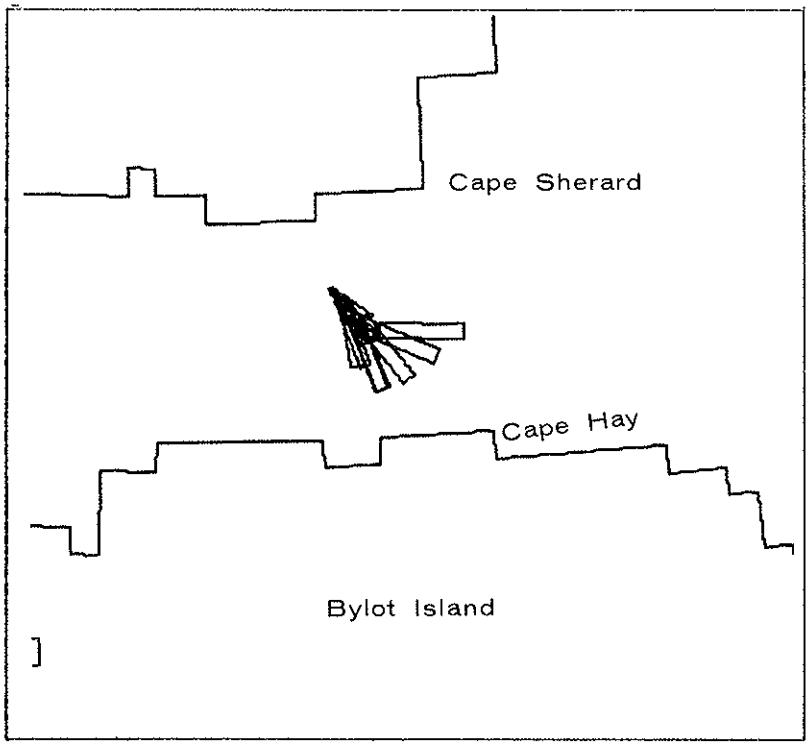

15 v) 3 S 20-3 - Site three; Blowout under 20 knot southerly wind; viewed three days after initial release of oil.

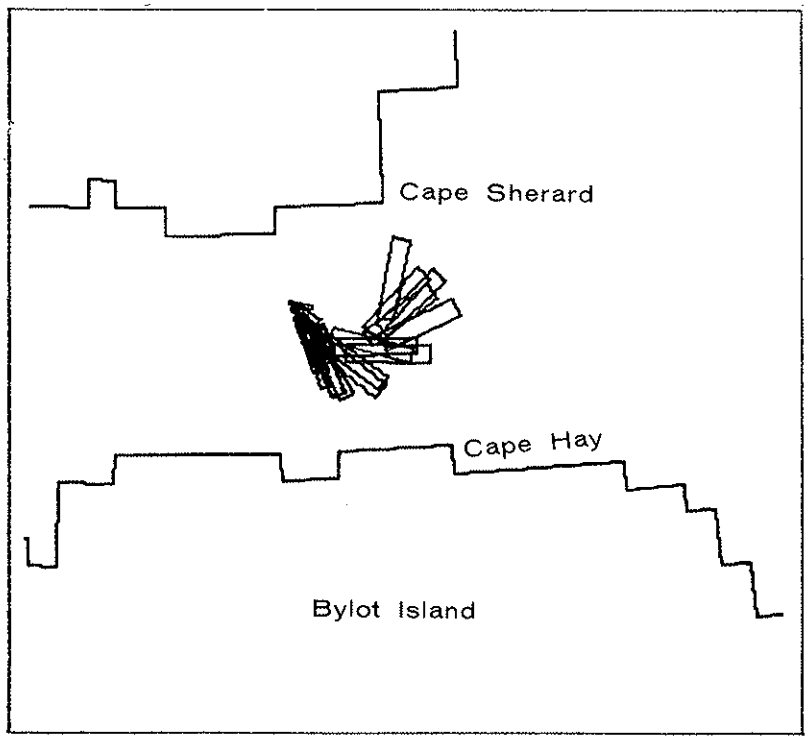

15 w) 3 S 20-5 - Site three; Blowout under 20 knot southerly wind; viewed five days after initial release of oil.

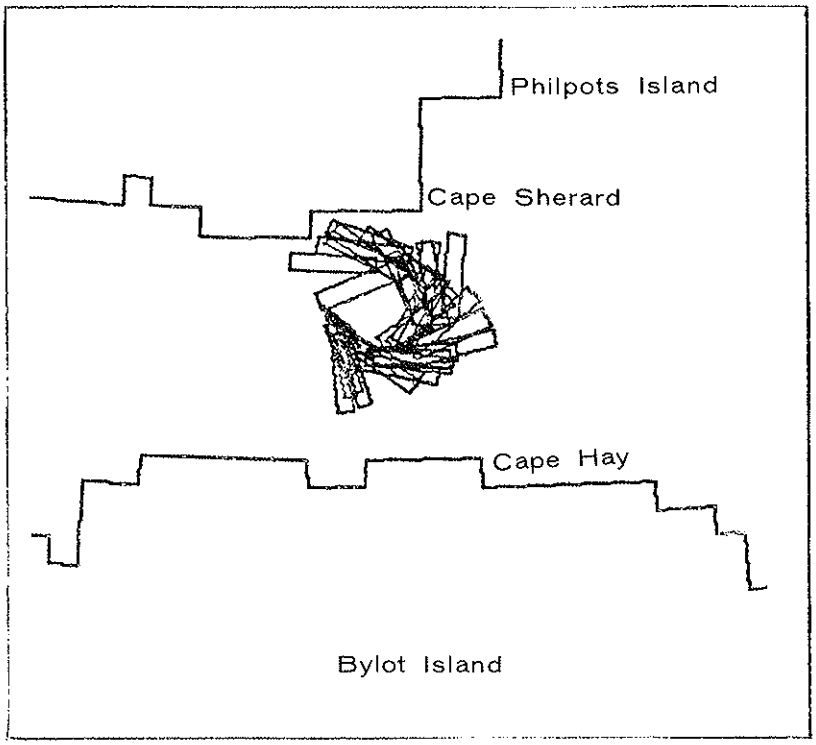

16 a) 4 N 10-1 - Site four; Blowout under 10 knot northerly wind; viewed one day after initial release of oil.

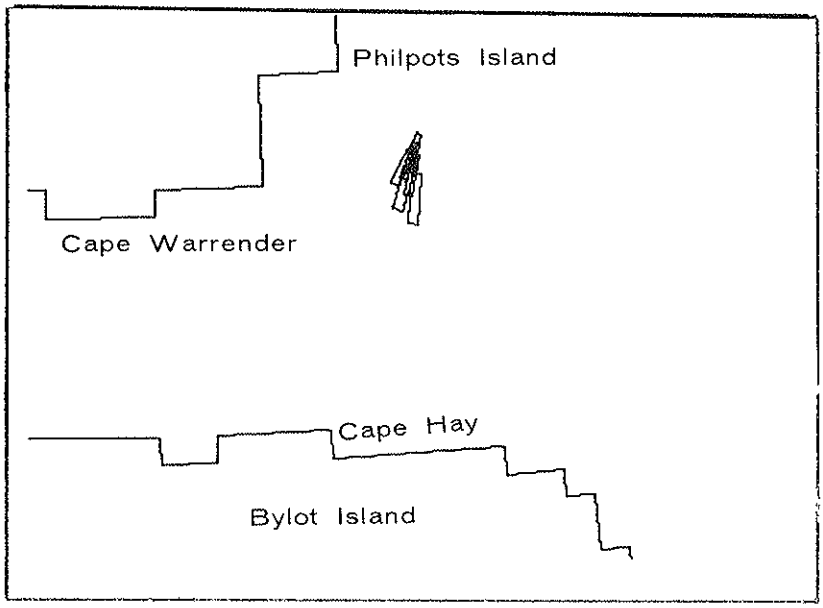

16 b) 4 N 10-3 - Site four; Blowout under 10 knot northerly wind; viewed three days after initial release of oil.

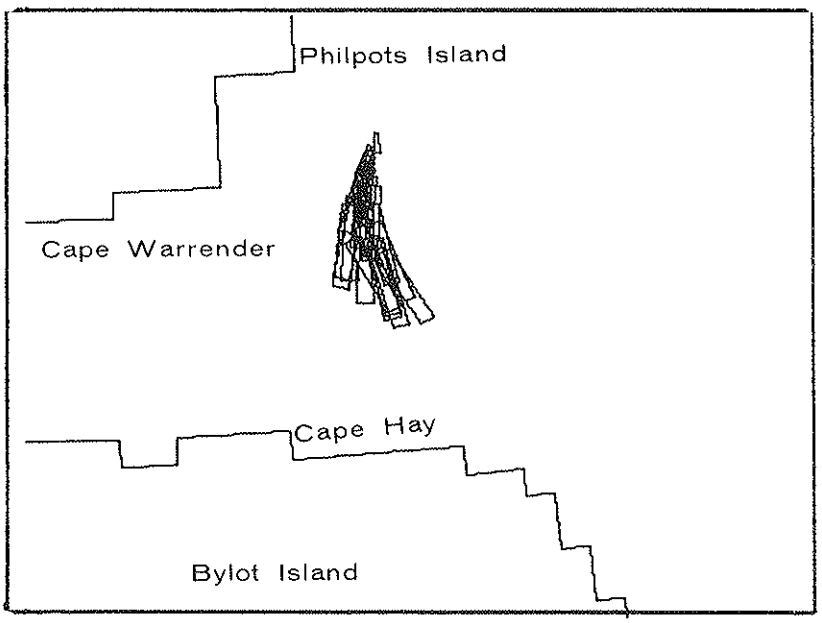

FIGURE 16 SCENARIOS OF OIL DRIFT IN THE AREA OF A SITE NO. 4 BLOWOUT UNDER TIME-INDEPENDENT NORTH, EAST, WEST AND SOUTH WINDS

16 c) 4 N 10-4 - Site four; Blowout under 10 knot northerly wind; viewed four days after initial release of oil.

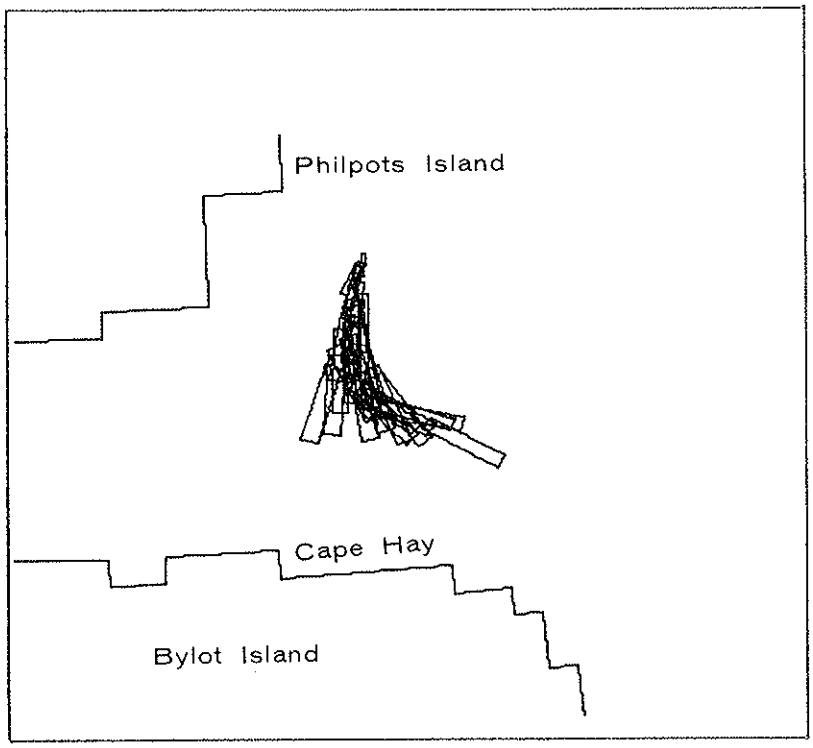

16 d) 4 N 10-6 - Site four; Blowout under 10 knot northerly wind; viewed six days after initial release of oil.

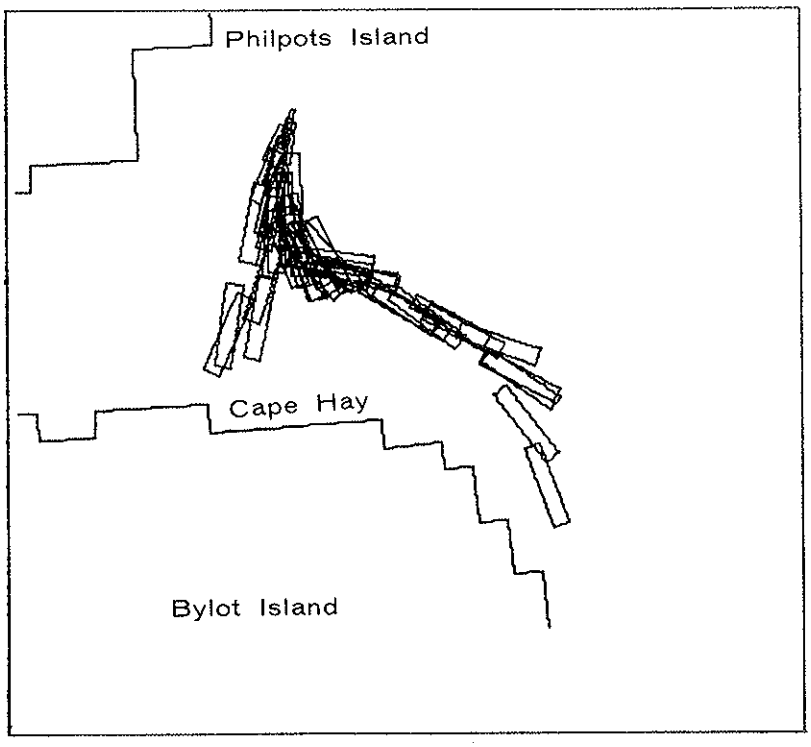

16 e) 4 N 10-7 - Site four; Blowout under 10 knot northerly wind; viewed seven days after initial release of oil.

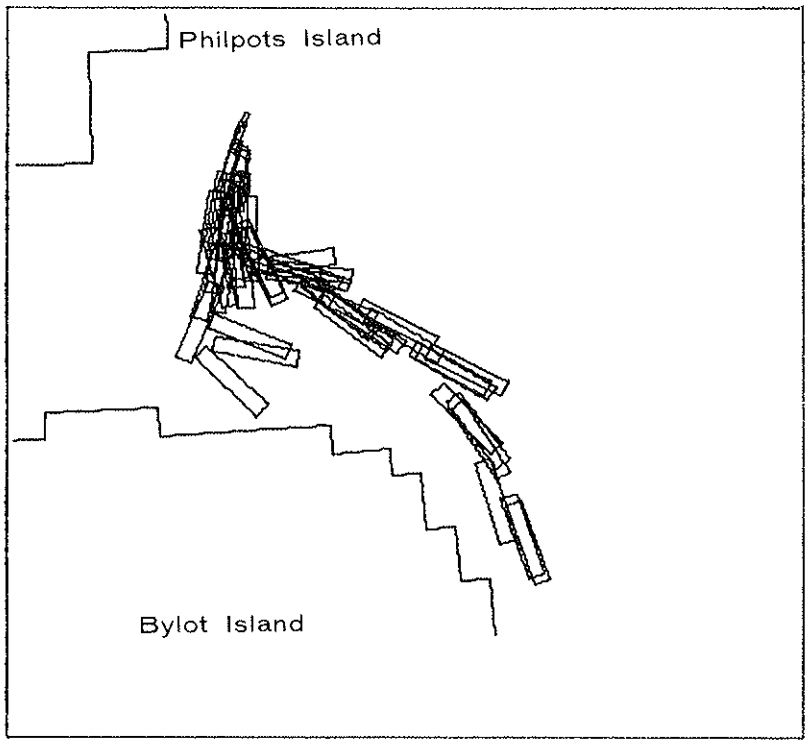

16 f) 4 N 20-3 - Site four; Blowout under 20 knot northerly wind; viewed three days after initial release of oil.

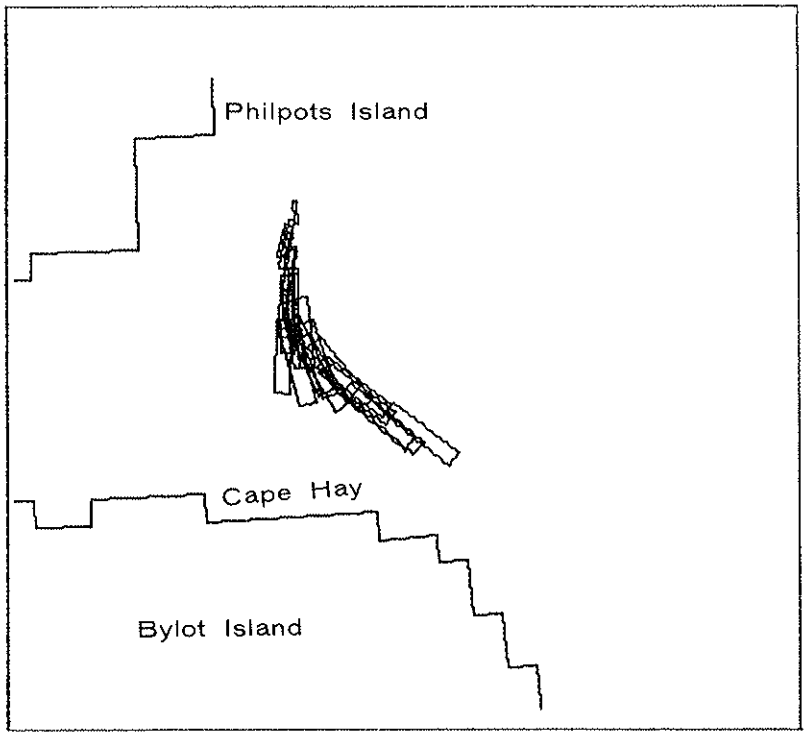

16 g) 4 N 20-4 - Site four; Blowout under 20 knot northerly wind; viewed four days after initial release of oil.

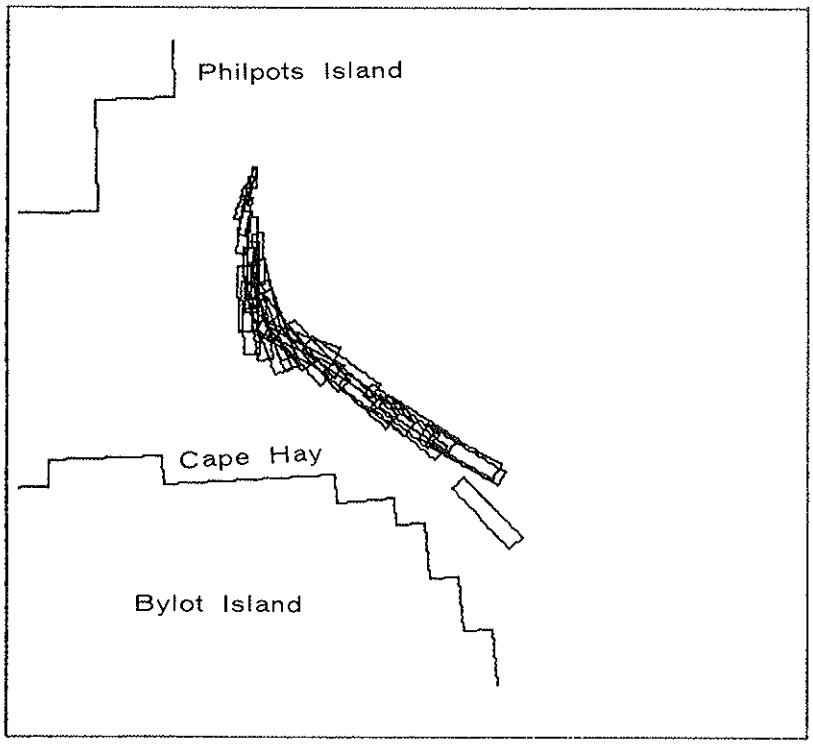

16 h) 4 N 20-5 - Site four; Blowout under 20 knot northerly wind; viewed five days after initial release of oil.

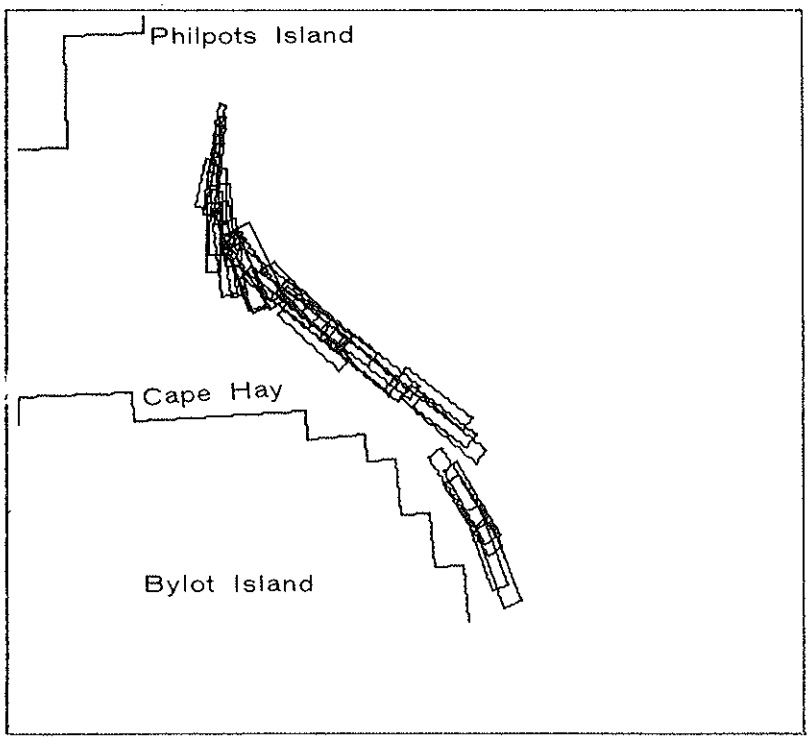

16 i) 4 N 20-7 - Site four; Blowout under 20 knot northerly wind; viewed seven days after initial release of oil.

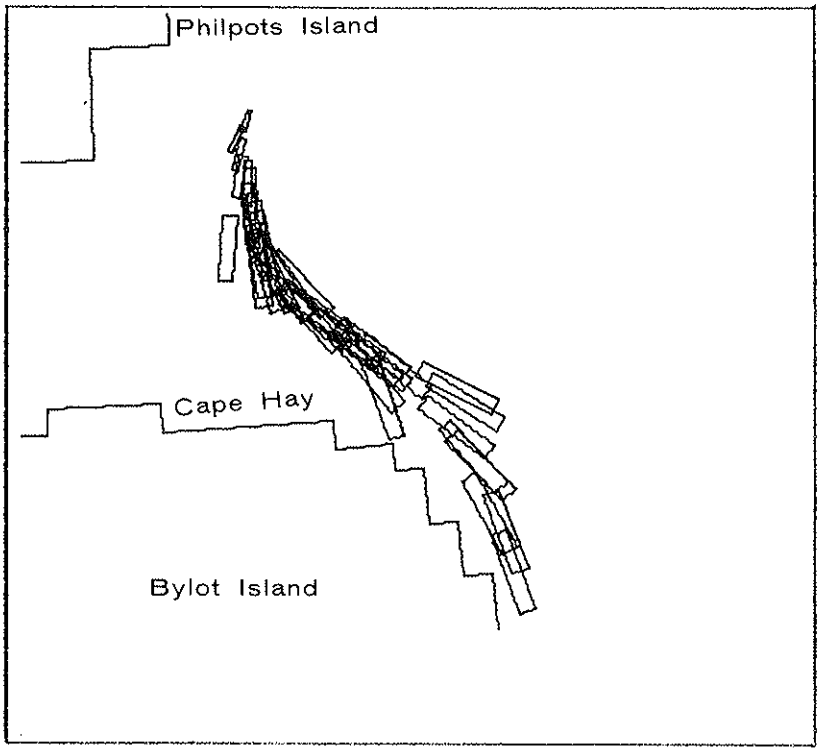

16 j) 4 E 10-3 - Site four; Blowout under 10 knot easterly wind; viewed three days after initial release of oil.

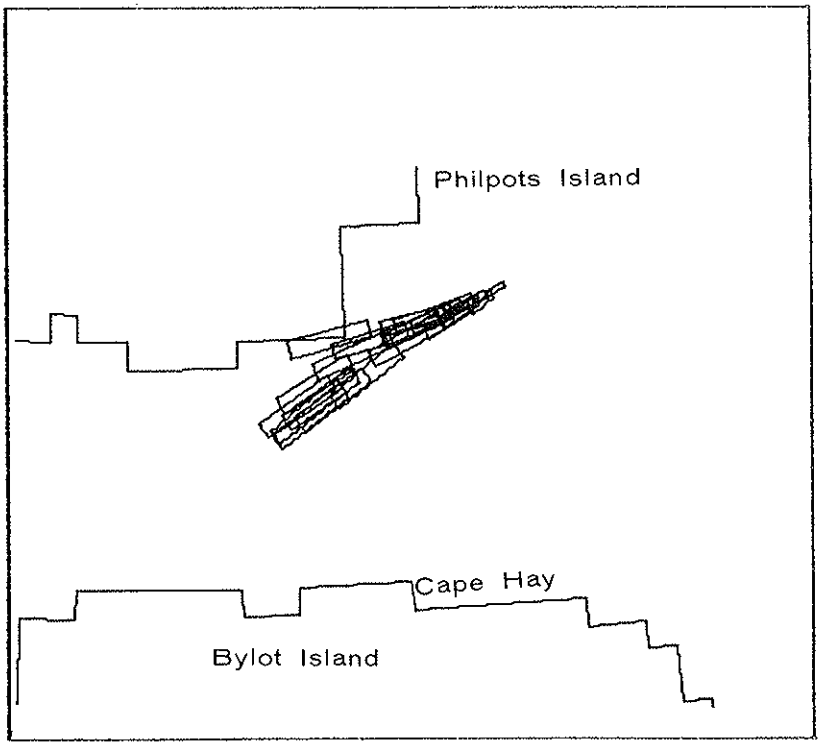

16 k) 4 E 10-4 - Site four; Blowout under 10 knot easterly wind; viewed four days after initial release of oil.

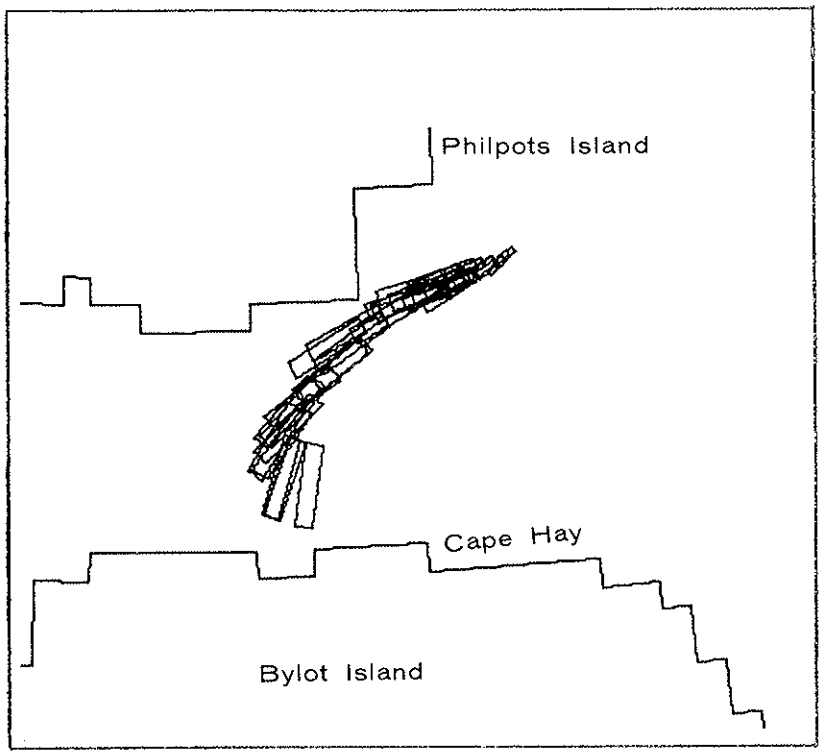

16 l) 4 E 10-6 - Site four; Blowout under 10 knot easterly wind; viewed six days after initial release of oil.

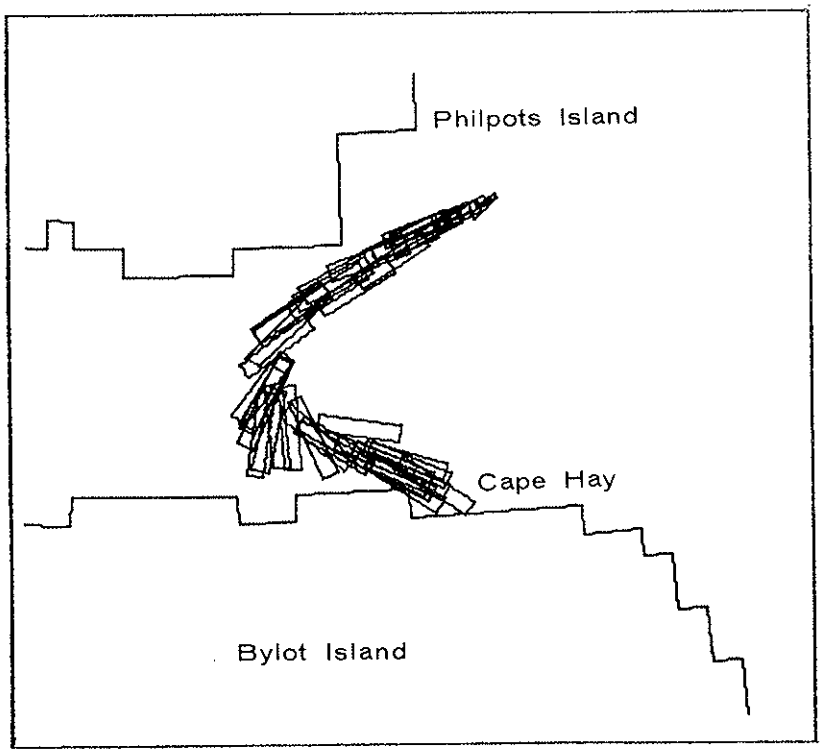

16 m) 4 E 20-2 - Site four; Blowout under 20 knot easterly wind; viewed two days after initial release of oil.

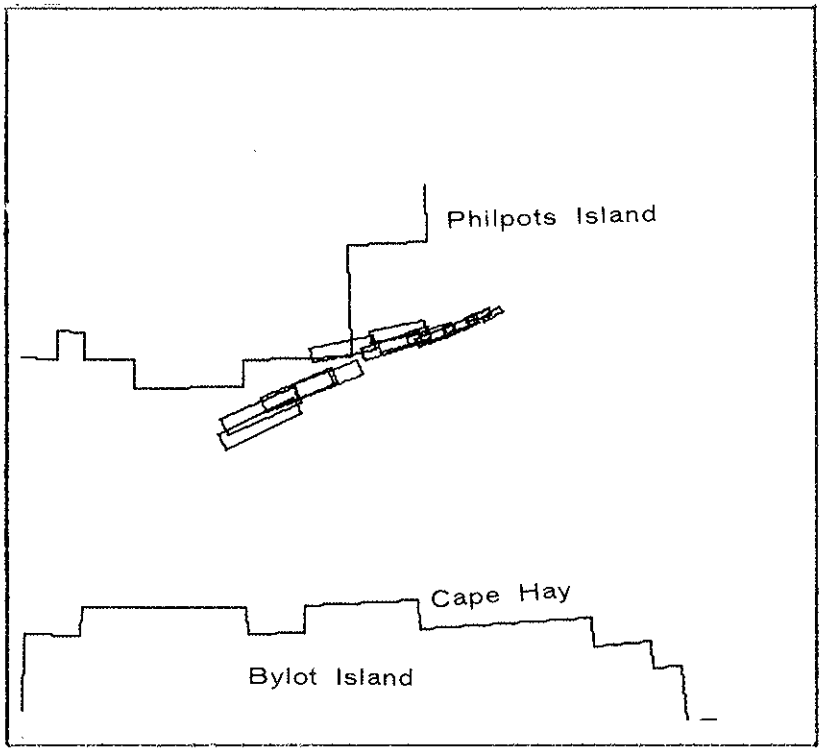

16 n) 4 E 20-4 - Site four; Blowout under 20 knot easterly wind; viewed four days after initial release of oil.

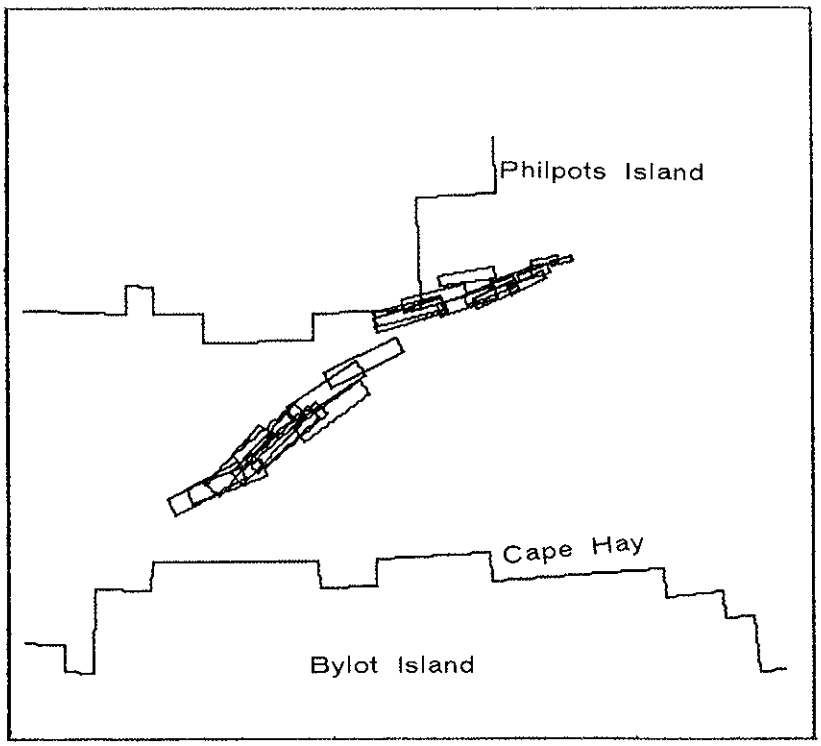

16 o) 4 E 20-6 - Site four; Blowout under 20 knot easterly wind; viewed six days after initial release of oil.

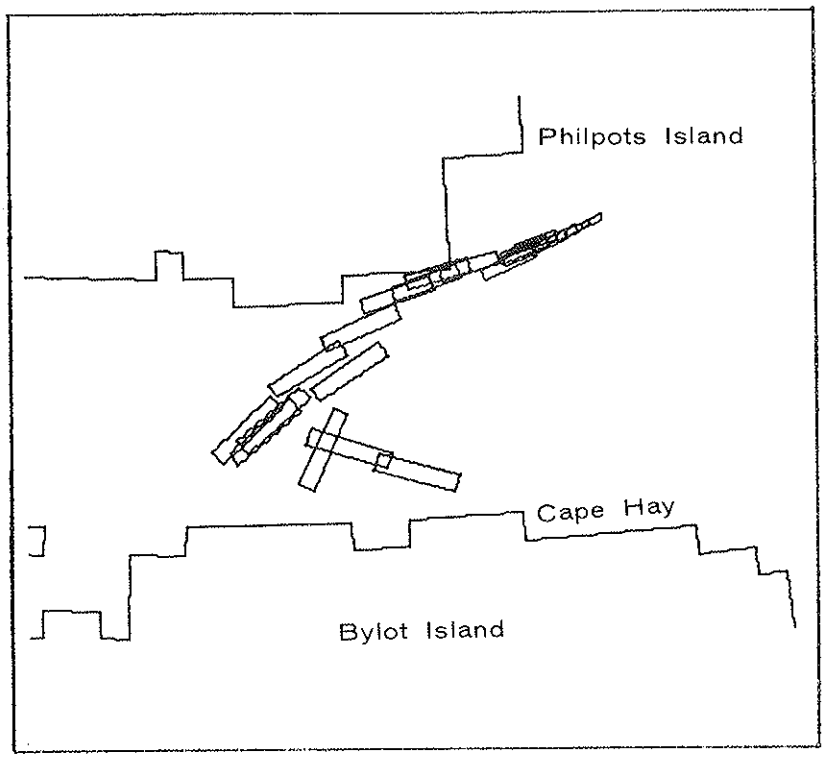

16 p) 4 W 10-2 - Site four; Blowout under 10 knot westerly wind; viewed two days after initial release of oil.

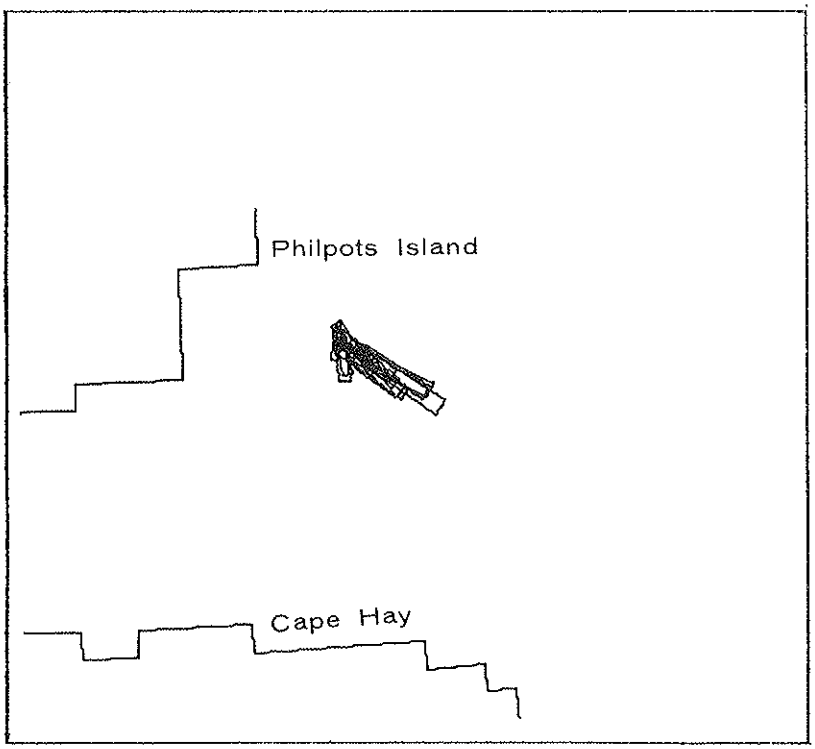

16 q) 4 W 10-5 - Site four; Blowout under 10 knot westerly wind; viewed five days after initial release of oil.

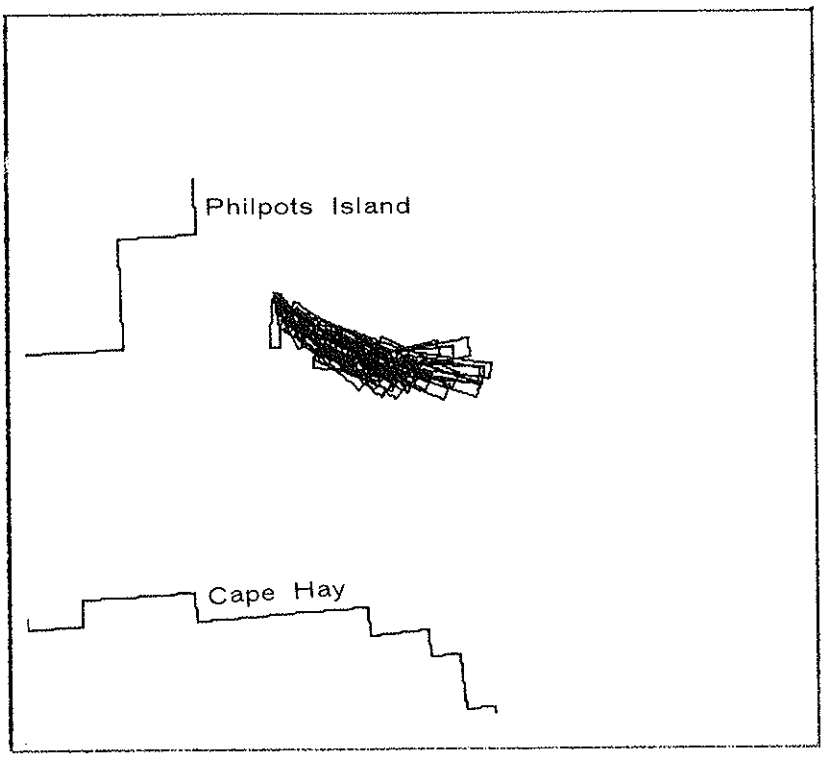

16 r) 4 W 10-7 - Site four; Blowout under 10 knot westerly wind; viewed seven days after initial release of oil.

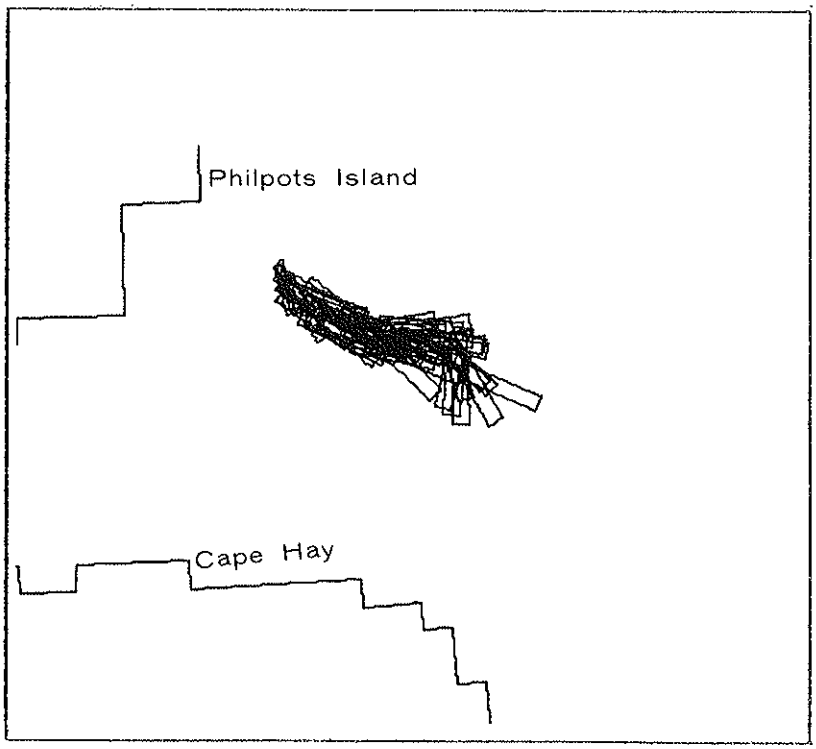

16 s) 4 W 20-2 - Site four; Blowout under 20 knot westerly wind; viewed two days after initial release of oil.

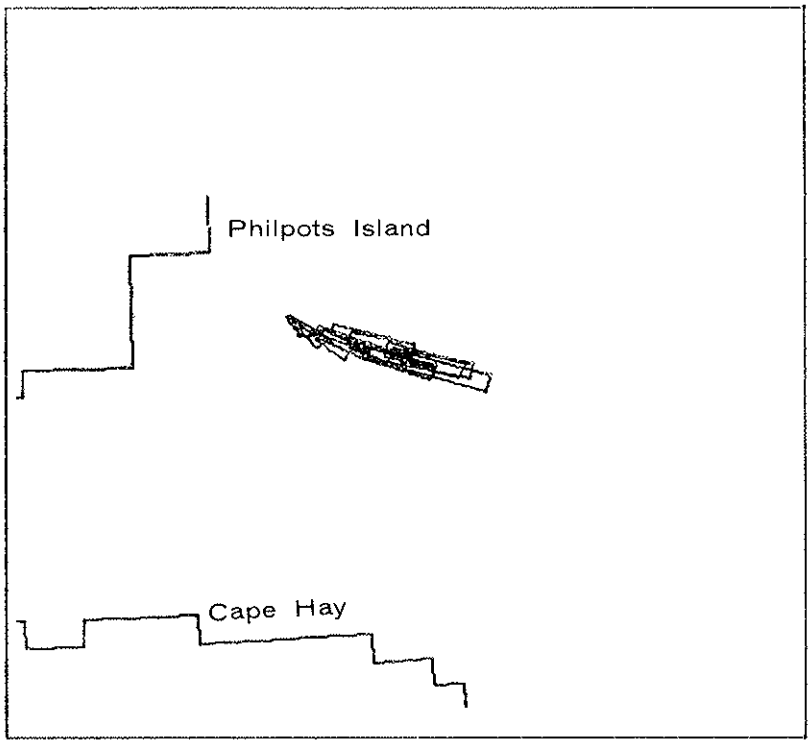

16 t) 4 W 20-5 - Site four; Blowout under 20 knot westerly wind; viewed five days after initial release of oil.

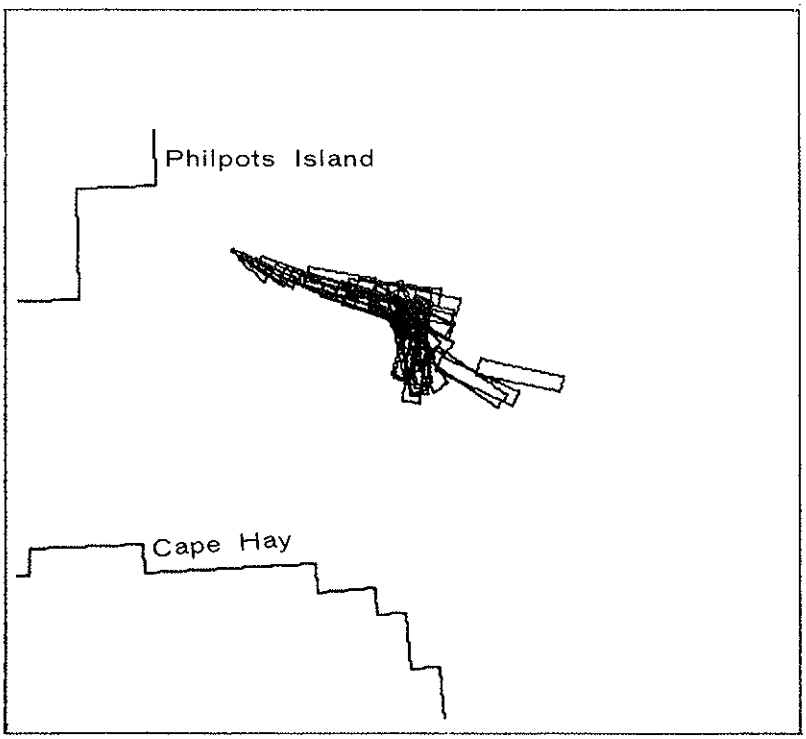

16 u) 4 W 20-7 - Site four; Blowout under 20 knot westerly wind; viewed seven days after initial release of oil.

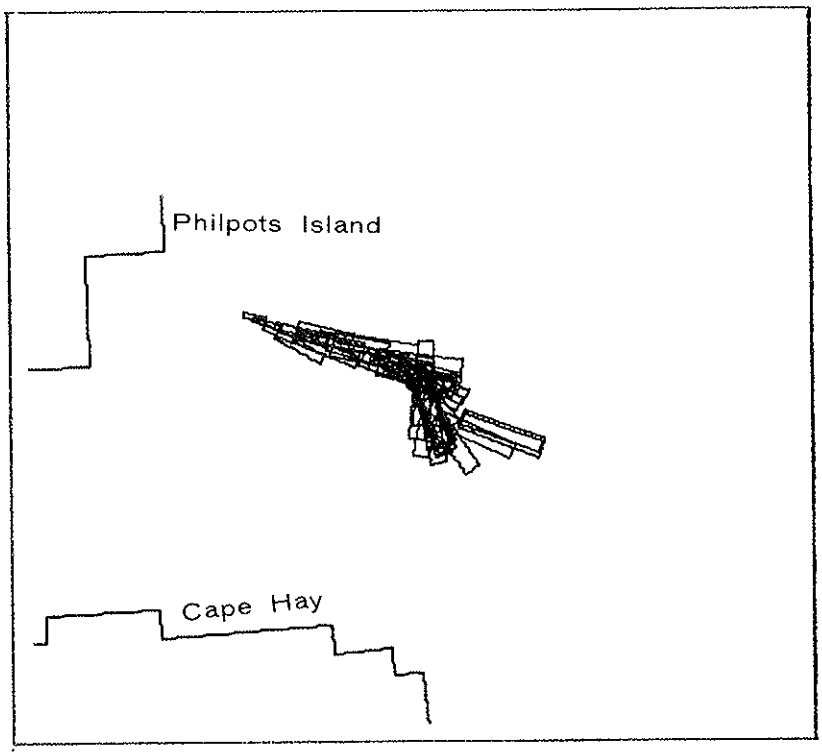

16 v) 4 S 10-2 - Site four; Blowout under 10 knot southerly wind; viewed two days after initial release of oil.

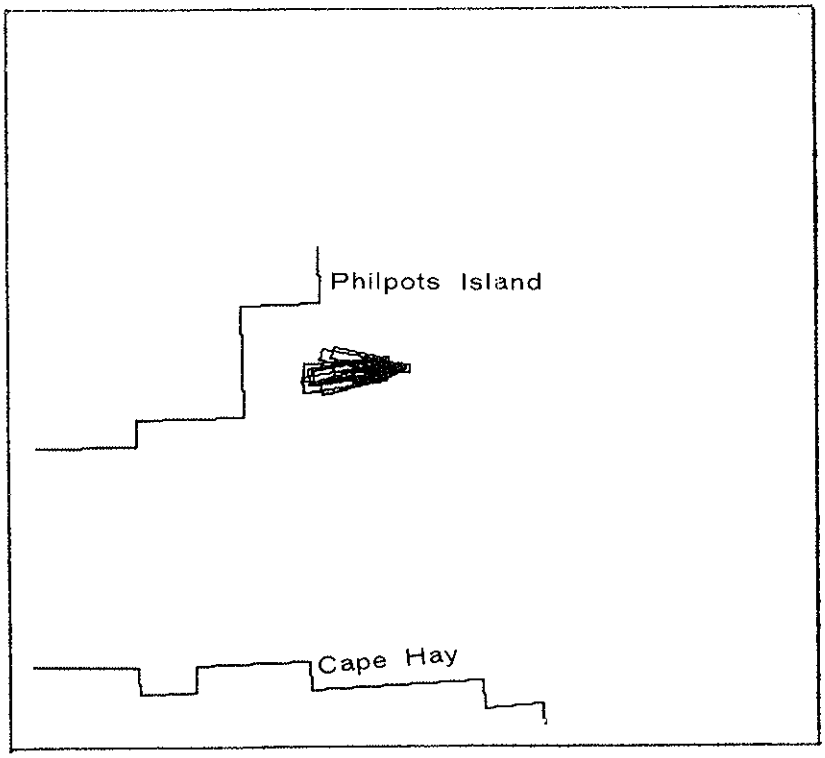

16 w) 4 S 10-4 - Site four; Blowout under 10 knot southerly wind; viewed four days after initial release of oil.

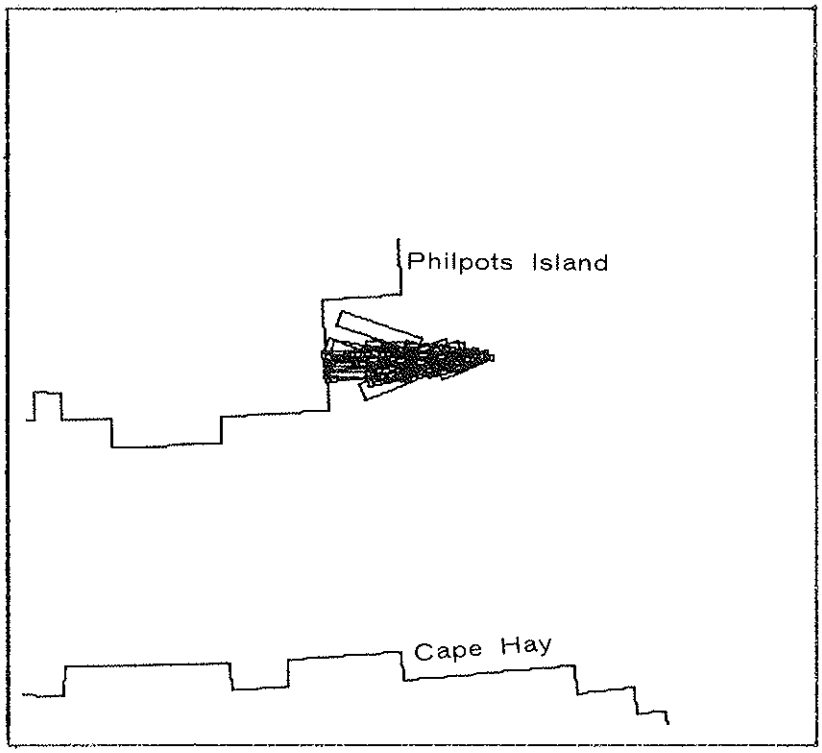

16 x) 4 S 20-2 - Site four; Blowout under 20 knot southerly wind; viewed two days after initial release of oil.

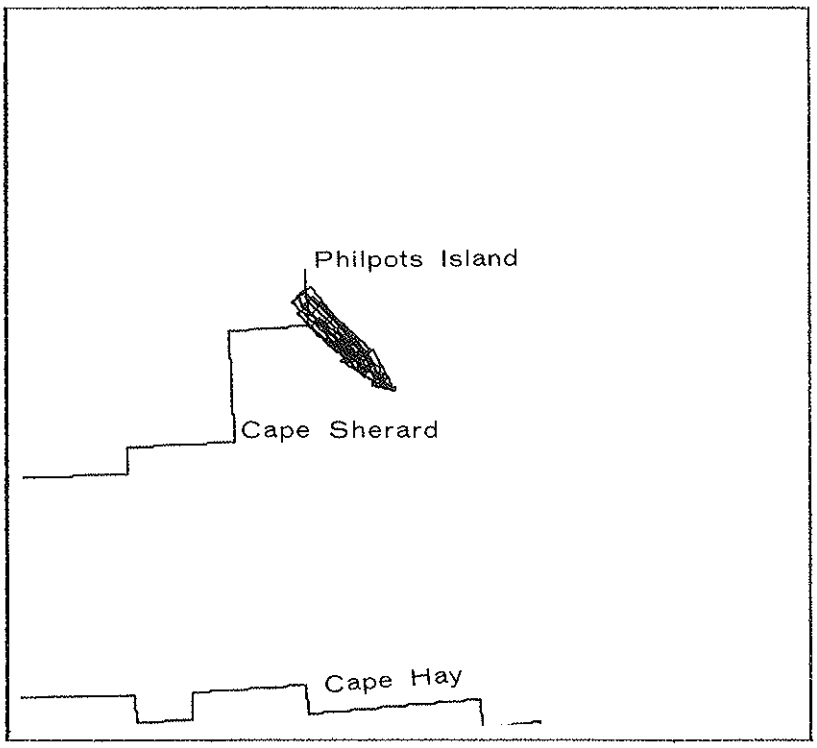

16 y) 4 § 20-3 - Site four; Blowout under 20 knot southerly wind; viewed three days after initial release of oil.

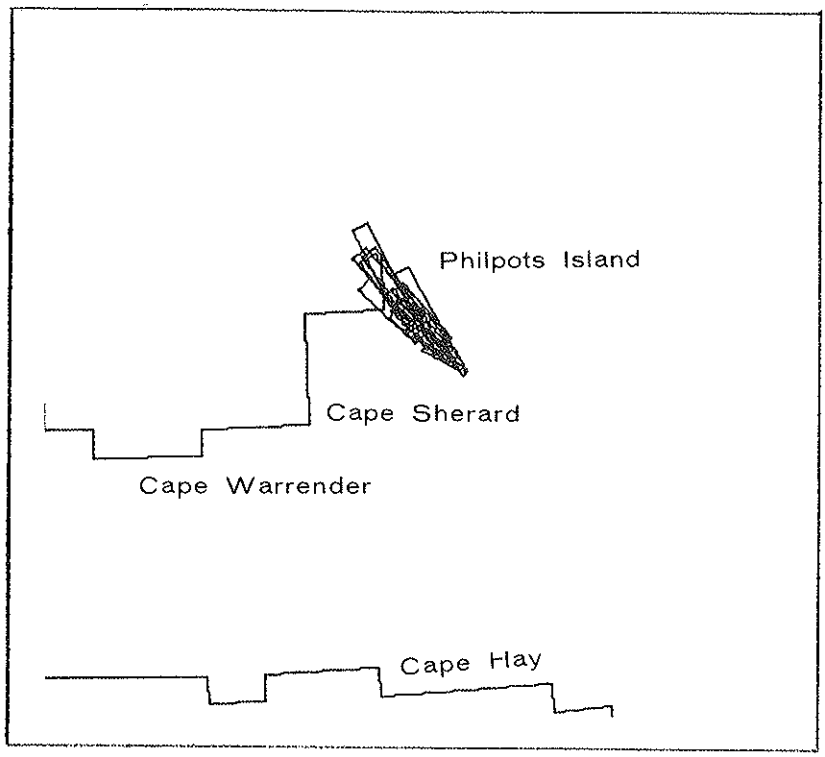

17 a)

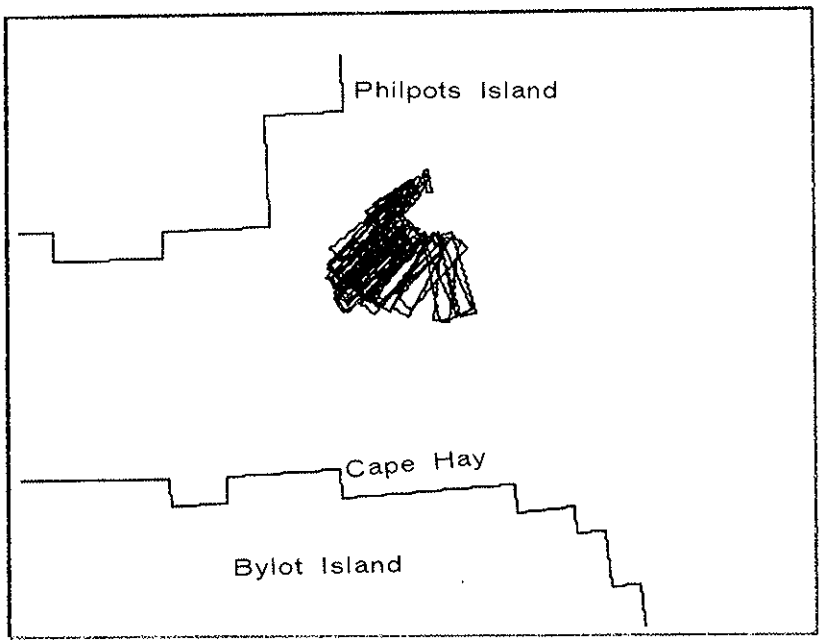

17 b)

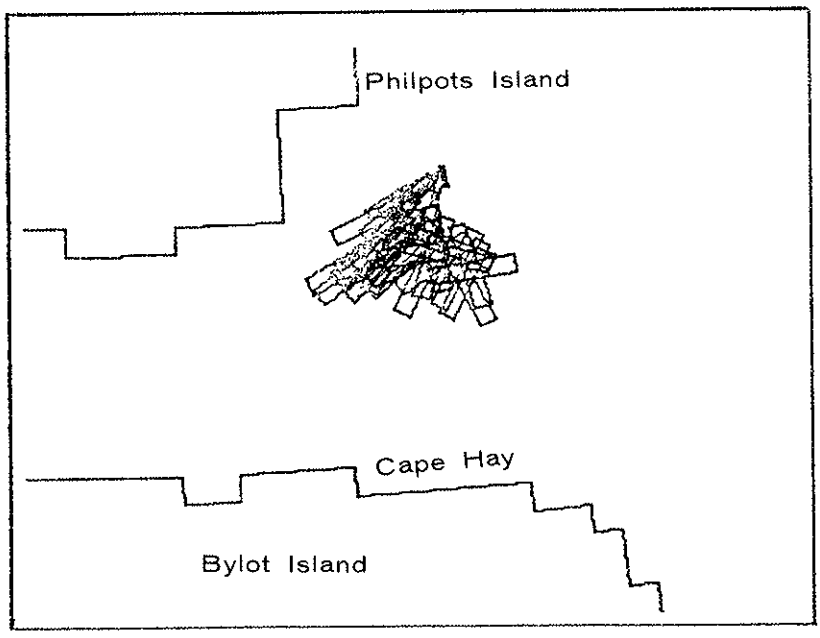

FIGURE 17a, b: THE DAY 3 CONFIGURATIONS OF A SITE NO. 4 BLOWOUT UNDER THE NOMINALLY NORTHERLY WINDS OF APPENDIX B FOR

(a) $D = 2 \times 10^5 cm^2/s$

(b) $D = 2 \times 10^6 cm^2/s$

18 a)

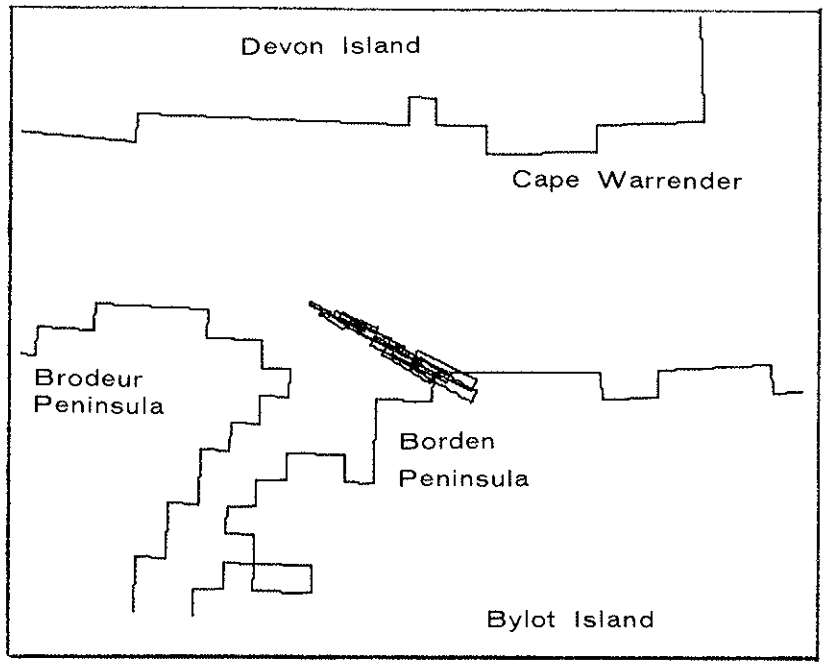

18 b)

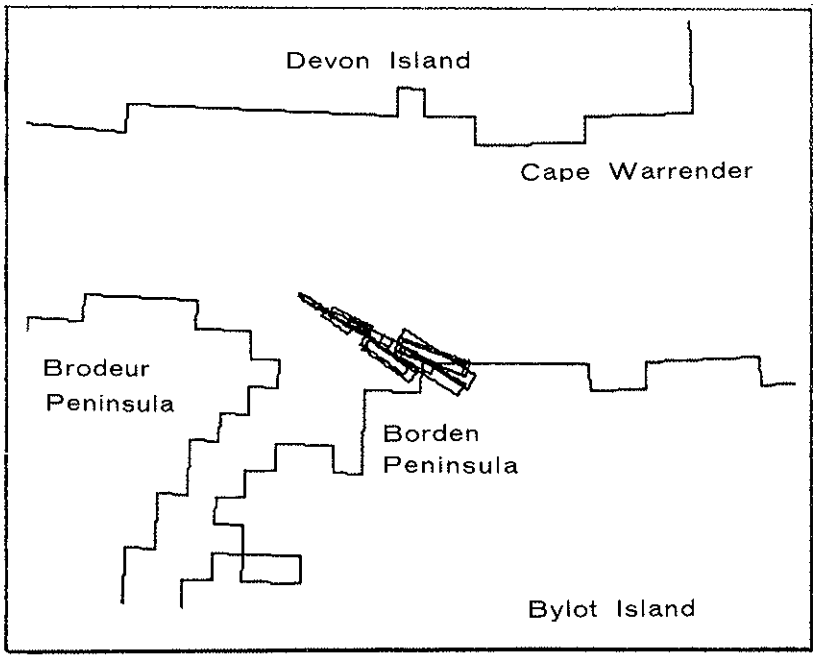

FIGURE 18 a,b: THE DAY 4 CONFIGURATION OF A SITE NO. 2 BLOWOUT UNDER THE NOMINALLY NORTHERLY WINDS OF APPENDIX B FOR

(a) $D = 2 \times 10^5 \text{ cm}^2/\text{s}$

(b) $D = 2 \times 10^6 \text{ cm}^2/\text{s}$

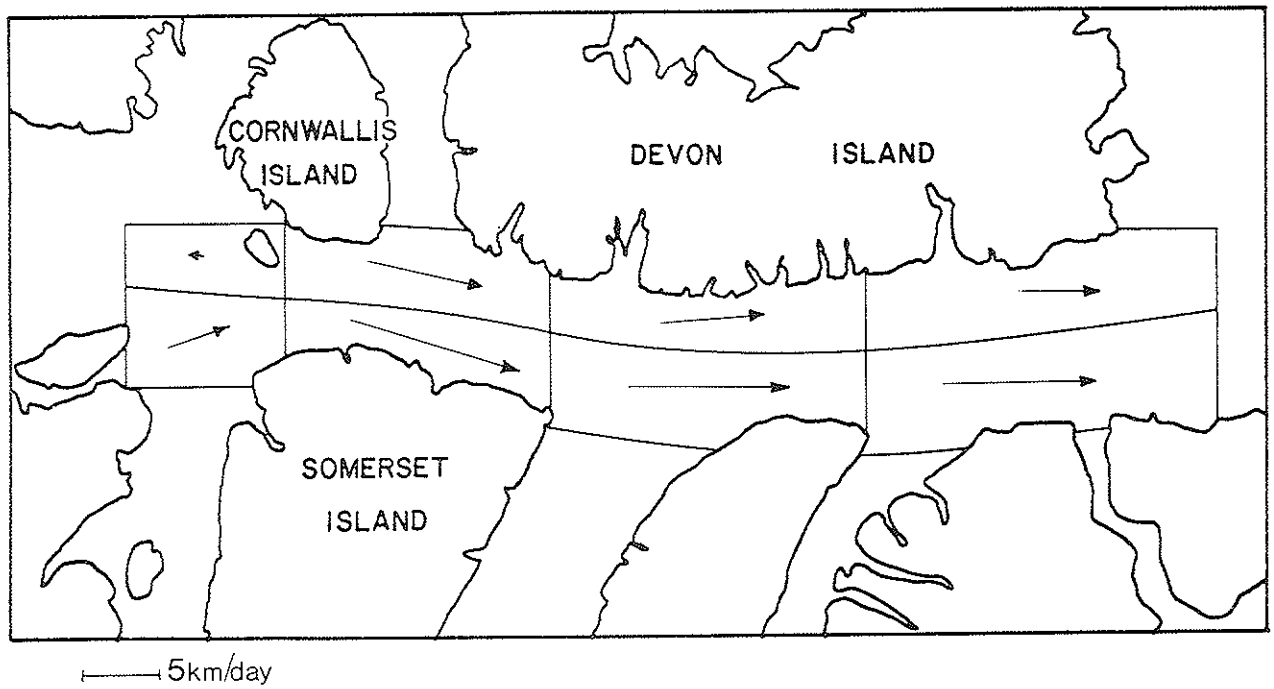

FIGURE 19: AVERAGE ICE VELOCITY VECTORS FOR THE SEPTEMBER TO MAY PERIOD IN EIGHT SECTORS OF EASTERN PARRY CHANNEL.

REFERENCES

Ahlstrom, S.W., "A Mathematical Model for Predicting the Transport of Oil Slicks". Battelle Pacific Northwest Laboratories, Richland, Washington, (1975).

Bishnoi, P.R. and B.B. Maini, "Laboratory Study of Behaviour of Oil and Gas Particles in Salt Water relating to Deep Oil-Well Blowouts", AMOP Technical Seminar, Edmonton, Alberta, (1979).

Blaikely, D.R., E.F.L. Dietzel, A.W. Glass and P.J. Kleek, "SLIKTRAK - A Computer Simulation of Offshore Oil Spills Cleanup Effects and Associated Costs". Proc. of Oil Spill Conference, New Orleans, La., (1977).

Blokker, D.C., "Spreading and Evaporation of Petroleum Products on Water", Proc. of 4th Int. Harbour Conf., Antwerp, Belgium, (1964).

Buckley, J. and B. Humphrey, "Fate of Dispersed Oil in the Environment", Part II: A Boomed Oil Spill, AMOP Technical Seminar, Edmonton, Alberta, (1979).

Fay, J.A., "Physical Processes in the Spread of Oil on a Water Surface". Proceedings of Joint Conference on Prevention and Control of Oil Spills, Washington, D.C. 544 pp., (1971).

FENCO, "An Oilspill Motion Model for Eastern Lancaster Sound", FENCO Consultants Ltd., Calgary, 57 pp., (1978).

Fissel, D.B., D.D. Lemon and G.R. Wilton, "A Preliminary Report on Physical Oceanographic and Iceberg Movement Studies in North-Western Baffin Bay", Submitted to Petro-Canada Ltd., (1978).

Fissel, D.B., and J.R. Marko, "A Surface Current Study on Eastern Parry Channel, N.W.T., Summer 1977", Institute of Ocean Sciences, Patricia Bay, 66 pp., (1978).

Fissel, D.B. and G.R. Wilton, "Sub-Surface Current Measurements in Eastern Lancaster Sound, N.W.T. - summer, 1977", Institute of Ocean Sciences, Patricia Bay, 72 pp., (1978).

Hill, S.H., D.B. Fissel and H. Serson, "A Study of Wind and Atmospheric Pressure in Eastern Parry Channel, N.W.T. - Summer, 1977". (1978).

Imperial Oil Ltd. "Environmental Impact Statement for Exploratory Drilling, Davis Strait Region", (1978).

Jeffrey, P.G., "Large-Scale Experiments on the Spreading of Oil at Sea and Its Disappearance by Natural Factors", Proc. of Joint Conf. on Prevention and Control of Oil Spills, pp. 469-474, (1973).

Kreider, R.E., "Identification of Oil Leaks and Spills", Proceedings of Joint Conference on Prevention and Control of Oil Spills, Washington, D.C., (1971).

MacKay, D. and P.J. Leinonen, "Mathematical Model of the Behaviour of Oil Spills on Water with Natural and Chemical Dispersion". Fisheries and Environment Canada, 84 pp., (1977).

Marko, J.R., "A Satellite Imagery Study of Eastern Parry Channel", Institute of Ocean Sciences, Patricia Bay, 134 pp., (1978).

Milne, A.R. and B.D. Smiley, "Offshore Drilling in Lancaster Sound". Institute of Ocean Sciences, Patricia Bay, 95 pp., (1978).

Murray, S.P., W.C. Smith and D.J. Sonu, "Oceanographic Observations and Theoretical Analysis of Oil Slicks during the Chevron Spill, March 1970". Technical Report No. 87, Coastal Studies Institute, Louisiana State University, Baton Rouge, La. 106 pp., (1970).

Murray, S.P., "Turbulent Diffusion of Oil in the Ocean". Limnology and Oceanography, XVII, pp. 651-660, (1972).

Neralla, V.R., W.S. Liu, S. Venkatesh and M.B. Danard, "Techniques for Predicting Sea Ice". A Symposium on Sea Ice Processes and Models, Seattle, Washington, pp. 87-97, (1977).

Okubo, A, "Oceanic Diffusion Diagrams", Deep Sea Research 18. pp. 789-802, (1971).

Sahota, H.S., Y.T. Tam, A.S. Rizkalla and M.B. Danard, "Prediction of the Motion of Oil Spills in Northern Canadian Waters", prepared for Atmospheric Environment Service, Downsview, Ontario, (1978).

Smith, J.E., "Torrey Canyon" Pollution and Marine Life. Cambridge University Press, (1970).

Topham, D.R., "Hydrodynamics of an Oilwell Blowout". Institute of Ocean Sciences, Patricia Bay, 52 pp., (1975).

APPENDIX A

COMPUTER PROGRAM LISTINGS

APPENDIX A

SIMULATOR PROGRAM DESCRIPTION

The oilspill simulator OILSIM was designed as a general purpose set of programs for assessing the likely levels of pollution at sites in the vicinity of a potential oil spill. It is designed to track individual parcels of oil at each time step of the program until:

a) a parcel leaves the area of the study
b) the amount of oil in a given parcel is reduced to zero due to dissipation and/or shoreline contact.

In each case the parcel is deleted from the list of active tracked oil masses.

The direction and velocity associated with the diffusive component of motion were expressed as:

$$V = RAN(R) * SQRT(3.) * SQRT(C*t)$$
$$D + RAN(R) * 360.$$

where RAN (R) = A random number $0. < RAN(R) < 1.$
C = Diffusion Coefficient (=D in text)
t = length of time step in seconds

The spatial spreading of each parcel was written as:

$$AREA = 1.6\,(a + 20000)^{1.52} \text{ in meters}$$

where a = parcel age in seconds
AREA was allowed a maximum value = 154.675 square kilometers

Losses due to shoreline (beach) contact was calculated from

$$L = OIL * (ac-pac)/(AREA-pac)$$

where L = oil loss
OIL = amount of oil in parcel
ac = area of beach contact
pac = previous area of beach contact

ac > pac, otherwise L = 0.

Losses are calculated for each parcel at each time step. Area plots and beach contact totals are tabulated at daily intervals (8 time steps).

The routines used in the model are:

MAIN - Main program, reads in all data needed for run.

LAND - Defines the water, shore and inland pixels on the grid.

CURS - Updates the current grid.

WIND - Updates the wind grid.

DATE - Computes time and date given time frame number.

BEACH - Computes beach contact, plots area of spill and reports beach contacts.

CLEAN - Removes parcels with Zero oil content.

PIXELS - Converts Radian latitudes and longitudes into grid coordinates.

DTOR - Converts latitudes and longitudes as DDD.MMHH into Radians.

RTOD - Inverses effect of "DTOR" function.

RAN - Generates a random number in the range $0<x<1$.

OSPI, OSPZ, OSPROJ - Oblique stereographic projection routines.

PLOTS, PLOT, SYMBOL, NUMBER - Calcomp plot routines.

The model uses several data files. These will be defined and described in detail:

UNIT NO. 2 - Current definition file (Format varies with Curs routine).

REC NO. 1 - Format (13) - Contains No. of following records.

REC NO. 2-N - Format (515, G15.7) Starting and ending X, starting and ending Y, direction and velocity (cm/s).
The current defined by direction and velocity is assigned to the rectangle defined by the starting and ending X and Y.

UNIT NO. 3 - Wind definition file (format varies with wind routine)

REC. NO. 1 - Format (12) - Number of rectangles (NR)

REC NO. 2 - NR + 1 - Format (415) - Starting and ending X, starting and ending Y.

REC NO. NR + 2 - Format (12) - Number of data sets (NS).

AREC NO. NR + 3 - N - Format (15, G15.7) Direction and velocities of NS data sets by NR rectangles.

Note: Direction is the direction of wind origin.

UNIT NO. 4 - Pixel definition file.

REC Format (2014) 5 data set per card.
Data set format (IY, 15X, IEX, IV)

IY - Pixel Y line.
ISX - Starting X.
IEX - Ending X.
IV - Value assigned to all pixels on line IY, ISX, through IEX such that;
IV = 0 - Pixel contains water only.
= 1 - Pixel contains land and water.
= 2 - Pixel contains land only.
= 3 - If anything goes into this pixel ignore it.

UNIT NO. 7 - Beach and shoreline definition file.
REC NO. 1 - Format (15) number of beach definitions.
Beach Definitions:

REC TYPE A - Format (I5, 5X, A40) number of pixels on beach (NP) and beach name.
REC TYPE B - Format (1615) NP pairs of X,Y pixel number pairs.
REC NO. 2 - Format (15) number of shoreline definitions
Shoreline Definitions:

REC format (I5, 2G15.7) IPEN, RY, RX

where:

IPEN = Calcomp plot routine pen control variable.
RY = Radian latitude.
RX = Radian longitude.

The shoreline definitions allows the user to determine the shoreline to be plotted, together with smaller landmass features not included.

UNIT NO. 5 - Run control file.
REC NO. 1 - Format (A20) title to be printed on plots.
REC NO. 2 - Format (GI5) number of time frames, span of time frame in hours, hour, day, month and year of time frame No. 1.
REC NO. 3 - Format (I5) number of parcels to release (NP).
(NP) RECS - Format (2F10.4, I5, F10.2) latitude, longitude, time frame and number of barrels to release.

REC. NO. 5 - Format (F5.1, I5) percentage of wind to use and seed for random number generator 0<seed<100.

REC NO. 6 - Format (G20.10) diffusion coefficient.

Runstream

```
1:@RUN,/R MARKXX,OAS-ARCTIC/MARK01,MARK01,60,200
2:@SYM PRINT$,,PG1
3:@ASG,A SIMLAND.          PIXEL DEFINITION FILE
4:@USE 4.,SIMLAND.
5:@ASG,A SIMCUR.           CURRENT DEFINITION FILE
6:@USE 2.,SIMCUR.
7:@ASG,A SWIND10.          WIND DEFINITION FILE
8:@USE 3.,SWIND10.
9:@ASG,A SIMBEACH.         BEACH DEFINITION FILE
10:@USE 7.,SIMBEACH.
11:@ASG,U SPLOT7.,F2       PLOT FILE
12:@USE PLOT$.,SPLOT7.
13:@ASG,A SIM2.
14:@XQT SIM2.MAINT
15:SOUTH WIND 10 KNOTS <TITLE
16:  56   3    0    1    9    78    <TIME FRAME INFORMATION
17:  56                              <NO. OF PARCELS
18:  74.0750   89.3300   1   712.
19:  74.0750   89.3300   2   712.
20:  74.0750   89.3300   3   712.
21:  74.0750   89.3300   4   712.
                                     PARCEL DEFINITIONS
70:  74.0750   89.3300   53  712.
71:  74.0750   89.3300   54  712.
72:  74.0750   89.3300   55  712.
73:  74.0750   89.3300   56  712
74:  3    34
75:      1000000.                    <% OF WIND AND SEED

76:@EOF                              < DIFFUSION COEFFICIENT
```

```
C
C       PROGRAM --- SIM
C
C       PURPOSE --- LANCASTER SOUND OIL SPILL MODEL
C
C       METHOLOGY --- J. R. MARKO PHD.
C
C       PROGRAMMING --- C. R. FOSTER CCP (SYSTEMS)
C
C       BY --- ARCTIC SCIENCES LTD
C
C       SOURCE CODE --- FORTRAN 4
C
C       SOURCE COMPUTER --- UNIVAC 1106
C
      REAL RLAT(100),RLON(100),FLOW(100),SAM(100),CE(24,62),CN(24,62)
      REAL WE(24,62),WN(24,62),EVAP(5),W1(5),W2(5),AREA(100)
      REAL A1(100),A2(100),A3(100),SE(100),SN(100)
C
C     A1,A2,A3 HAVE NO MEANING IN THE MAIN PROGRAM,
C      THEY ONLY HAVE MEANING IN SUBROUTINE BEACH AND USE THE
C      MAIN PROGRAM AS A VEHICLE SO THAT CLEAN CAN KEEP TRACK
C      OF THEM.
C
      CHARACTER*20 TITLE
      INTEGER IB(100),ST(24,62),AGE(100)
      DATA EVAP /37.5,4.5,4.,3.5,3./
      DATA W1/7.5,7.,6.,5.,4./
      DATA W2/10.5,10.,9.,7.,6./
      ROOT3 = SQRT(3.)
      IPR = 1
      IPL = 1
C
C       READ THE TITLE CARD.
C
      READ (5,8999)TITLE
8999  FORMAT (A20)
C
C     READ THE TIME DEFINITION CARD.
```

```
      C
            READ (5,9000)IFRAM,ISPAN,IH,ID,IM,IYR
9000  FORMAT(6I5)
      C
      C     READ IN THE NUMBER OF PARCELS.
      C
            READ (5,9000)NSP
      C
      C       READ IN THE PARCELS.
      C
            DO 1 I=1,NSP
              READ (5,9001)WLAT,WLON,IB(I),FLOW(I)
9001          FORMAT(2F10.4,I5,F10.2)
              RLAT(I) = DTOR(WLAT)
              RLON(I) = DTOR(WLON)
          1 CONTINUE
      C
      C    READ IN % OF WIND & NUMBER OF LOOPS FOR THE RANDONM NUMBER GENERATOR.
      C
            READ (5,9003)PW,IPRN
9003  FORMAT(F5.1,I5)
      C
      C     READ IN THE DIFUSSION COEFFICIENT.
      C
            READ (5,9002)DIFUS
9002  FORMAT(G20.10)
            PW = PW/100.
            R = -1.
            TIMULT = FLOAT(ISPAN)*3600.
            INTERV = 24/ISPAN
      C
      C     INIALISE THE RANDONM NUMBER GENERATOR.
      C
            DO 2 I=1,IPRN
          2 X = RAN(R) * RAN(R)
      C
      C     READ IN THE LAND DEFINITION FILE.
      C
            CALL LAND (ST)
```

```
      NSPL = 0
      DO 30 I=1,IFRAM
C
C     CALCULATE CURRENT TIME FRAME TIME AND DATE.
C
      CALL DATE (IH1,ID1,IM1,IY1,I,ISPAN,IH,ID,IM,IYR)
C
C     UPDATE THE CURRENT GRID.
C
      CALL CURS (CE,CN,I)
C
C     UPDATE THE WIND GRID.
C
      CALL WIND (WE,WN,I)
      IF (NSPL.EQ.0)GO TO 15
C
C     FOR EACH PARCEL COMPUTE NEW POSITION.
C
      DO 5 J=1,NSPL
      CALL PIXELS (RLAT(J),RLON(J),IX,IY)
      CME = (CE(IY,IX) + PW*WE(IY,IX))*TIMULT
      CMN = (CN(IY,IX) + PW*WN(IY,IX))*TIMULT
C
C     COMPUTE AND ADD IN THE RANDONM COMPONENT.
C
      D1 = RAN(R)*ROOT3*SQRT (DIFUS*TIMULT)
      D2 = RAN(R)*6.2831852
      CER = CME + SIN(D2)*D1
      CNR = CMN+ COS(D2)*D1
      ITC = 0
  908 SE (J) = CER
      SN (J) = CNR
      DY = RLAT(J) + CNR/636239471.
      DX = RLON(J) - CER/(COS(DY)*636239471.)
      CALL PIXELS (DY,DX,IXT,IYT)
C
C   CHECK TO SEE IF PARCEL IS ON THE GRID
C
      IF (IXT.LT.1.OR.IXT.GT.62)GO TO 31
```

```
118             IF (IYT.LT.1.OR.IYT.GT.24)GO TO 31
119             IF (ST(IYT,IXT).GE.-1)GO TO 4
120             IF (ITC.EQ.25)GO TO 909
121             ITC = ITC + 1
122             CER = CER * .9
123             CNR = CNR * .9
124             GO TO 908
125           4 RLAT(J) = DY
126             RLON(J) = DX
127       C
128       C     COMPUTE THE INCREASE OF OIL TO EACH PARCEL, AND
129       C     COMPUTE THE LOSSES DUE TO EVAPORATION AND WIND.
130       C
131         909 AGE(J) = AGE(J) + ISPAN
132             IDAY = 1+ AGE(J)/24
133             IF (IDAY.GT.5)IDAY=5
134             SAM(J) = SAM(J) - EVAP(IDAY)
135             IF (SQRT(WE(IY,IX)**2 + WN(IY,IX)**2).GT.700.)GO TO 3
136             SAM(J) = SAM(J) - W1(IDAY)
137              GO TO 5
138       C
139       C     IF PARCEL OFF GRID ZERO OIL.
140       C
141          31 SAM(J) =0.
142             GO TO 5
143           3   SAM(J) = SAM(J) - W2(IDAY)
144           5 CONTINUE
145          15   IF (NSPL.EQ.NSP)GO TO 20
146             IF (I.LT.IB(NSPL+1))GO TO 20
147             NSPL = NSPL + 1
148             SAM (NSPL) = FLOW(NSPL)
149          20 IF (IPR.NE.1)GO TO 22
150       C
151       C       PRINT THE FRAME TITLE.
152       C
153             IF (I/8*8.NE.I)GO TO 22
154             WRITE (6,9600)I,IH1,ID1,IM1,IY1,NSPL
155        9600  FORMAT('1',//,30X,' TIME FRAME #',I3,//,10X,'TIME:',
156            &   I3,':00 GMT,',I4,'-',I2,'-',I2,//,10X,
```

```
157            &    'THERE ARE',I3,' ACTIVE ELEMENTS.',//)
158       C
159       C     COMPUTE THE AREA OF THE PARCELS.
160       C
161           22 DO 25 J = 1,NSPL
162              SAM(J) = AMAX1(SAM(J),0.)
163              AR = 1.6*(AGE(J)*3600.+20000.)**1.52
164              AREA(J) = AMIN1(AR,154675295.)
165           25 CONTINUE
166       C
167       C     PLOT THE SPILLS AND CHECK FOR CONTACT WITH THE BEACH.
168       C
169               CALL BEACH (I,NSPL,A1,A2,A3,RLAT,RLON,SE,SN,AREA,SAM,ST,IPR,IPL,
170            &  TITLE)
171       C
172       C     CLEAN UP ANY PARCELS THAT CONTAIN NO OIL.
173       C
174               CALL CLEAN(RLAT,RLON,FLOW,SAM,AREA,SE,SN,
175            &       A1,A2,A3,IB,AGE,NSPL,NSP)
176           30 CONTINUE
177              IF (IPL.EQ.1)CALL PLOTND
178              STOP
179              END
```

```
      SUBROUTINE LAND (S)
C
C     PROGRAM --- OILSIM
C
C      MODULE --- LAND
C
C     PURPOSE --- TO DEFINE THE PIXELS THAT ARE ON THE
C                   SHORE AS WELL AS INLAND.
C
C     PROGRAMMER --- C. R. FOSTER
C
C     SOURCE CODE --- FORTRAN 4
C
C     SOURCE COMPUTER --- UNIVAC 1106
C
C*****
C     DATA DEFINITIONS
C*****
      INTEGER C(5,4), S(24,62)
C*****
C     END OF DATA DEFINITIONS
C*****
C
C    THE STATUS VALUES ARE:
C
C        0 --- WATER
C        1 --- BEACH AREA
C        2 --- LAND (NO WATER CONTACT)
C        3 --- IGNORE
C
      DO 5 I=1,24
      DO 5 J=1,62
    5 S(I,J)=0
   10 READ(4,9000,END=25)((C(I,J),J=1,4),I=1,5)
 9000 FORMAT(20I4)
      DO 20 I=1,5
        IF (C(I,1).LT.0)GO TO 10
        IF (C(I,1).EQ.999)GO TO 25
        IF (C(I,1).GT.24)GO TO 20
```

```
40              I0 = C(I,1)
41              I1 = C(I,2)
42              I2 = C(I,3)
43              IV = C(I,4)
44              DO 15 J=I1,I2
45        15      S(I0,J) = IV
46        20 CONTINUE
47           GO TO 10
48        25 RETURN
49           END
```

```
      SUBROUTINE CURS (E,N,IO)
C
C       MODULE --- CURS / SIM
C
C       PURPOSE --- TO READ IN AND MAINTAIN THE CURRENT GRID
C
C       PROGRAMMING --- C. R. FOSTER CCP (SYSTEMS)
C
C     THIS VERSION READS ONLY 1 CURRENT GRID.
C
      REAL E(24,62), N(24,62)
      IF (IO.NE.1)RETURN
      READ (2,9000)NG
 9000 FORMAT(I3)
      DO 10 I=1,NG
      READ (2,9001)ISX,IEX,ISY,IEY,ID,V
 9001 FORMAT(5I5,G15.7)
      A = FLOAT(ID)/57.29577951
      CE = V*SIN(A)
      CN = V*COS(A)
      DO 2 J=ISX,IEX
      DO 2 K=ISY,IEY
        E(K,J) = CE
    2   N(K,J) = CN
   10 CONTINUE
      RETURN
      END
```

```
      SUBROUTINE WIND (E,N,IO)
C
C       MODULE --- WIND / SIM
C
C       PURPOSE --- TO READ IN AND MAINTAIN THE WIND GRID
C
C       PROGRAMMER --- C. R. FOSTER CCP (SYSTEMS)
C
      REAL E(24,62), N(24,62)
      INTEGER G(10,4)
C
C     IF NOT THE FIRST TIME THROUGH THEN SKIP TO UPDATE.
C
      IF (IO.GT.1)GO TO 10
C
C     READ IN THE NUMBER OF GRID PATTERNS.
C
      READ (3,9000)NG
9000  FORMAT(I2)
C
C     READ IN THE GRID PATTERNS.
C
      DO 1 I=1,NG
    1 READ (3,9001)(G(I,J),J=1,4)
9001  FORMAT(4I5)
      IA = 0
C
C     READ IN THE NUMBER OF GRIDS IN THIS FILE.
C
      READ (3,9000)IDT
    2 IF (IA.GE.IDT)RETURN
      IA =IA + 1
C
C     READ IN A NEW GRID.
C
      DO 5 I=1,NG
      READ (3,9002)ID,V
9002  FORMAT(I5,G15.7)
      A=FLOAT(MOD(ID+180,360))/57.29577951
```

```
40              V = V *51.4096
41              CE = V*SIN(A)
42              CN = V*COS(A)
43              ISX = G(I,1)
44              IEX = G(I,2)
45              ISY = G(I,3)
46              IEY = G(I,4)
47              DO 3 J=ISX,IEX
48              DO 3 K = ISY,IEY
49              E (K,J) = CE
50            3 N (K,J) = CN
51            5 CONTINUE
52      C
53      C       CHECK TO SEE IF AN UPDATE IS REQUIRED (EVERY 4 FRAMES).
54      C
55              RETURN
56           10 IF (MOD(IO,4).EQ.0)GO TO 2
57              RETURN
58              END
```

```
C
C       MODULE --- DATE
C
C       PURPOSE --- COMPUTES THE DATE GIVEN STARTING TIME,
C                    LENGTH OF INTERVAL & # OF INTERVALS SINCE START.
C
C       PROGRAMMER --- C. R. FOSTER
C                      ARCTIC SCIENCES LTD,
C                       SIDNAY, B.C.
C
C       SOURCE CODE --- FORTRAN 4
C
C       SOURCE COMPUTER --- UNIVAC 1106, IOS, PAT BAY.
C
      SUBROUTINE DATE (IH,ID,IM,IY,I,ISPAN,IH1,ID1,IM1,IY1)
      INTEGER DAYS(12)
      DATA DAYS /31,28,31,30,31,30,30,31,30,31,30,31/
      ID = ID1
      IM = IM1
      IY = IY1
      IH = (I-1)*ISPAN
    1 IF (IH.LT.24)GO TO 2
      IH = IH - 24
      ID = ID + 1
      GO TO 1
    2 IF (ID.LE.DAYS(IM))RETURN
      ID = ID - DAYS(IM)
      IM = IM + 1
      IF (IM.LE.12)GO TO 2
      IM = 1
      IY = IY + 1
      DAYS(2) = 28
      IF (IY/4*4.EQ.IY)DAYS(2)=29
      GO TO 2
      END
```

```
      FUNCTION DTOR (X)
C
C      SUB MODULE --- DTOR
C
C      PURPOSE --- TO CONVERT DEGREES AS DDD.MMFFFFFFF TO RADIANS
C
C      PROGRAMMER --- C. R. FOSTER
C
C      SOURCE CODE --- FORTRAN 4
C
C      SOURCE COMPUTER --- UNIVAC 1106
C
      DTOR = (FLOAT(IFIX(X)) + AMOD(X,1.)/.6) / 57.29577951
      RETURN
      END
```

```
      FUNCTION RTOD (X)
C
C      SUB MODULE --- RTOD
C
C      PURPOSE --- TO CONVERT RADIANS TO DEGRESS AS DDD.MMFFF
C                  INVERSES EFFECT OF DTOR.
C
C      PROGRAMMER --- C. R. FOSTER
C
C      SOURCE CODE --- FORTRAN 4
C
C      SOURCE COMPUTER --- UNIVAC 1106
C
      X1 = X * 57.29577951
      RTOD = FLOAT(IFIX(X1)) + AMOD(X1,1.)*.6
      IF (AMOD(RTOD,1.).GE.0.5999)RTOD = RTOD + 0.4
      RETURN
      END
```

```
C
C       MODULE --- PIX
C
C       PURPOSE --- CONVERTS PIXELS NUMBERS INTO RADIAN LATS & LONS.
C
C       PROGRAMMER --- C. R. FOSTER CCP
C                       ARCTIC SCIENCES LTD,
C                        SIDNEY, B.C.
C
C       SOURCE CODE --- FORTRAN 4
C
C       SOURCE COMPUTER --- UNIVAC 1106, IOS, PAT BAY.
C
      SUBROUTINE PIX (IY,IX,LAT,LON)
      REAL LAT,LON
      LON = 1.3195736+FLOAT(IX-1)*.0052883
      LAT = 1.2748175+FLOAT(IY-1)*.0014544
      RETURN
      END
```



```
C
C       MODULE --- PIXELS
C
C       PURPOSE --- CONVERTS LATS & LONS IN RADIANS INTO PIXEL NUMBERS.
C
C       PROGRAMMER --- C. R. FOSTER CCP
C                       ARCTIC SCIENCES LTD
C                        SIDNEY, B.C.
C
C       SOURCE CODE --- FORTRAN 4
C
C       SOURCE COMPUTER --- UNIVAC 1106, IOS, PAT BAY.
C
      SUBROUTINE PIXELS (LAT,LON,IX,IY)
      REAL LAT,LON
      IX = 1+(LON-1.3169293)/.0052883
      IY = 1+(LAT-1.2740902)/.0014544
      RETURN
      END
```

```
C
C       MODULE --- CLEAN
C
C       PURPOSE --- ELIMINATES PARCELS THAT HAVE NO OIL LEFT.
C
C       PROGRAMMER --- C. R. FOSTER CCP
C                       ARCTIC SCIENCES LTD,
C                        SIDNEY, B.C.
C
C       SOURCE CODE --- FORTRAN 4
C
C       SOURCE COMPUTER --- UNIVAC 1106, IOS, PAT BAY.
C
      SUBROUTINE CLEAN (RLT,RLN,F,SM,AR,SE,SN,A1,A2,A3,
     &      IB,AG,NS,NSP)
      REAL RLT(100),RLN(100),F(100),SM(100),AR(100)
      REAL A1(100), A2(100), A3(100), SE(100),SN(100)
      INTEGER IB(100), AG(100), ID(100)
      N = 0
      NN=0
      DO 5 I=1,NSP
      IF (I.GT.NS)GO TO 3
      IF (SM(I).LT.0.1)GO TO 5
      NN=NN+1
    3 N=N+1
      ID(N)=I
    5 CONTINUE
      IF (N.EQ.0)RETURN
      DO 10 I=1,N
      IDP = ID(I)
      RLT(I) = RLT(IDP)
      RLN(I) = RLN(IDP)
      F(I) = F(IDP)
      SM(I) = SM(IDP)
      AR(I) = AR(IDP)
      SE(I) = SE(IDP)
      SN(I) = SN(IDP)
      IB(I) = IB(IDP)
```

```
      AG(I) = AG(IDP)
      A1(I) = A1(IDP)
      A2(I) = A2(IDP)
      A3(I) = A3(IDP)
   10 CONTINUE
      NS = NN
      NSP = N
      RETURN
      END
```

```
      FUNCTION RAN(X)
C
C      ROUTINE NAME --- RAN
C
C      PURPOSE --- INTERFACE ROUTINE FOR RANDOM NUMBER GENERATION
C                    SINCE THERE IS NO RAN ROUTINE ON THE UNIVAC
C                    THIS ROUTINE INTERFACES CALLS TO RAN WITH
C                    CALLS TO GGUBF IN THE IMSL LIBRARY.
C
C                  RAN MUST BE INITIALISED BY A CALL WITH X < 0.0
C
C      PROGRAMMER --- C. R. FOSTER CCP
C
C      SOURCE CODE --- FORTRAN
C
C      SOURCE COMPUTER --- UNIVAC 1106
C
      IF (X.LT.0.)GO TO 10
    5 RAN = GGUBF(ISEED)
      RETURN
   10 ISEED = 172635421.
      X = 0.0
      GO TO 5
      END
```

```
      SUBROUTINE BEACH (IFR,NS,SME,SMN,ASL,RLT,RLN,SE,SN,AREA,SAM,
     &       ST,IPR,IPLI,TITLE)
C
C       MODULE --- BEACH
C
C       PURPOSE --- KEEPS TRACK OF OIL ON BEACHES
C
C       PROGRAMMER --- C. R. FOSTER CCP
C
C       DATE --- 19 FEB 79
C
       REAL RLT(100),RLN(100),SE(100),SN(100),AREA(100),SAM(100)
       REAL BAM(24,62), ASL(100), HAM(10), SME(100), SMN(100)
       INTEGER ST(24,62)
       INTEGER NPTS(15),ICH(10,2),IX(15,30),IY(15,30)
        REAL XR(120),YR(120), R(4),X(4),Y(4)
       INTEGER IPENS (120)
       CHARACTER*20 TITLE
       CHARACTER*40 ID(15)
       DATA R/.19739556,2.944197094,3.338988213,6.085789747/
       IF (IFR.GT.1)GO TO 80
       DO 5 I=1,100
         SME(I) =0.
     5   SMN(I) =0.
C
C     INITIALIZE & SETUP    (PART 1)
C
C 1) READ BEACH DEFINITION CARDS
C
       READ(7,9000)NBEACH
9000   FORMAT(16I5)
       DO 10 I=1,NBEACH
         READ(7,9001)NP,ID(I)
9001     FORMAT(I5,5X,A40)
         NPTS(I) = NP
         READ (7,9000)(IX(I,J),IY(I,J),J=1,NP)
    10 CONTINUE
C
C 2)  SET BEACH OIL COUNTER MATRIX TO 0.0
```

```
      C
            DO 20 I=1,24
            DO 20 J=1,62
         20 BAM(I,J)=0.
      C
      C      SET AREA LOST COUNTER STORAGE TO 0.
      C
            DO 25 I=1,100
         25 ASL(I) = 0.0
      C
      C 3) SET UP FOR PLOTTING IF NEEDED.
      C
            IF (IPL1.NE.1)CALL PLOTS('SML','BLK','BLK','INK')
      C
      C 4) PRIME THE STEREO-GRAPHIC PROJECTION ROUTINES.
      C
           CALL OSP1 (.035,.035,.05,.05)
            CALL OSP2 (1.2944,1.4439,XINCH,7.)
      C
      C   CHECK PHASE   (PART  2)
      C
         80 DO 90 I=1,NS
            SME(I)=SME(I) + SE(I)
            SMN(I)=SMN(I) + SN(I)
         90 CONTINUE
        100 IPL = IPLI
      C
      C      PLOT OUTLINE IF CALLED FOR.
      C
            IF (IFR/8*8.NE.IFR)IPL=0
            IF (IPL.NE.1)GO TO 105
            IF (IFR.NE.8)CALL FRAME
              CALL PLOT (6.,4.,-3)
              CALL SYMBOL (-4.,-3.8,.21,'DAY # ',0.,6)
              CALL NUMBER (999.,999.,.21,FLOAT(IFR/8),0.,-1)
            CALL SYMBOL (-4.,-4.1,.21,TITLE,0.,20)
              CALL PLOT (-5.5,-3.5,3)
              CALL PLOT (5.,-3.5,2)
              CALL PLOT (5.,3.5,2)
```

```
79              CALL PLOT (-5.5,3.5,2)
80              CALL PLOT (-5.5,-3.5,2)
81        C
82        C     PLOT THE RECTANGLES THAT REPRESENT EACH PARCEL OF OIL.
83        C
84          105 DO 180 I=1,NS
85              IF (SAM(I).LT.0.1)GO TO 179
86              IF (ABS(SME(I)).LT.0.1 .AND. ABS(SMN(I)).LT.0.1)GO TO 179
87              D=SQRT (SME(I)**2+SMN(I)**2)
88              ANG=ACOS(SME(I)/D)
89              IF (SMN(I).LT.0.0)ANG = 6.283155307-ANG
90              WM = SQRT(AREA(I)/5.)
91              SM = WM*5.
92              DP = SQRT (SM*SM+WM*WM)/2.
93              DO 110 J=1,4
94              AR = AMOD(ANG+R(J),6.283155307)
95              X1 = DP*COS(AR)
96              Y1 = DP*SIN(AR)
97              Y(J) = RLT(I) + Y1/6362394.71
98              X(J) = RLN(I) - X1/(COS(Y(J))*6362364.71)
99              IF (IPL.NE.1)GO TO 110
100             CALL OSPROJ (Y(J),X(J),X1,Y1)
101             IP = 3
102             IF (J.NE.1)IP=2
103             CALL PLOT (X1,Y1,IP)
104             IF (J.NE.4)GO TO 110
105             CALL OSPROJ(Y(1),X(1),X1,Y1)
106             CALL PLOT (X1,Y1,2)
107         110 CONTINUE
108       C
109       C      CHECK FOR BEACH CONTACT
110       C
111       C
112       C     COMPUTE THE AREA OF SHORE OVERLAP.
113       C
114             ARMIC = AREA(I)/100.
115             DO 115 K=1,10
116         115 HAM(K) = 0.0
117             NH = 0
```

```
118             SL = 0.
119             Y23 = Y(2)-Y(3)
120             X23 = X(2)-X(3)
121             Y14 = Y(1)-Y(4)
122             X14 = X(1)-X(4)
123             DO 175 J=1,10
124               FJM = FLOAT(J-1)/10.
125               XA = X(3) + FJM*X23
126               YA = Y(3) + FJM*Y23
127               XB = X(4) + FJM*X14
128               YB = Y(4) + FJM*Y14
129               DO 170 K= 1,10
130                 FKM = FLOAT(K-1)/10.
131                 XP = XA + (XB-XA)*FKM
132                 YP = YA + (YB-YA)*FKM
133                 CALL PIXELS (YP,XP,ICX,ICY)
134                 IF (ST(ICY,ICX).EQ.-1)GO TO 171
135       170     CONTINUE
136               GO TO 175
137       C
138       C     STORE THE OVERLAP NUMBERS
139       C
140         171 ARP = FLOAT(11-K)*ARMIC
141             SL = SL + ARP
142             NH = NH + 1
143             HAM(NH) = ARP
144             ICH(NH,1) = ICY
145             ICH(NH,2) = ICX
146         175 CONTINUE
147       C
148       C    ACCOUNT FOR SHORE OVERLAP OF PREVIOUS AREAS LOST.
149       C
150             IF (NH.EQ.0)GO TO 179
151             IF (SL.LE.ASL(I))GOTO 179
152             OILOST = 0.
153             DO 176  K = 1, NH
154               ICY = ICH(K,1)
155               ICX = ICH(K,2)
156               AM  = HAM (K)
```

```
157               OILOSS = AM*SAM(I)/(AREA(I)-ASL(I))
158               BAM(ICY,ICX) = BAM(ICY,ICX) + OILOSS
159           176 OILOST = OILOST + OILOSS
160               SAM(I) = SAM(I) - OILOST
161               ASL(I) = SL
162           179 IF (IFR/8*8.NE.IFR)GO TO 180
163               SME(I) = 0.
164               SMN(I) = 0.
165           180 CONTINUE
166               IF (IFR/8*8.NE.IFR)RETURN
167               IF (IPR.GE.1)WRITE (6,9070)
168          9070 FORMAT(' ')
169          C
170          C      PLOT THE SHORE LINE
171          C
172               IF (IFR.NE.8)GO TO 187
173               READ (7,9000)NLINE
174               DO 185 I=1,NLINE
175               READ (7,9020)IPENS(I),RBLAT,RBLON
176          9020 FORMAT(I5,2G15.7)
177               CALL OSPROJ (RBLAT,RBLON,XR(I),YR(I))
178           185 CONTINUE
179           187 DO 190 I=1,NLINE
180           190 CALL PLOT (XR(I),YR(I),IPENS(I))
181          C
182          C     PRINT BEACH TOTALS
183          C
184               DO 195 I=1,NBEACH
185               BT = 0.
186               NP = NPTS(I)
187               DO 193 J=1,NP
188               AM = BAM(IY(I,J),IX(I,J))
189               IF (AM.LT.0.1)GO TO 193
190               WRITE (6,9060)IX(I,J),IY(I,J),AM
191          9060 FORMAT(' PIXEL (',I2,',',I2,') CONTAINS',F9.1,' BARRELS.')
192               BT = BT + AM
193           193 CONTINUE
194               IF (BT.GT.0.5)WRITE (6,9061)ID(I),BT
195          9061 FORMAT(5X,A40,' IS CONTAMINATED BY',F9.1,' BARRELS.')
```

```
196         195 CONTINUE
197             RETURN
198             END
```

APPENDIX B

TIME-VARYING WINDFIELDS

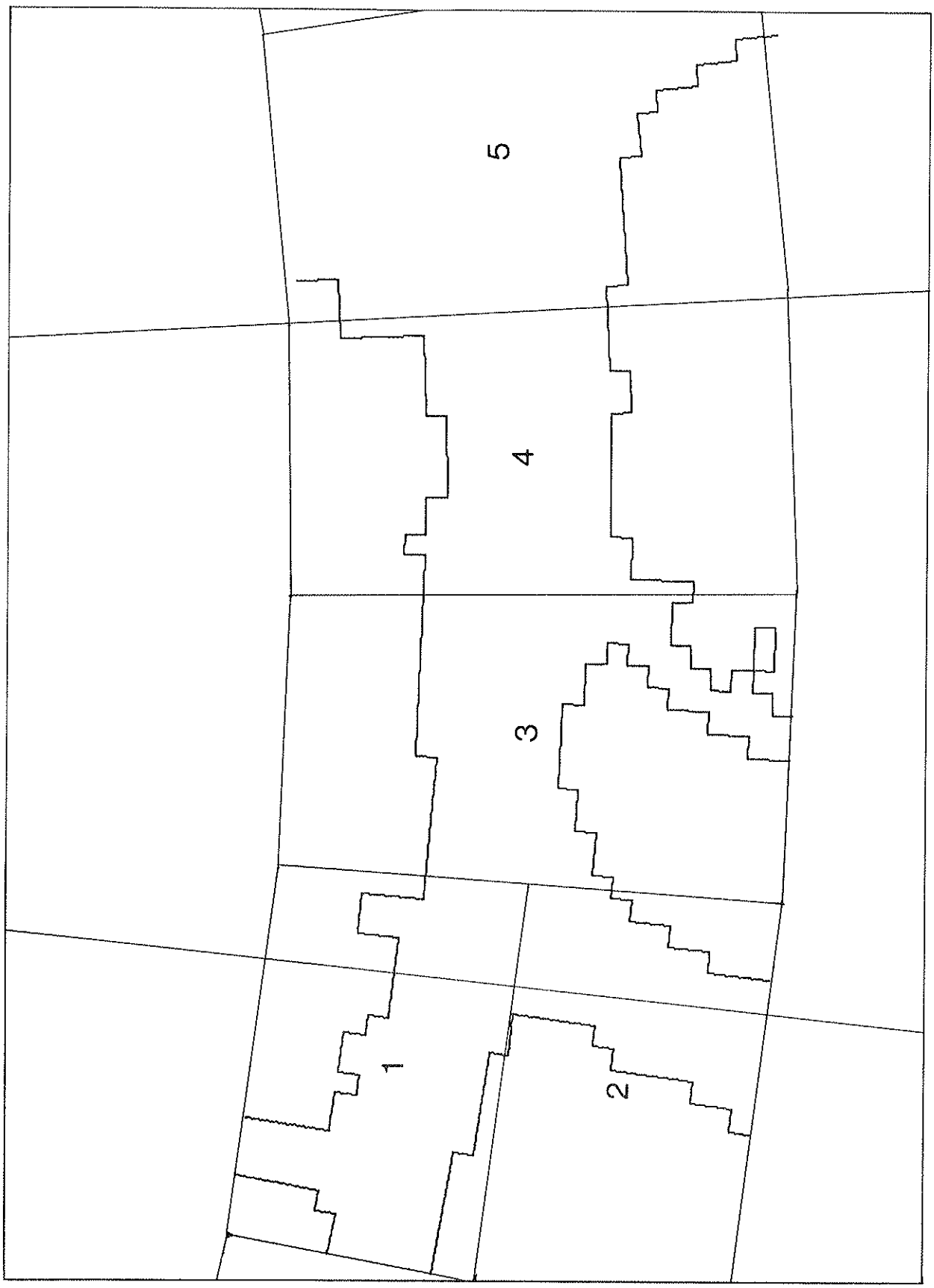

A LOCATOR MAP FOR THE WIND FIELDS LISTED IN THIS APPENDIX.

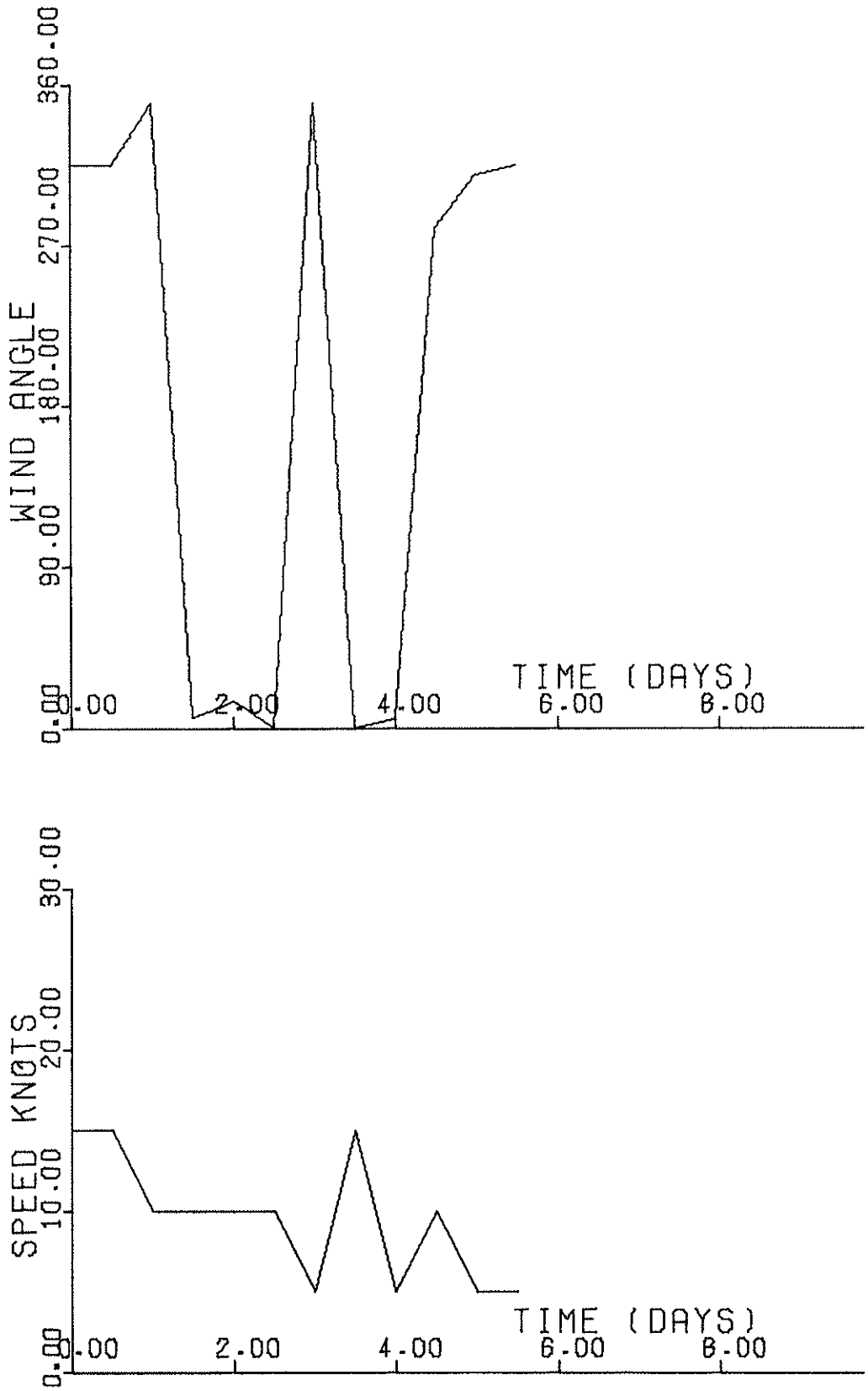

SECTOR NO. 1

A TIME-DEPENDENT NOMINALLY NORTHERLY WINDFIELD IN FIVE SECTORS OF EASTERN PARRY CHANNEL.

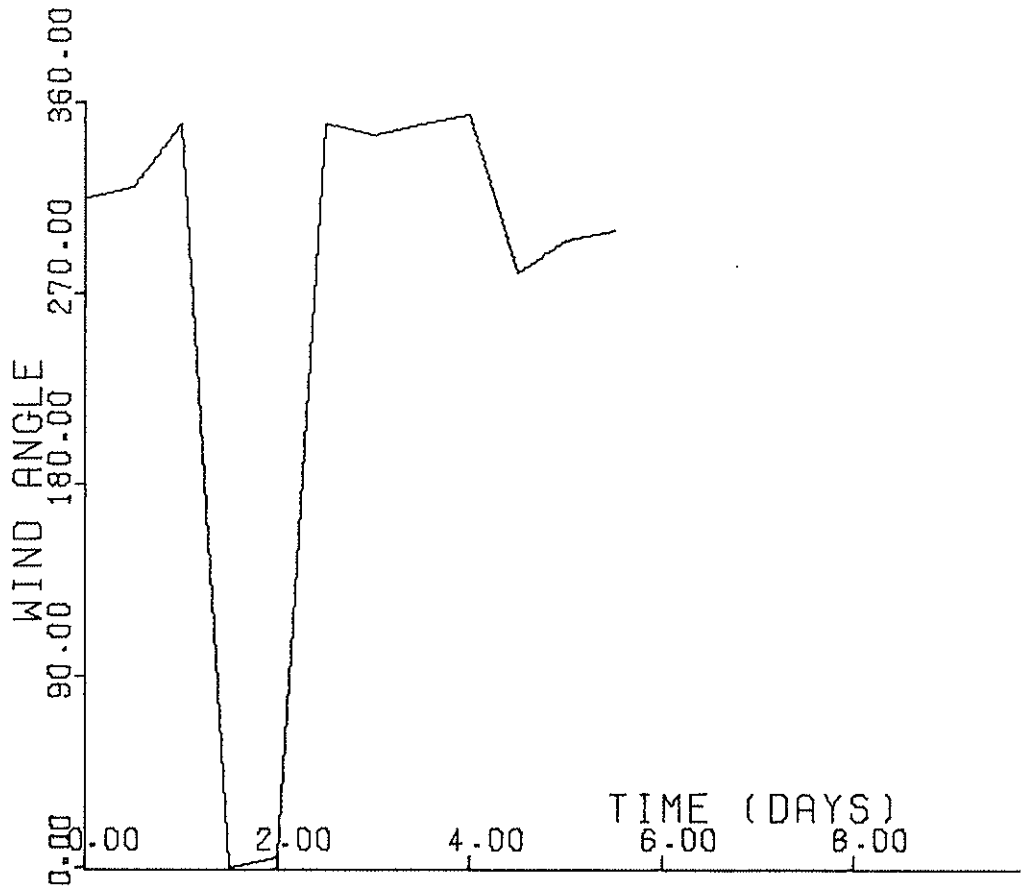
WIND ANGLE
360.00
270.00
180.00
90.00
0.00
0.00
2.00
4.00
6.00
8.00
TIME (DAYS)

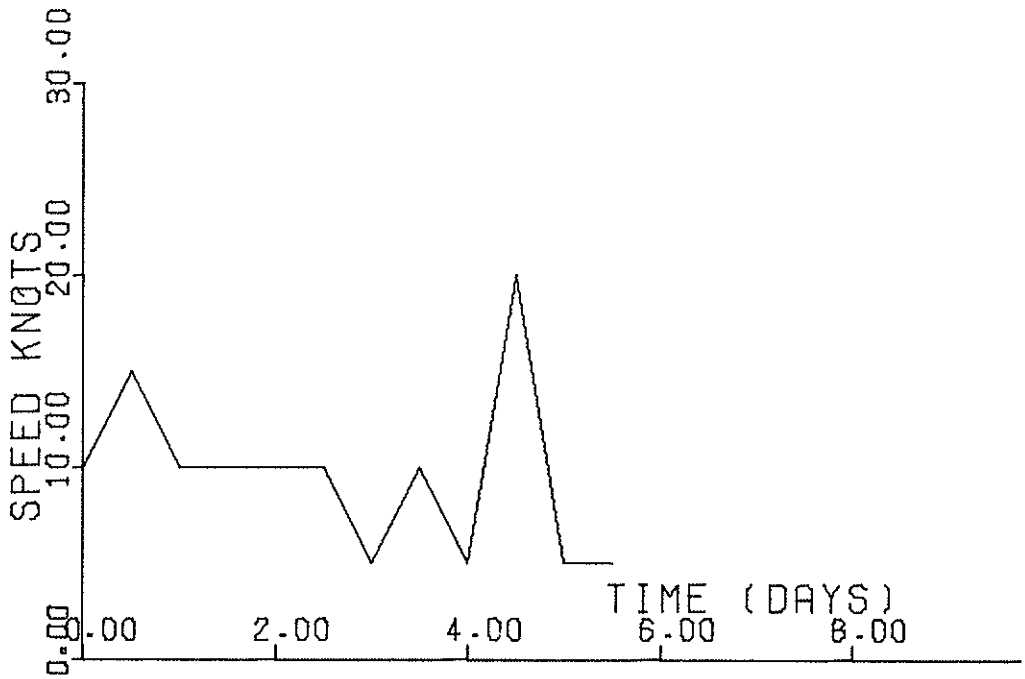
SPEED KNOTS
30.00
20.00
10.00
0.00
0.00
2.00
4.00
6.00
8.00
TIME (DAYS)

SECTOR NO. 2

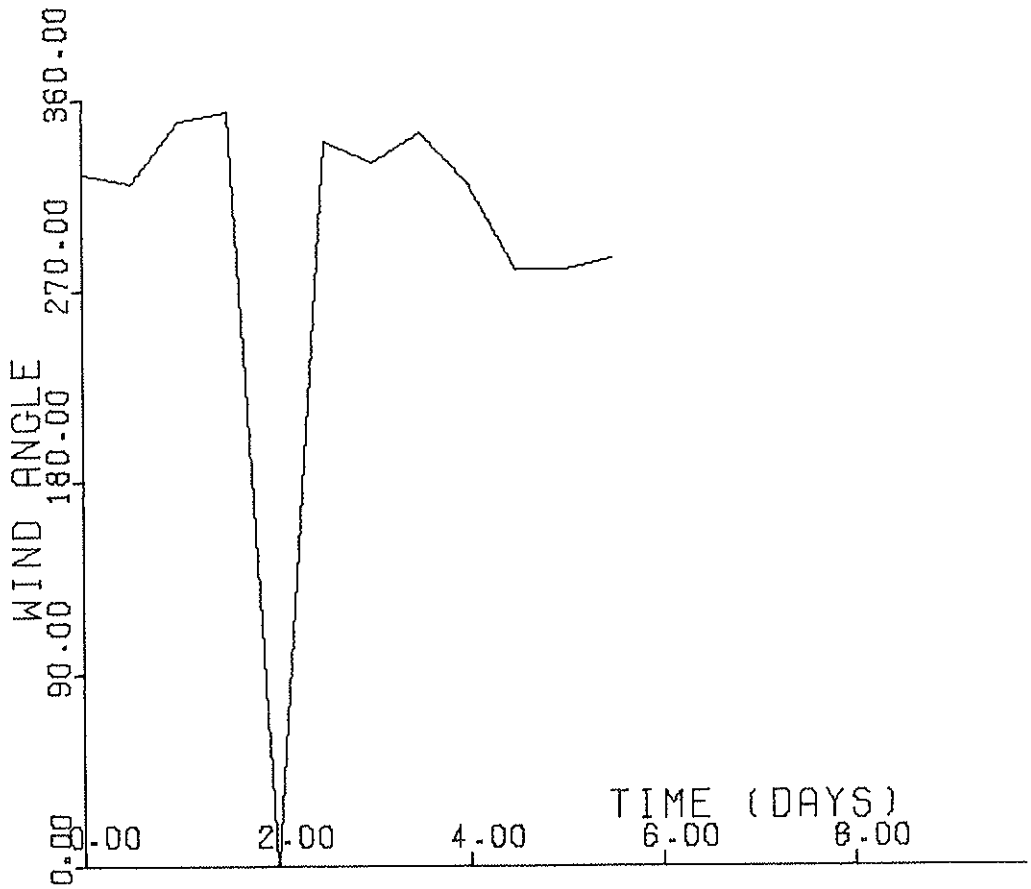
WIND ANGLE
360.00
270.00
180.00
90.00
0.00
0.00
2.00
4.00
6.00
8.00
TIME (DAYS)

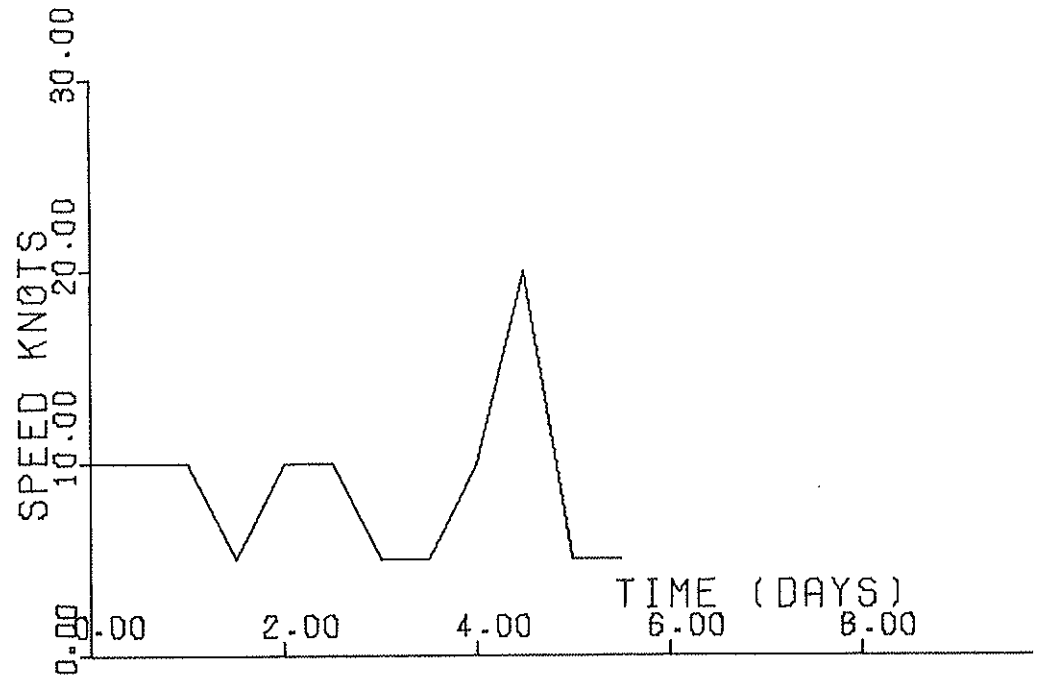
SPEED KNOTS
30.00
20.00
10.00
0.00
0.00
2.00
4.00
6.00
8.00
TIME (DAYS)

SECTOR NO. 3

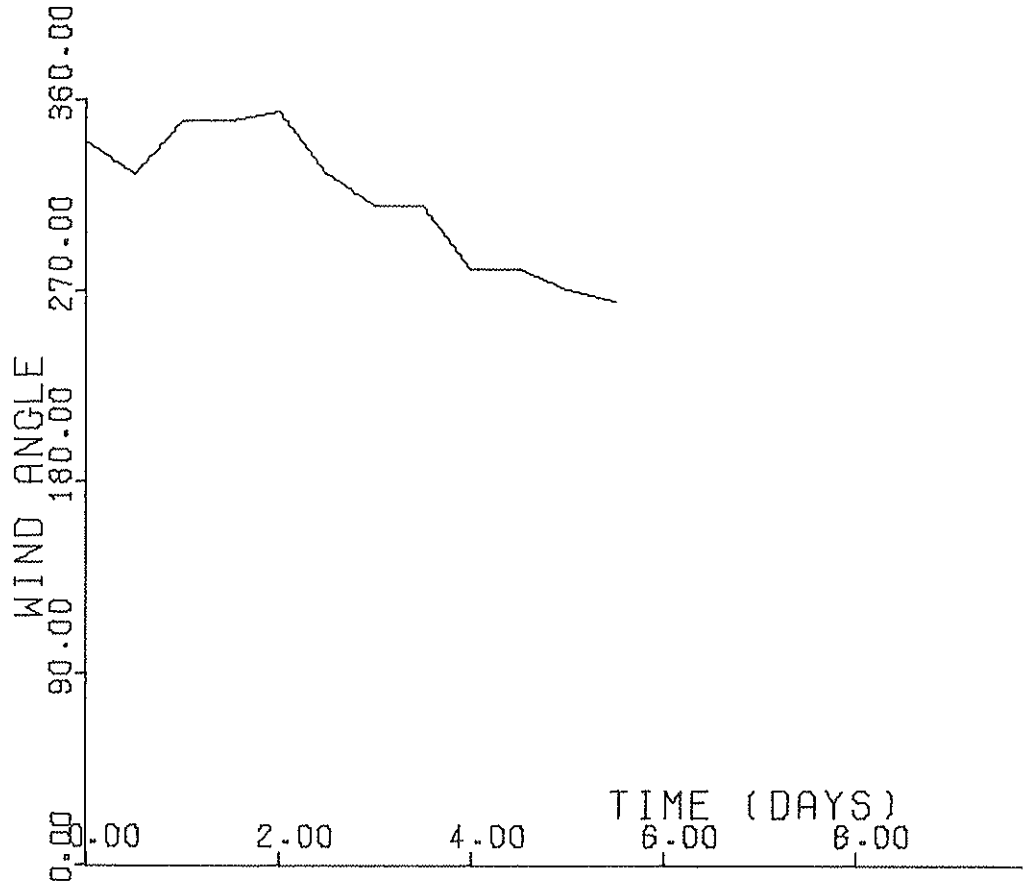
WIND ANGLE
360.00
270.00
180.00
90.00
0.00
0.00
2.00
4.00
6.00
8.00
TIME (DAYS)

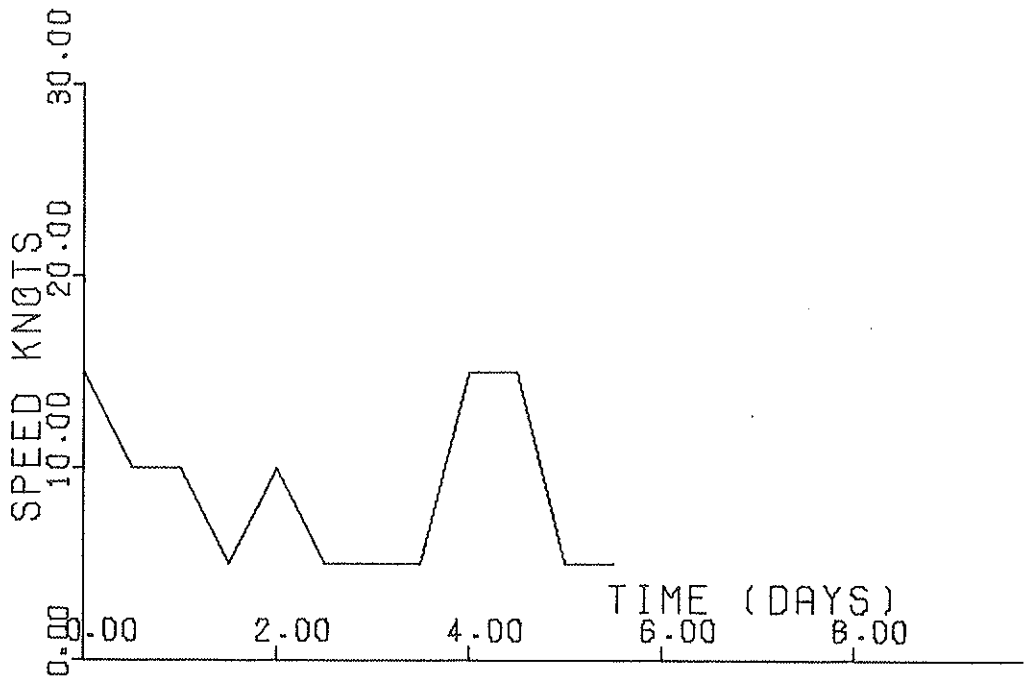
SPEED KNOTS
30.00
20.00
10.00
0.00
0.00
2.00
4.00
6.00
8.00
TIME (DAYS)

SECTOR NO. 4

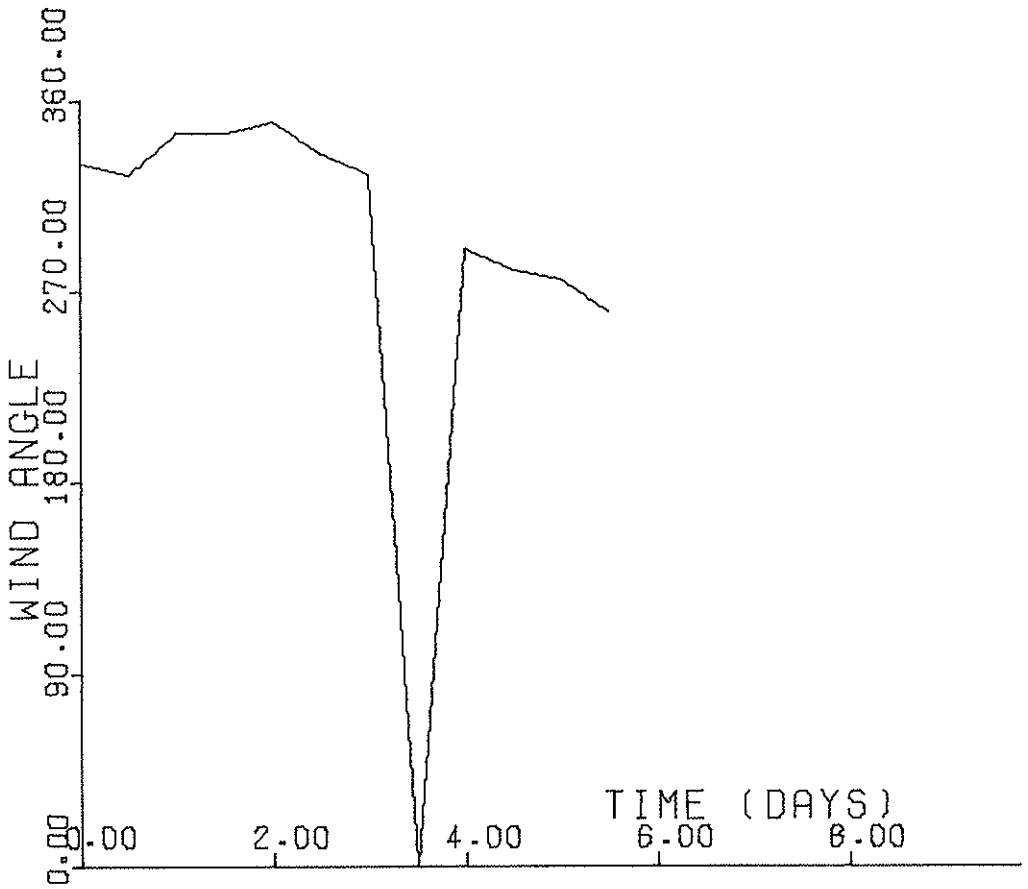
WIND ANGLE
360.00
270.00
180.00
90.00
0.00
0.00
2.00
4.00
6.00
8.00
TIME (DAYS)

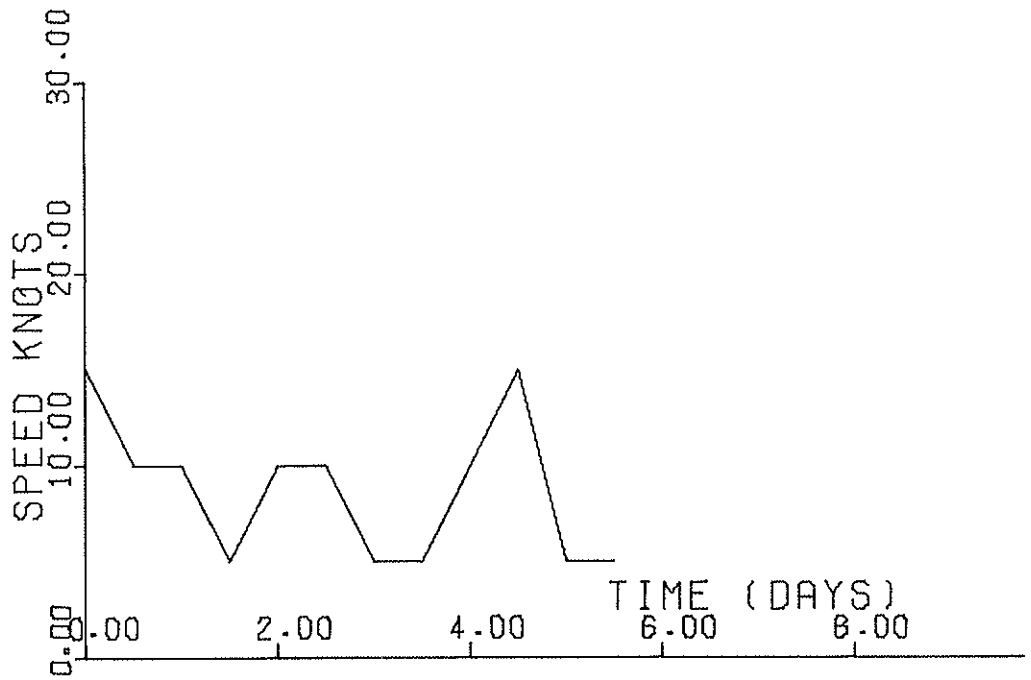
SPEED KNOTS
30.00
20.00
10.00
0.00
0.00
2.00
4.00
6.00
8.00
TIME (DAYS)

SECTOR NO. 5

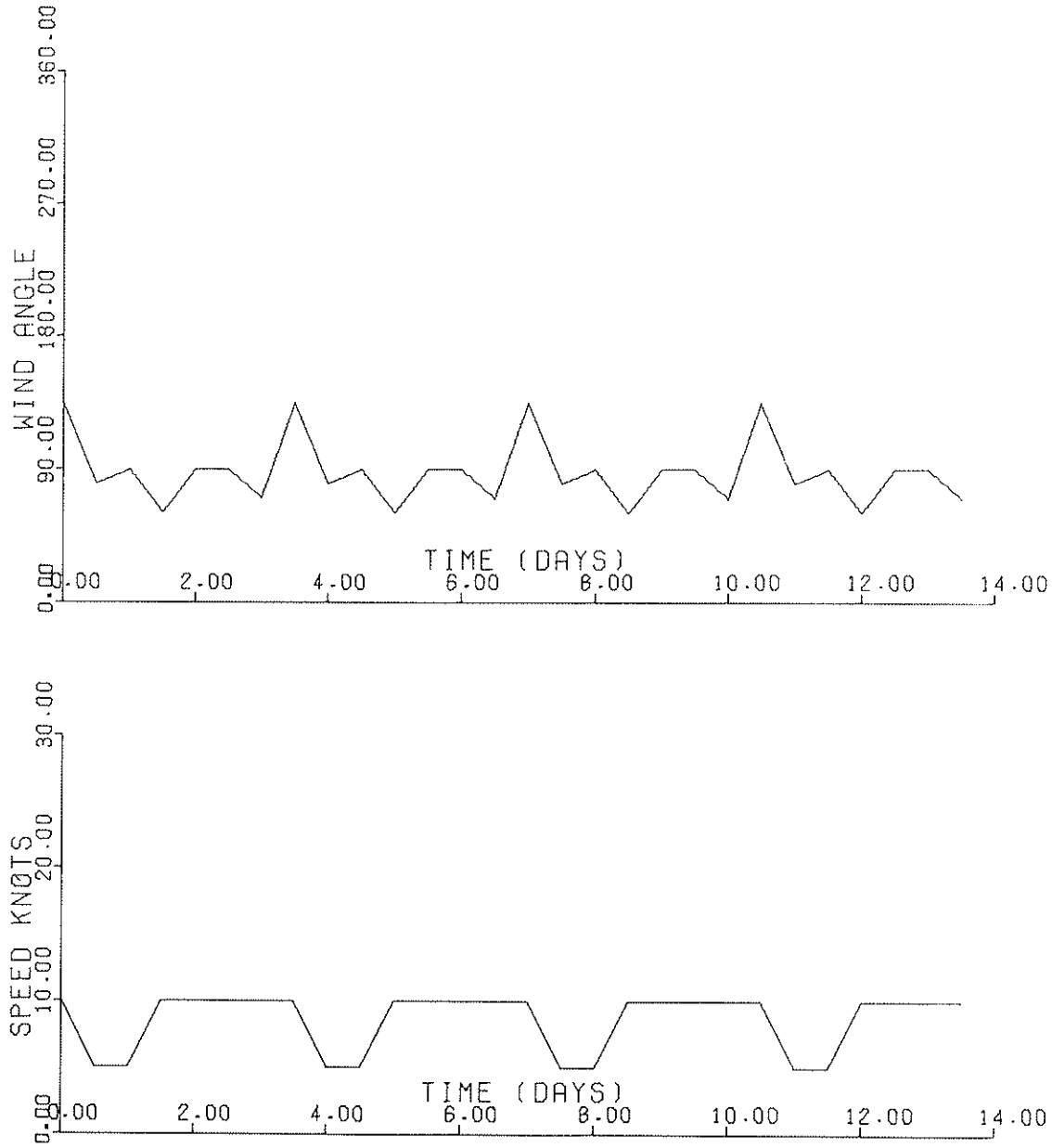

SECTOR NO. 1

A TIME DEPENDENT NOMINALLY EASTERLY WINDFIELD IN FIVE SECTORS OF EASTERN PARRY CHANNEL

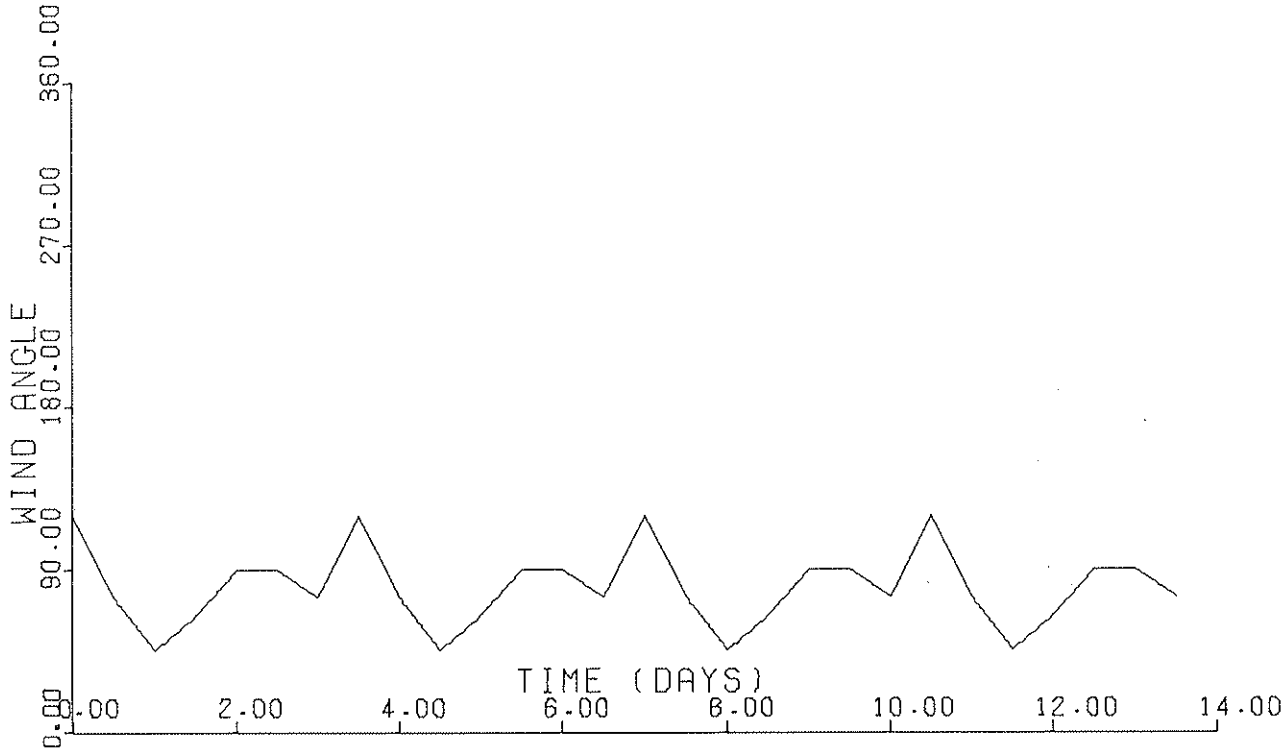
WIND ANGLE
360.00
270.00
180.00
90.00
0.00
TIME (DAYS)
0.00
2.00
4.00
6.00
8.00
10.00
12.00
14.00

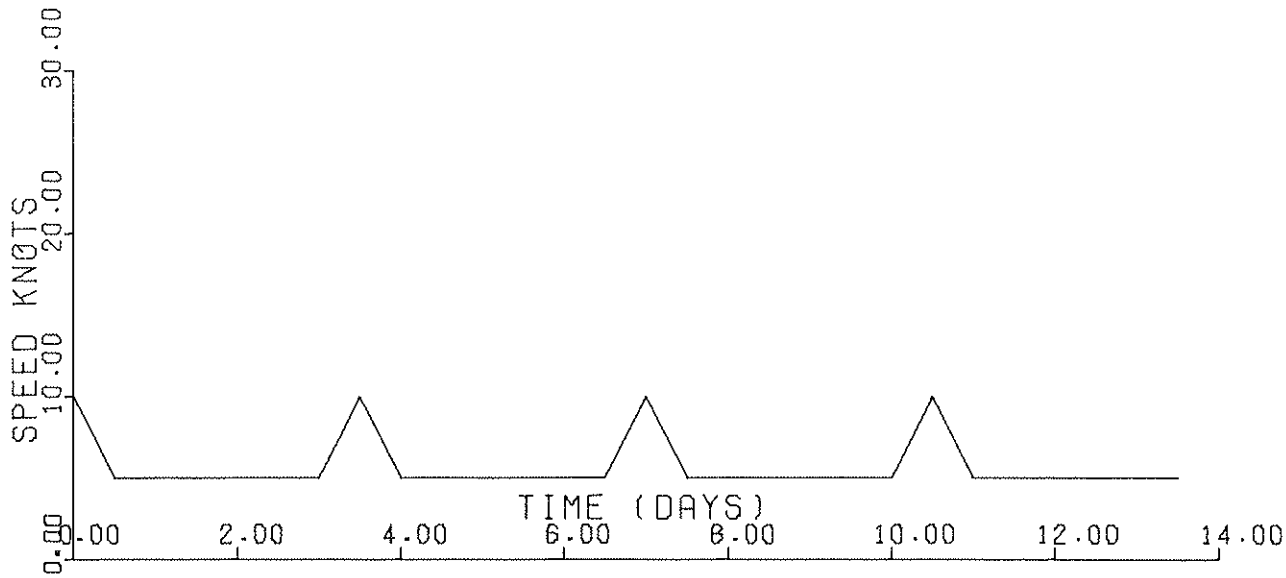
SPEED KNOTS
30.00
20.00
10.00
0.00
TIME (DAYS)
0.00
2.00
4.00
6.00
8.00
10.00
12.00
14.00

SECTOR NO. 2

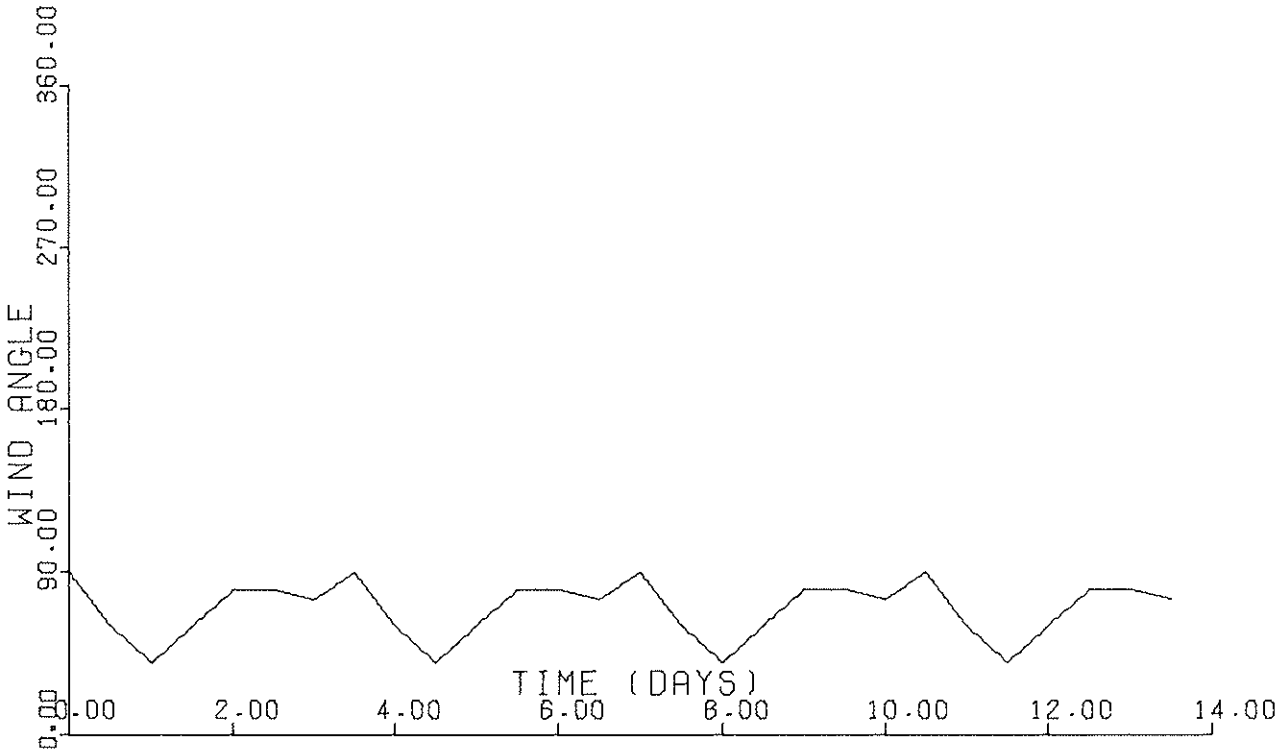
WIND ANGLE
360.00
270.00
180.00
90.00
0.00
TIME (DAYS)
0.00
2.00
4.00
6.00
8.00
10.00
12.00
14.00

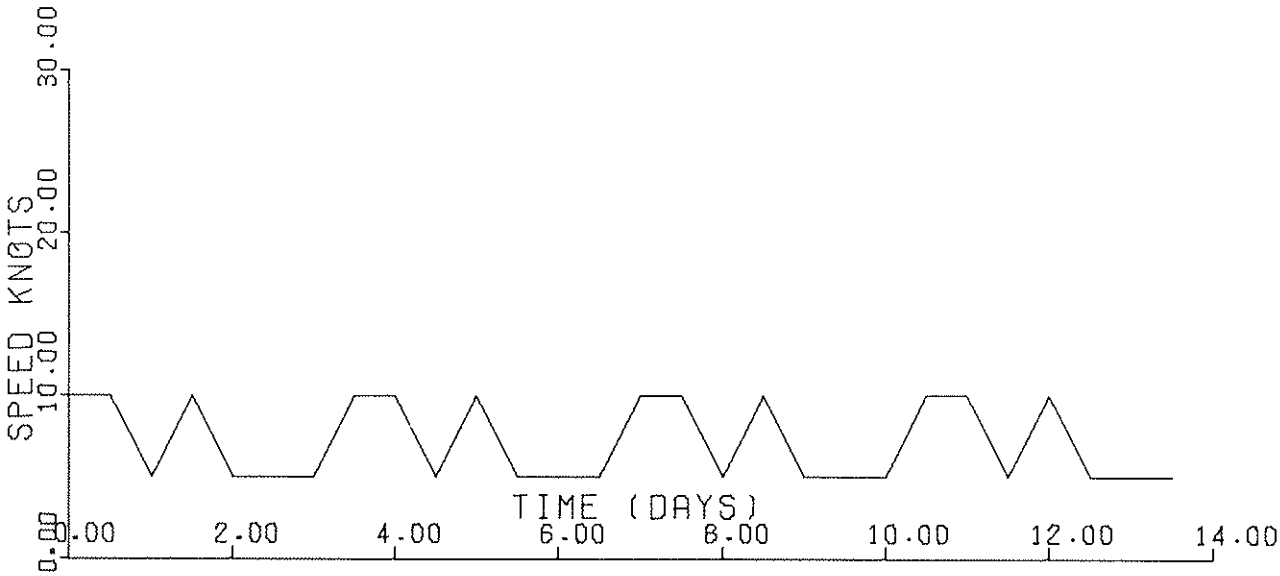
SPEED KNOTS
30.00
20.00
10.00
0.00
TIME (DAYS)
0.00
2.00
4.00
6.00
8.00
10.00
12.00
14.00

SECTOR NO. 3

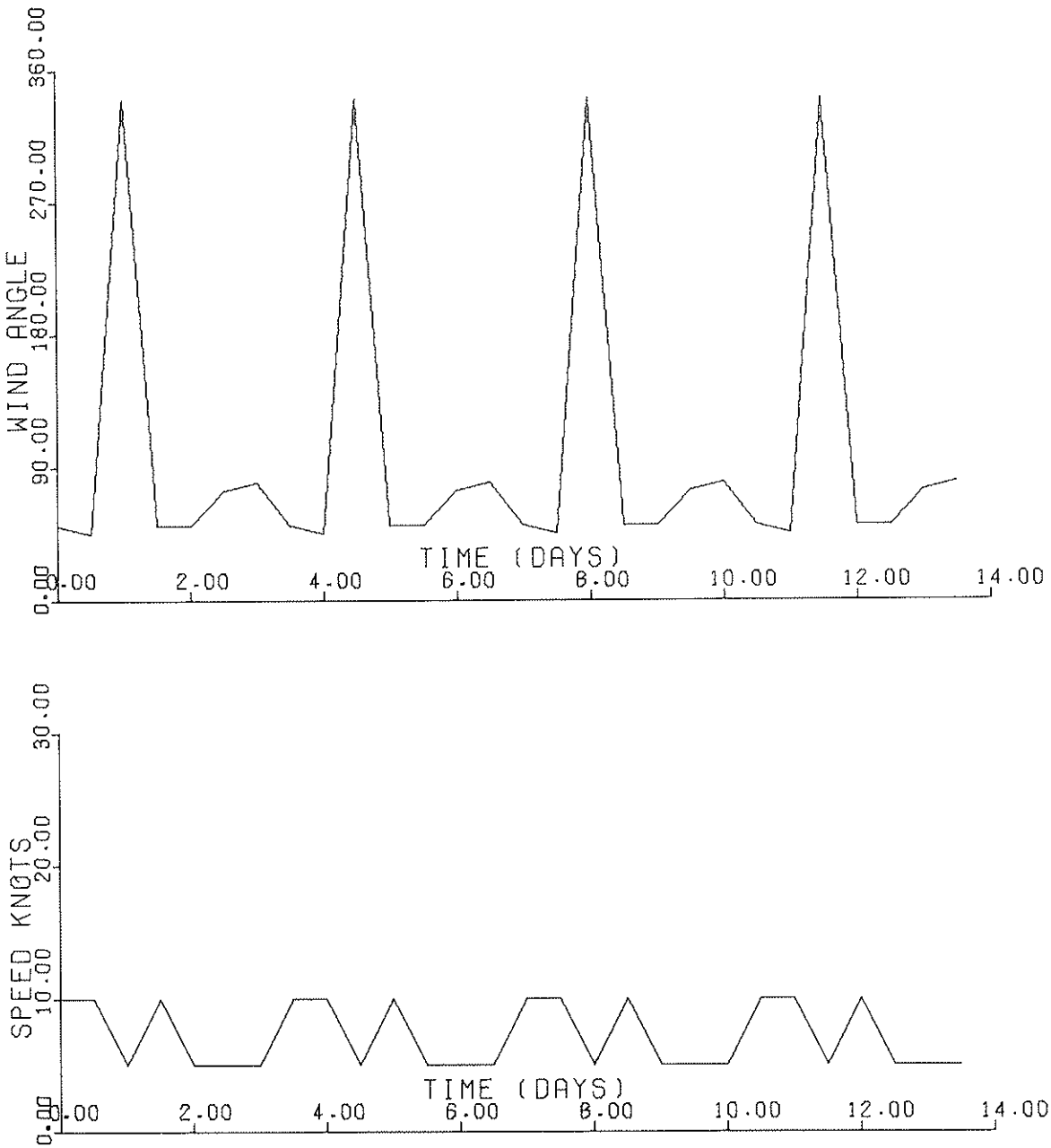
WIND ANGLE
360.00
270.00
180.00
90.00
0.00
TIME (DAYS)
0.00
2.00
4.00
6.00
8.00
10.00
12.00
14.00
SPEED KNOTS
30.00
20.00
10.00
0.00
TIME (DAYS)
0.00
2.00
4.00
6.00
8.00
10.00
12.00
14.00

SECTOR NO. 4

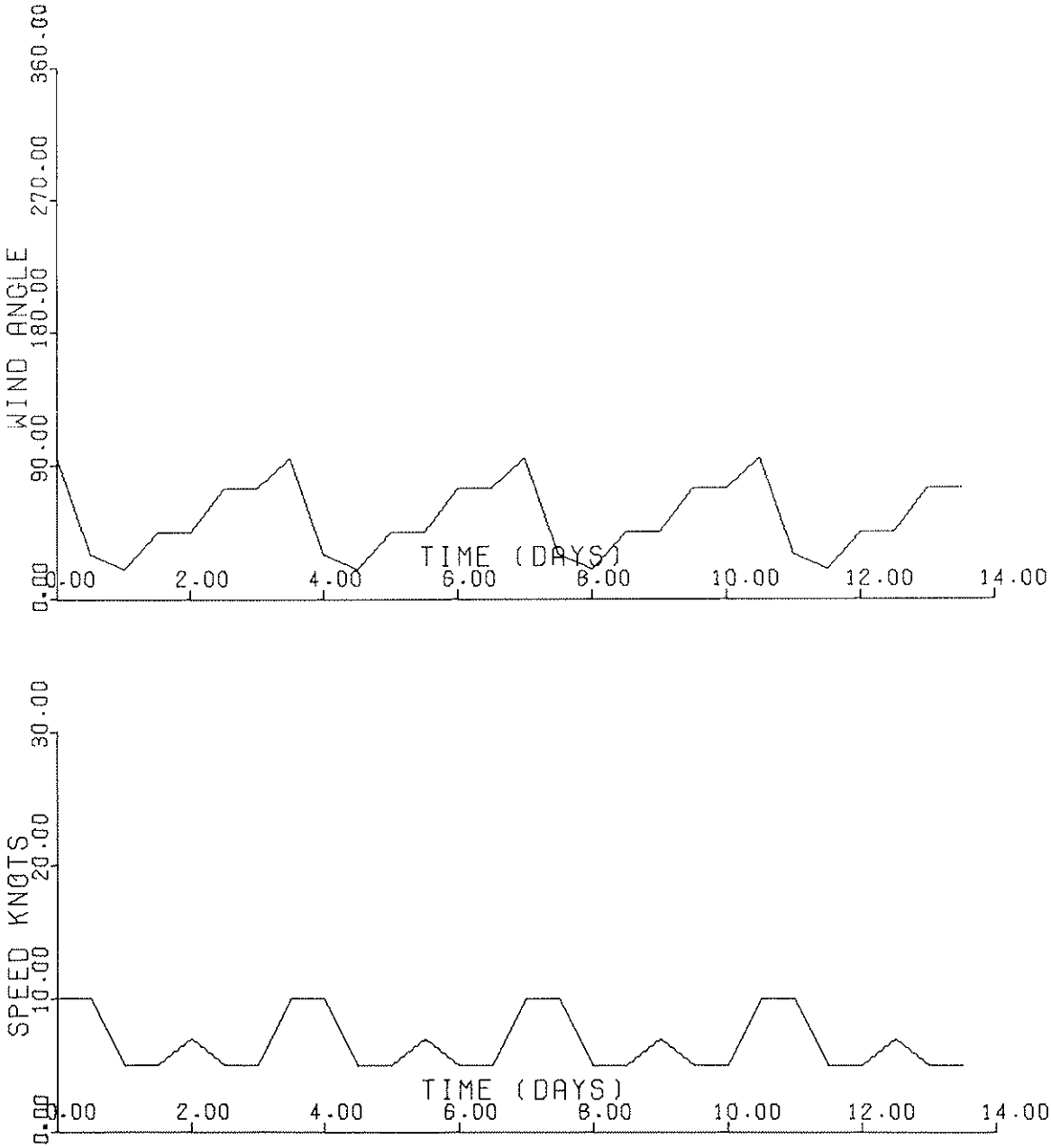
WIND ANGLE
360.00
270.00
180.00
90.00
0.00
TIME (DAYS)
0.00
2.00
4.00
6.00
8.00
10.00
12.00
14.00
SPEED KNOTS
30.00
20.00
10.00
0.00
TIME (DAYS)
0.00
2.00
4.00
6.00
8.00
10.00
12.00
14.00

SECTOR NO. 5

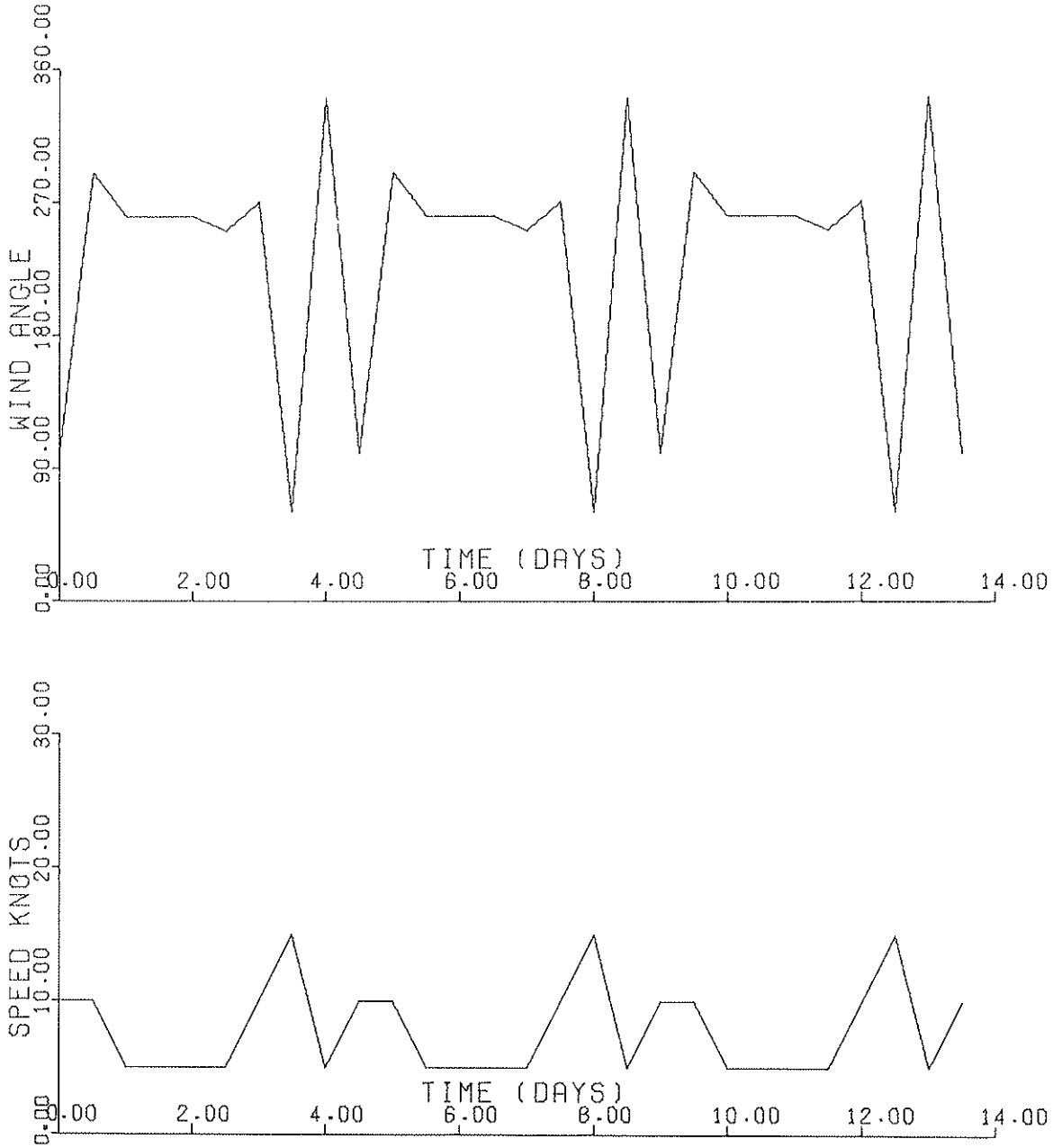

SECTOR NO. 1

A TIME DEPENDENT NOMINALLY WESTERLY WINDFIELD IN FIVE SECTORS OF EASTERN PARRY CHANNEL.

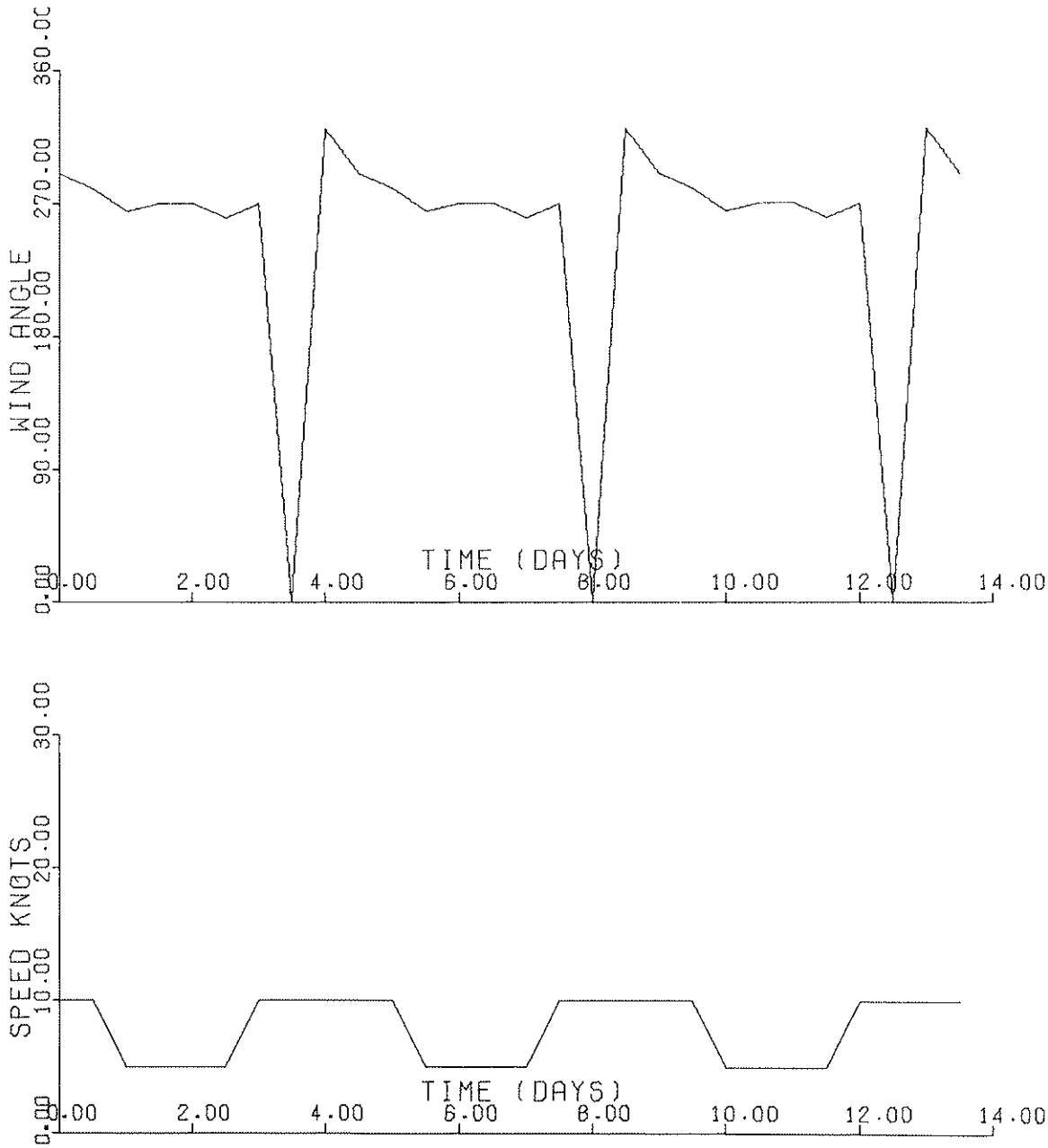
WIND ANGLE
360.00
270.00
180.00
90.00
0.00
TIME (DAYS)
0.00
2.00
4.00
6.00
8.00
10.00
12.00
14.00
SPEED KNOTS
30.00
20.00
10.00
0.00
TIME (DAYS)
0.00
2.00
4.00
6.00
8.00
10.00
12.00
14.00

SECTOR NO. 2

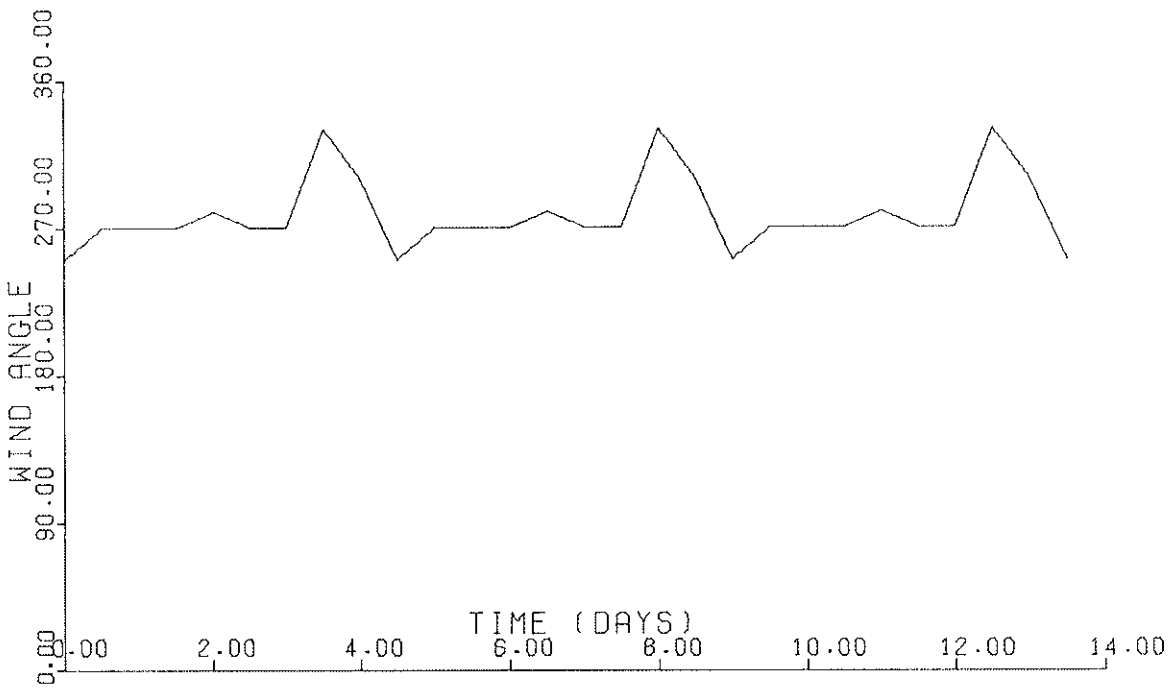
WIND ANGLE
360.00
270.00
180.00
90.00
0.00
TIME (DAYS)
0.00
2.00
4.00
6.00
8.00
10.00
12.00
14.00

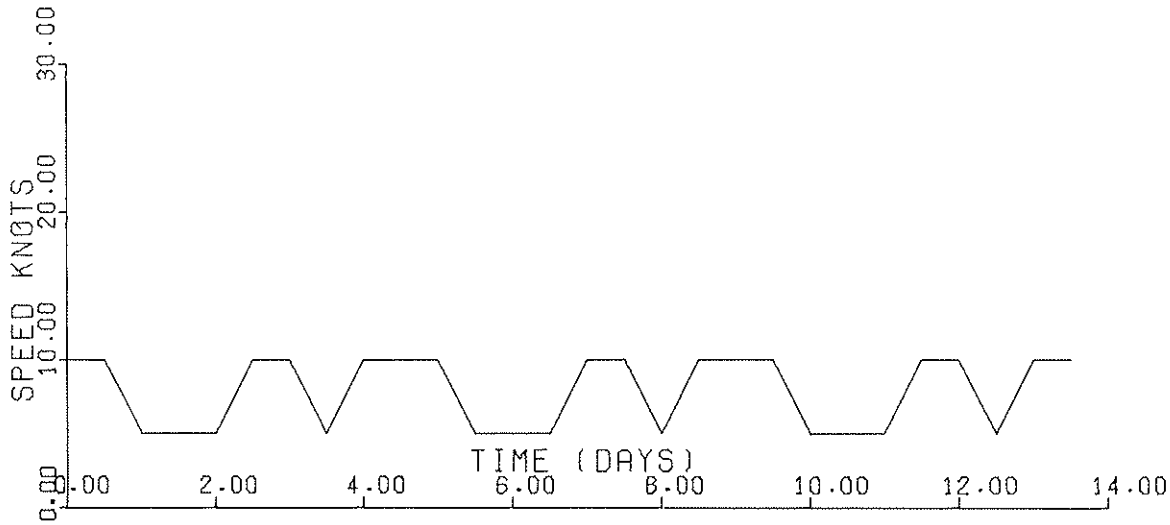
SPEED KNOTS
30.00
20.00
10.00
0.00
TIME (DAYS)
0.00
2.00
4.00
6.00
8.00
10.00
12.00
14.00

SECTOR NO. 3

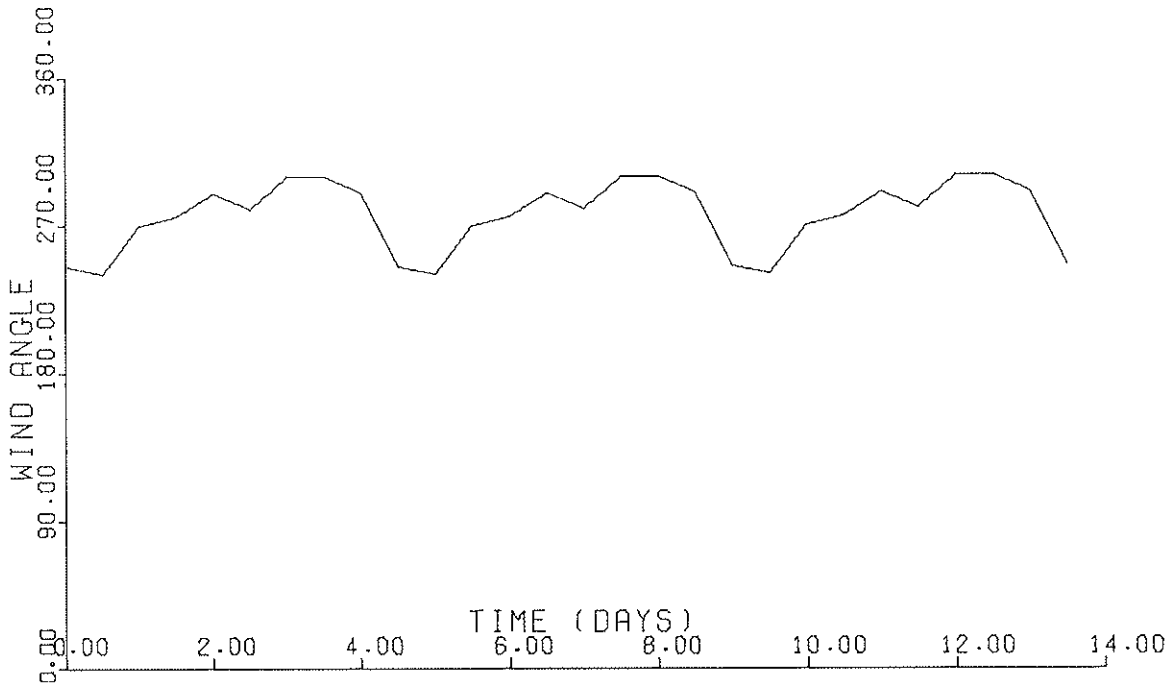
WIND ANGLE
360.00
270.00
180.00
90.00
0.00
TIME (DAYS)
0.00
2.00
4.00
6.00
8.00
10.00
12.00
14.00

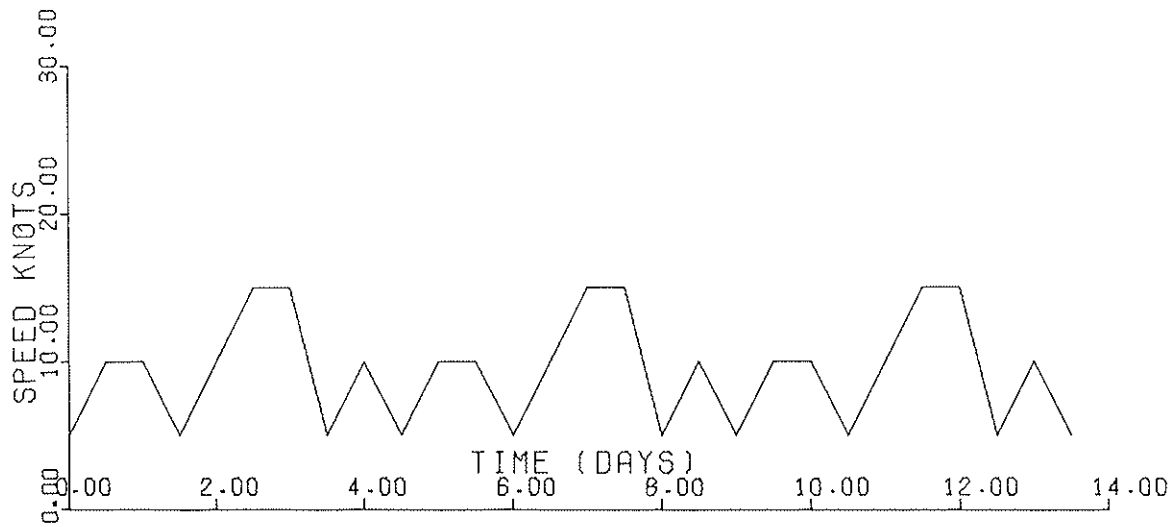
SPEED KNOTS
30.00
20.00
10.00
0.00
TIME (DAYS)
0.00
2.00
4.00
6.00
8.00
10.00
12.00
14.00

SECTOR NO. 4

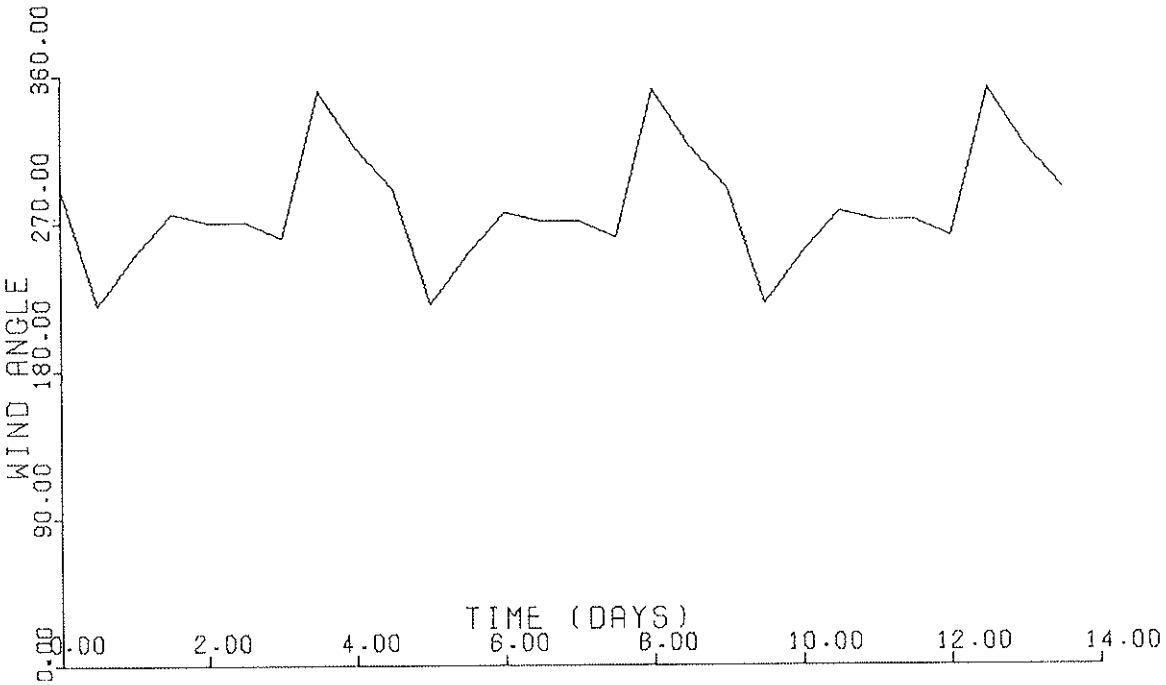
WIND ANGLE
360.00
270.00
180.00
90.00
0.00
TIME (DAYS)
0.00
2.00
4.00
6.00
8.00
10.00
12.00
14.00

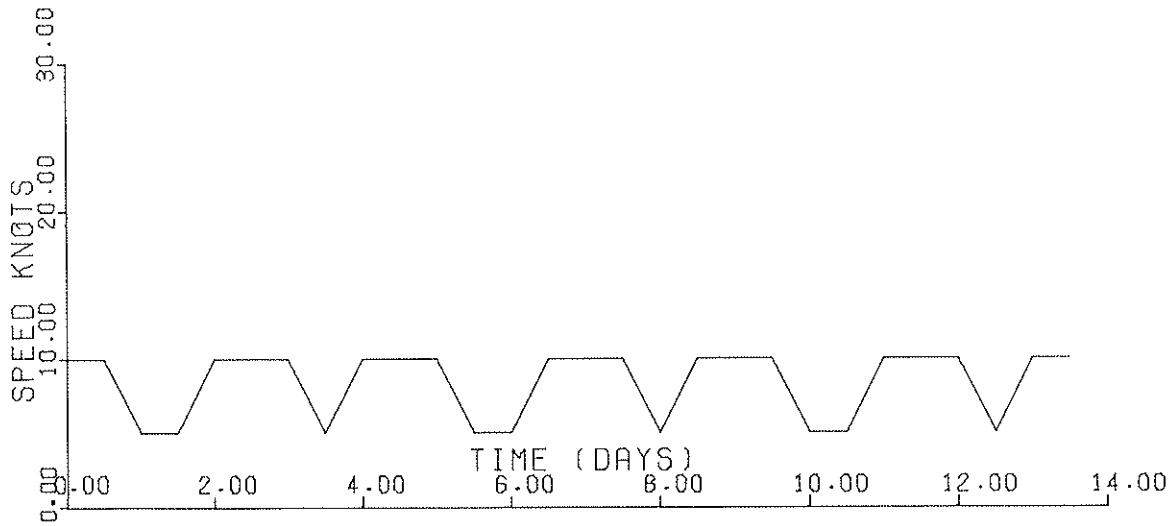
SPEED KNOTS
30.00
20.00
10.00
0.00
TIME (DAYS)
0.00
2.00
4.00
6.00
8.00
10.00
12.00
14.00

SECTOR NO. 5